Indian J Chem
FEBRUARY 1992
CODEN : IJOCAP 31A(2) 71-140 (1992)
ISSN : 0019-5103

INDIAN JOURNAL OF CHEMISTRY

SECTION A

(Inorganic, Bio-inorganic, Physical, Theoretical & Analytical Chemistry)

Published by
PUBLICATIONS & INFORMATION DIRECTORATE, CSIR, NEW DELHI
in association with
THE INDIAN NATIONAL SCIENCE ACADEMY, NEW DELHI

NEW TITLES FROM PID

BODY'S BATTLES

by **Bal Phondke**

This attractive and lavishly illustrated book unfolds the dramatic story of our inner defence organisation, the diversity and specificity of its armament, and the methodical way in which it maintains a round the clock vigil to meet squarely every imaginable threat to the human body and also how it wins the Body's Battles most of the time.

ISBN 81- 85038-99-6

84 pages, price Rs. 9.00

MINING THE OCEAN

by **T.K.S. Murthy**

This well illustrated book written especially for the non-specialist, reveals the timeless secrets of the seas. It unfolds in exquisite detail the bounty that seas hold in reserve and highlights man's attempts at mining the Oceans.

ISBN 81-7236-014-2

106 pages, price Rs. 12.00

LIFE : FROM CELL TO CELL

by **Bal Phondke**

The exciting story of Life—an eternal journey from cell to cell is told in this profusely illustrated popular sciences volume especially written for young readers.

ISBN 81-85038-91-0

74 pages, price Rs. 8.00

LEARN SCIENCE YOURSELF

A compendium of exciting science experiments and do-it-yourself projects that are not only educative but also of practical utility.

ISBN 81-85038-93-7

128 pages, price Rs. 10.00

INSIGHT INTO SCIENTIFIC RESEARCH

by **Rais Ahmed & Madhulika Rakesh**

This is an unusual piece of research reported in a clear and direct manner, addressed as much to the scholars as to the managers and policy-makers of research.

ISBN 81-85038-96-1

xiv+154 : pages; price : Rs. 140.00

Copies available from:

Senior Sales & Distribution Officer, *Publications & Information Directorate, CSIR, Dr. K.S. Krishnan Marg, New Delhi - 110 012*

INDIAN JOURNAL OF CHEMISTRY

Section A: Inorganic, Bio-inorganic, Physical, Theoretical & Analytical Chemistry

Published by the Publications & Information Directorate (CSIR), Hillside Road, New Delhi 110 012
Director: Dr G P Phondke

The Indian Journal of Chemistry is issued monthly in two sections: A and B. Communications regarding contributions for publication in the journal should be addressed to the Editor, Indian Journal of Chemistry, Publications & Information Directorate, Hillside Road, New Delhi 110 012.

Correspondence regarding subscriptions and advertisements should be addressed to the Sales & Distribution Officer, Publications & Information Directorate, Hillside Road, New Delhi 110 012.

The Publications & Information Directorate (CSIR) assumes no responsibility for the statements and opinions advanced by contributors. The Editorial Board in its work of examining papers received for publication is assisted, in an honorary capacity by a large number of distinguished scientists, working in various parts of India.

Annual Subscription: Rs. 400.00 £ 100.00 $ 150.00; 50% discount admissible to research workers and students and 25% discount to non-research individuals on annual subscription.

Single Copy: Rs. 40.00 £ 10.00 $ 15.00

Payments in respect of subscriptions and advertisements may be sent by cheque, bank draft, money order or postal order marked payable to Publications & Information Directorate, Hillside Road, New Delhi 110 012.

Claims for missing numbers of the journal will be allowed only if received within 3 months of the date of issue of the journal plus the time normally required for postal delivery of the journals and the claim.

Author Index

Indian Journal of Chemistry

Sect. A: Inorganic, Bio-inorganic, Physical, Theoretical & Analytical

VOLUME 31A NUMBER 2 FEBRUARY 1992

CONTENTS

Contd.

Authors for correspondence are indicated by (*)

Indian Journal of Chemistry
Vol. 31A, February 1992, pp. 71-76

Photopolymerization of methyl methacrylate using dichloroacetic acid and dimethylaniline combination as photoinitiator

Premamoy Ghosh* & Gauri Sankar Mukherjee[†]

Department of Plastics and Rubber Technology, Calcutta University, 92, A.P.C. Road, Calcutta 700 009, India

Received 5 August 1991; revised and accepted 13 November 1991

Photopolymerization of methyl methacrylate (MMA) in bulk and in solution at 40°C using dichloroacetic acid-dimethylaniline (DCAA-DMA) combination as photoinitiator has been studied kinetically. Initiator exponent and k_p^2/k_t values are ~0.27 and 1.30×10^{-2} $dm^3 \cdot mol^{-1} \cdot s^{-1}$ respectively, while the monomer exponent is 1.0 in benzene and pyridine but < 1.0 in chloroform, carbon tetrachloride and cyclohexanone. End group analysis of the polymers prepared indicates that initiation of polymerization takes place by radicals derived from each initiating component on photo-decomposition of the complex between DCAA and DMA formed *in situ*. The radical generation process is dependent on the nature of the solvent used. The role of different solvents in modifying the initiation or radical generation process is analysed. The kinetic non-ideality in respect of low initiator exponent (< 0.5) is explained on the basis of significant initiator dependent termination through primary radicals or via degradative transfer to initiator.

Chloroacetic acids are known to form acid-base complexes when allowed to react with alkyl, aryl or aralkyl amines[1]. Previously, we reported[2] the results of studies on the effectiveness of acetic acid and its three chloro derivatives in combination with dimethylaniline for polymerization of MMA. In the present paper we report the results of investigation on the kinetics and related features of photopolymerization of methyl methacrylate (MMA) using dichloroacetic acid (DCAA) and dimethylaniline (DMA) combination as photoinitiator.

Materials and Methods

Methyl methacrylate (MMA) received from Western Commercial Corporation was purified by usual procedures[3,4]. Dichloroacetic acid (DCAA) (Analar, BDH) was purified by recrystallization by cooling and stored in a desiccator at 5°C. Dimethylaniline (DMA) (E. Merck) was kept on KOH pellets and was purified by distillation. Solvents used were of A.R. quality and were purified by distillation following standard procedures[5].

Polymerization of MMA was studied dilatometrically in nitrogen atmosphere in the presence of light (visible and near UV) at 40°C using a 125 W Hg-vapour lamp (Philips India Ltd.) without any filter. The dilatometer was made of borosilicate glass. The polymerization was followed to a low conversion (≤10%) and the polymers produced were isolated by precipitation with excess of petroleum ether as non-solvent. The polymer was then washed with non-solvent and dried at 50°C in a vacuum oven. Intrinsic viscosities, $[\eta]$ of the polymers in benzene solution were determined at 30°C by standard procedures[3,4]. Molecular weight, $\bar{M}_n$ and hence the degree of polymerization, $\bar{P}_n$ of the polymers were calculated from the following relationship[6].

$$[\eta] = 8.69 \times 10^{-5} \bar{M}_n^{0.76} \quad \ldots (1)$$

Results

Complexation between DCAA and DMA

Examination of UV absorption spectra of dilute solution of DCAA (6.5×10^{-3} mol.dm^{-3}), DMA (4×10^{-5} mol.dm^{-3}) and a mixture thereof (DCAA:DMA = 6.5×10^{-3} mol.dm^{-3}: 4×10^{-5} mol.dm^{-3}) revealed the formation of an in situ equilibrium complex between DCAA and DMA[2].

Photopolymerization of MMA in bulk at 40°C

Neither DCAA nor DMA was capable of inducing the polymerization of MMA in 200 min either in the dark or in the presence of light. When used in combination, however, they readily initiated the polymerization of MMA under photo condition. The in situ complex, I ($[I] = K_c[DCAA][DMA]$, K_c = equilibrium constant) is believed to be the actual initiating species. Photopolymerization was usually associated with an inhibition period (IP) ranging between 50 and 80 min depending on [I]. Higher [I]

[†]Present address: Defence Research & Development Organization, DMSRDE, Kanpur.

produced lower IP and higher rate of polymerization (R_p). IP arises probably due to impurities such as traces of oxygen in the nitrogen-flushed system. A much higher IP was observed when the polymerization was carried out in air or benzoquinone (0.01%). R_p was calculated from the slope of the linear plots of % conversion versus time[7].

Initiator exponent

The slope of the plot of log R_p versus log[DCAA][DMA], Fig. 1, giving the value of the initiator exponent, is 0.28 for the bulk polymerization and 0.26 for polymerization in chloroform-diluted systems; in each case however, the initiator exponent value is less than 0.5, which is the expected initiator order for normal free radical polymerization.

k_p^2/k_t value

The kinetic parameter k_p^2/k_t was evaluated in the usual manner[8] from R_p and $\overline{P}_n$ data with the help of Eq. (2). From the slope of the linear plot of $1/\overline{P}_n$ versus $R_p/[M]^2$, Fig. 2 the value of k_p^2/k_t was found to be 1.29×10^{-2} dm^3 mol^{-1} s^{-1} for bulk systems and 1.31×10^{-2} dm^3 mol^{-1} s^{-1} for chloroform-diluted system and the calculated k_p^2/k_t values are in good agreement with each other and with those reported for free radical polymerization[6-12]. The kinetic features with respect to k_p^2/k_t value remains practically unchanged on shifting over from bulk polymerization to solution polymerization.

$$1/\overline{P}_n = 1.85(k_t/k_p^2)(R_p/[M]^2) + C_M + C_I K_C[DCAA][DMA]/[M] \quad \ldots (2)$$

Apparent activation energy, E_a

The apparent activation energy for the bulk polymerization, E_a, ($E_a = E_p - E_t/2$) determined in the usual manner[8] is 20.79 kJ mol^{-1}. This appears to be in good agreement with the E_a value for the photopolymerization of MMA[8-10].

Initiators transfer parameter ($C_I K_e$)

The value of the initiator transfer parameter defined as the product of C_I and K_e at 40°C in the bulk polymerization of MMA, where C_I is the chain transfer constant of the initiating complex, was determined as 9×10^{-2} dm^3 mol^{-1} from the slope of the plot of $\{1/\overline{P}_n - 1.85\ (k_t/k_p^2).\ (R_p/[M]^2)\}$ versus [DCAA][DMA]/[M], Fig. 3, according to the Mayo equation (2) in the following form Eq. (2A)

$$1/\overline{P}_n - 1.85(k_t/k_p^2)(R_p/[M]^2 + C_M + C_I K_e \cdot [DCAA][DMA]/[M] \quad \ldots (2A)$$

The effect of possible modes of chain termination other than the bimolecular mode on $\overline{P}_n$ is considered

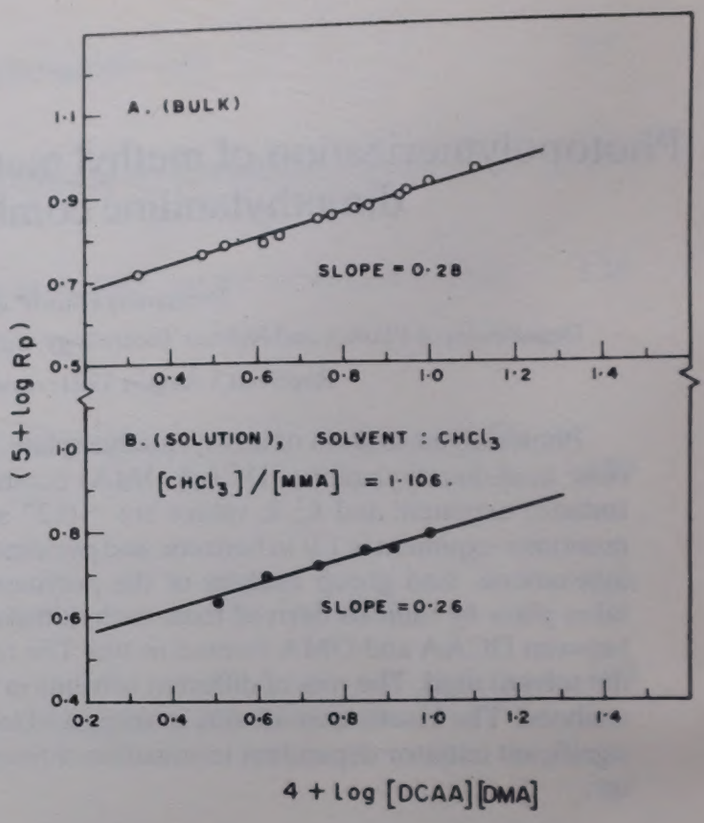

Fig. 1—Photopolymerization of MMA at 40°C using DCAA-DMA combination as photoinitiator: plot of log R_p versus log [DCAA][DMA]

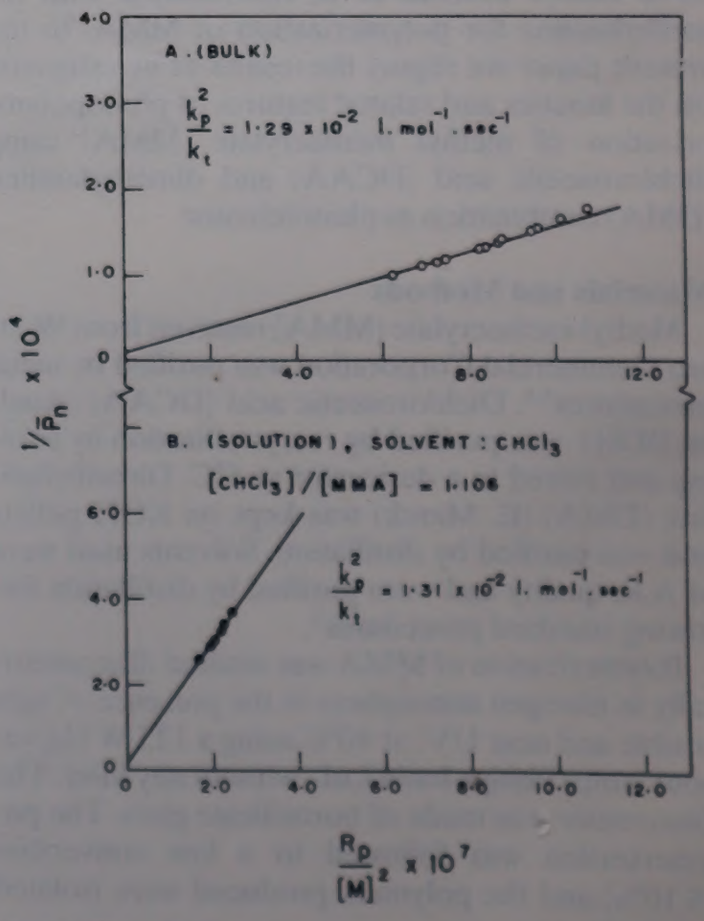

Fig. 2—Photopolymerization of MMA in bulk at 40°C using DCAA-DMA combination as photoinitiator: Plot of $1/P_n$ versus $R_p/[M]^2$

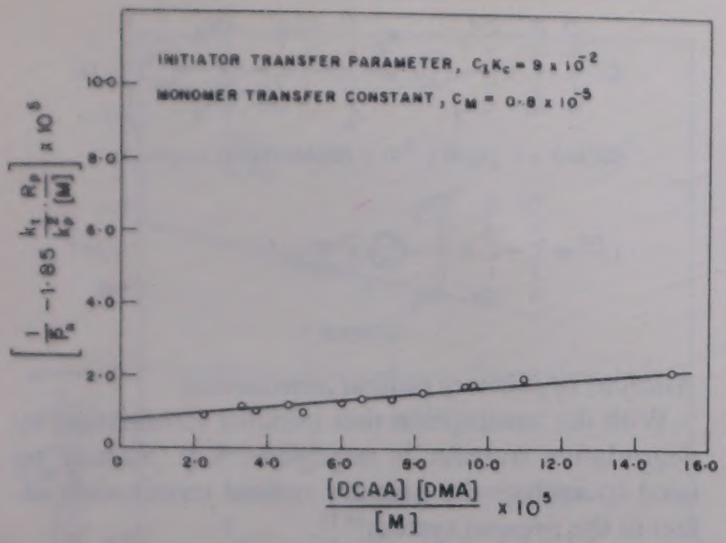

Fig. 3—Photopolymerization of MMA in bulk using DCAA-DMA combination as photoinitiator: Plot of $[(1/\bar{P}_n) - 1.85\,(k_t/k_p^2)(R_p/[M]^2)]$ versus [DCAA][DMA]/[M]

negligible over the initiator concentration range studied.

Monomer transfer constant (C_M)

The intercept of the slope of the above plot (Fig. 3) based on Eq. (2A) gives the value of monomer transfer constant, C_M as 0.8×10^{-5} and this value appears to be in good agreement with some literature values for the same[3,13].

Monomer exponent and role of solvents

At fixed concentration of the initiating components, photopolymerization of MMA in solution was carried out at 40°C using solvents such as benzene, pyridine, cyclohexanone, chloroform and carbon tetrachloride in various volume proportions separately. The monomer order for each solvent system was calculated from the plot of log R_p versus log [M], (Fig. 4). With benzene and pyridine the monomer exponent was 1.0, conforming to the normal kinetics of radical polymerization. But with cyclohexanone, chloroform and carbon tetrachloride, the monomer exponents were 0.80, 0.65 and 0.46 respectively, thereby indicating the kinetics of radical polymerization with respect to monomer order to be non-ideal in nature. With chloromethanes first an enhancement of rate and then a decrease in the rate with increasing dilution was observed. Thus, cyclohexanone, chloroform and carbon tetrachloride are rate enhancing solvents for the present system.

The rate enhancing abilities of cyclohexanone and chloromethanes were further verified by measuring R_p at a particular initiator concentration ($[DCAA][DMA] = 10 \times 10^{-4}$ mol^2 dm^{-6} keeping temperature (40°C) and monomer concentration fixed using benzene (an inert additive) as a balancing

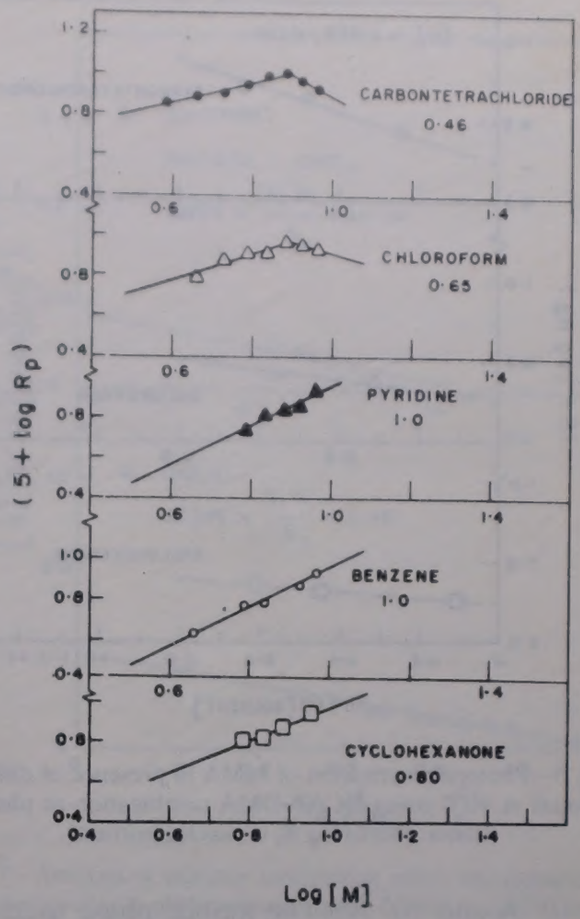

Fig. 4—Photopolymerization of MMA in presence of different solvents at 40°C using DCAA-DMA combination as photoinitiator: Plot of log R_p versus log [M]

solvent in the presence of various concentrations of the active solvents. Related data shown in Fig. 5 clearly indicate that increasing proportions of cyclohexanone, $CHCl_3$ and CCl_4 bring about progressive enhancement of R_p at a fixed [M]. The enhancement of R_p may be due to the abilities of these solvents to increase the R_i, the rate of chain initiation

End group analysis

Positive response to (rhodamine 6G reagent in benzene) dye interaction technique[14,15] for carboxyl end group and UV spectrophotometric data given and discussed elsewhere[2] clearly gave convincing evidence for the incorporation of both DCAA and DMA moieties as end groups in the present polymers.

Molecular weight distribution

The gel permeation chromatographic (GPC) analysis revealed a distribution ratio ($\bar{M}_w/\bar{M}_n$) of 3.12 for a polymer sample prepared at 40°C using 5×10^{-2} mol dm^{-3} of each of DCAA and DMA ($R_p = 1.22 \times 10^{-4}$ mol dm^{-3} s^{-1}). The data were obtained at 25°C on a GPC equipment (Waters Associates) using a combination of styragel columns (10^5

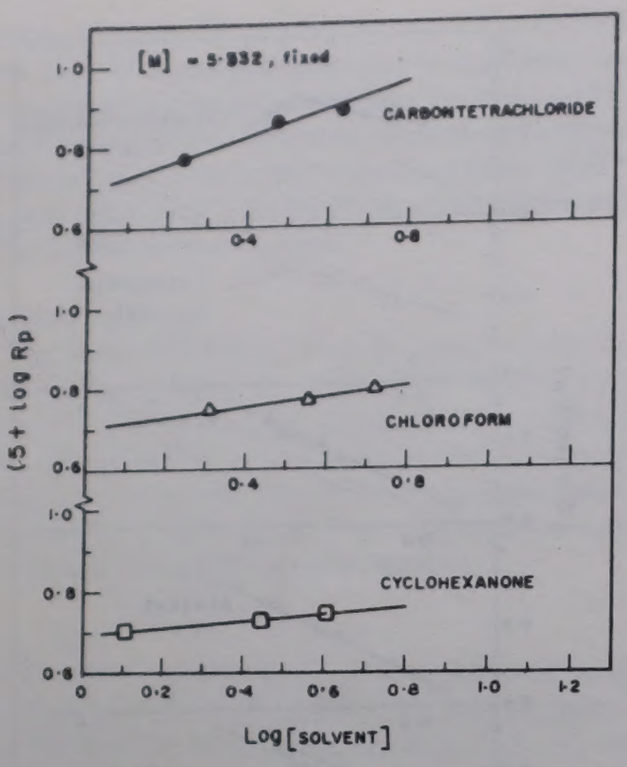

Fig. 5—Photopolymerization of MMA in presence of different solvents at 40°C using DCAA-DMA combination as photoinitiator: Plot of log R_p versus log [solvent]

Å, 10^4 Å and 10^3 Å). The mobile phase used was tetrahydrofuran with a flow rate of 1.5 ml/min.

Discussion

Mechanism

Kinetic data in respect of k_p^2/k_t value, apparent activation energy, inhibitory effect of air (O_2) and benzoquinone and results of end group analysis indicate a radical mechanism. The radical generation process may be considered to follow an initial complexation reaction in situ between DCAA and DMA followed by the photodecomposition of the complex into radicals as depicted in Scheme 1.

Spectrophotometric studies indicate the formation of complex, I from DCAA and DMA when they are mixed together[2].

Analysis of kinetic non-idealities

Low initiator exponent (< 0.5) in each of bulk and solution systems indicates that termination in the present polymerization is significantly initiator dependent. The initiator dependency of the termination process may arise due to (i) primary radical termination characterized by the rate constant k_{prt} and/or (ii) termination by direct reaction with the initiating complex, I via degradative chain transfer characterized by the rate constant k_t'.

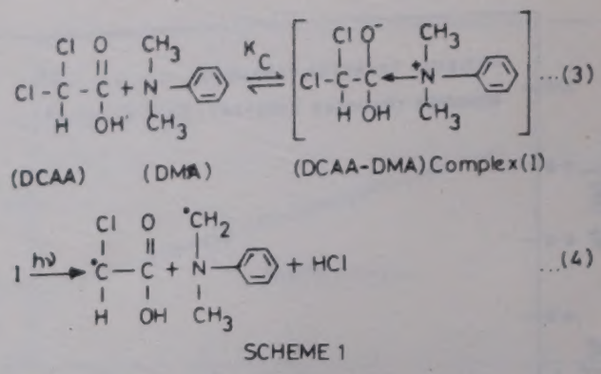

Analysis of primary radical termination

With the assumption that initiator termination by degradative transfer is negligible, Eq. (5) may be used to analyse the primary radical termination effect in the present system[16,17].

$$\log \frac{R_p^2}{[DCAA][DMA][M]^2} = \log(f k_d K_c \cdot k_p^2/k_t) - 0.8684 \frac{k_{prt} R_p}{k_i k_p [M]^2} \quad \ldots (5)$$

where all the terms have their usual significances. A negative slope, obtained for each of bulk and solution (solvent:$CHCl_3$) polymerization of MMA when the left hand side of Eq. (5) is plotted against $R_p/[M]^2$ in each case (Fig. 6) taking data corresponding to the use of different concentrations of DCAA and DMA, indicate measurable occurrence of termination through reaction with primary radicals. The intercept of the plots give the values of fk_dK_c as 2.02×10^{-5} dm^3 mol^{-1} s^{-1} and 2.15×10^{-5} dm^3 mol^{-1} s^{-1} for the bulk and chloroform diluted system respectively. The $k_{prt}/k_i k_p$ value obtained from the slope of the above plot (Fig. 6) is 5.24×10^5 mol sec dm^{-3} for the bulk system and 1.0×10^5 mol s dm^{-3} for the diluted system. The $k_{prt}/k_i k_p$ values show that the primary radical termination effect is more prominent in the bulk system than in the chloroform diluted system.

Analysis of initiator termination via degradative initiator chain transfer

This degradative process may be expressed as

$$M^{\cdot} + I \xrightarrow{k_t'} \text{polymer product} \quad \ldots (6)$$

(initiator termination through degradative chain transfer with no reinitiation)

Now we have,

Rate of initiation, $R_i = 2fk_d[I]$

$$= 2fk_dK_c[DCAA][DMA] \quad \ldots (7)$$

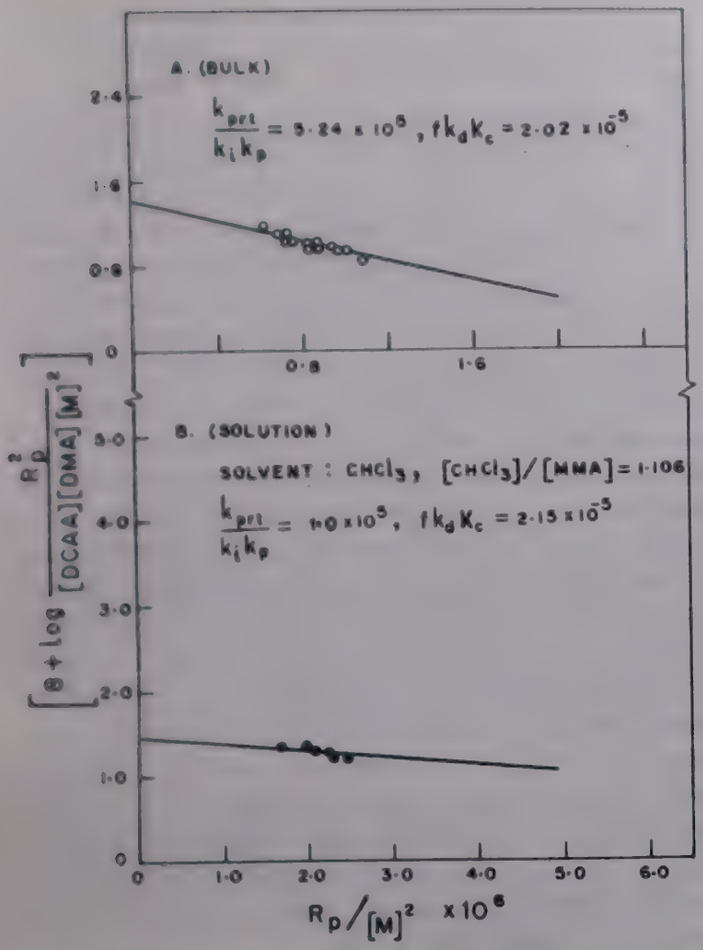

Fig. 6—Analysis of primary radical termination effect in photopolymerization of MMA at 40°C using DCAA-DMA combination as photoinitiator: Plot of $\log (R_p^2/([DCAA][DMA][M]^2)$ versus $R_p/[M]^2$

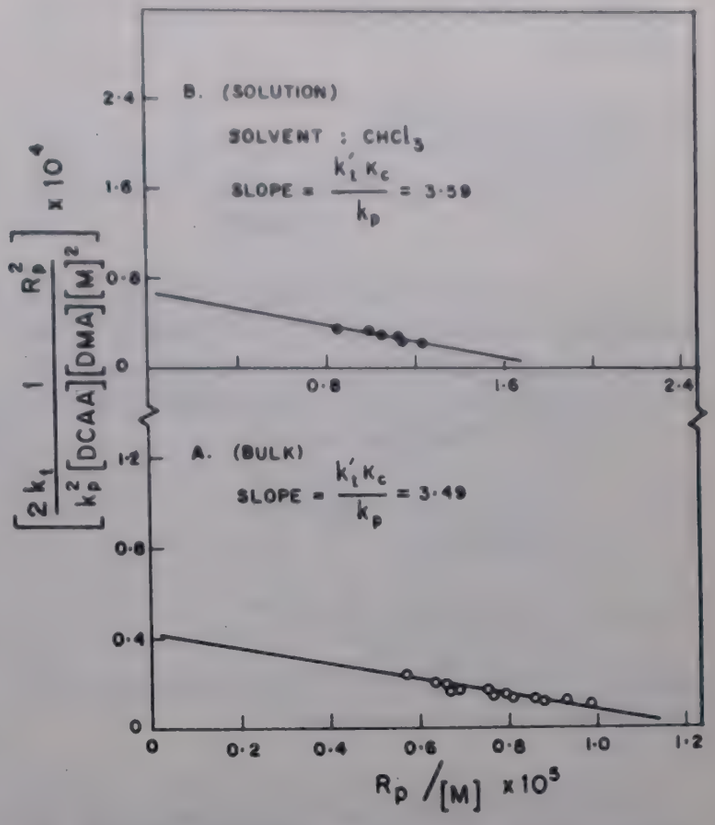

Fig. 7—Analysis of initiator termination effect via degradative initiator transfer in photopolymerization of MMA at 40°C using DCAA-DMA combination as photoinitiator: Plot of $\{2k_tR_p^2/(k_p^2[DCAA][DMA][M]^2)\}$ versus $R_p/[M]$

and considering significant termination by degradative initiator transfer as shown in Eq. (6) along with the usual bimolecular termination, we have:

Rate of termination, $R_t = 2k_t[M^\cdot]^2 + k_t'[I][M^\cdot]$

or, $R_t = 2k_t[M^\cdot]^2 + k_t'K_c[DCAA][DMA][M]$ ... (8)

Elimination of the chain radical concentration term gives

$$R_t = \frac{2k_t}{k_p^2}\cdot\frac{R_p^2}{[M]^2} + \frac{k_t'K_c}{k_p}\cdot\frac{[DCAA][DMA]R_p}{[M]} \quad \ldots (9)$$

At steady state, $R_t = R_i$

Therefore, Eq. (10) may be derived combining Eqs (7) and (9)

$$2\cdot\frac{k_t}{k_p}\cdot\frac{R_p^2}{[DCAA][DMA][M]^2} = 2fk_dK_c - \frac{k_t'K_c}{k_p}\cdot\frac{R_p}{[M]} \quad \ldots (10)$$

Using data for polymerization in the presence of chloroform as a solvent (S), ([S]/[M] = 1.106) and for bulk polymerization ([S]/[M] = zero), the left hand side of Eq. (10) was plotted against $R_p/[M]$ and in each case a straight line with a negative slope was obtained, (Fig. 7) giving a good evidence for chain termination reaction via degradative initiator transfer. The slope of the plot in each gives the value of the initiator termination parameter $k_t'K_c/k_p$; the average value of this parameter is 3.54 $dm^3\ mol^{-1}$. The value of k_dK_c calculated from the intercept is 2.10×10^{-5} $dm^3\ mol^{-1}\ s^{-1}$ for bulk polymerization and the value of the parameter is somewhat higher (3.10×10^{-5} $dm^3\ mol^{-1}\ s^{-1}$) for polymerization in chloroform. The fk_dK_c values obtained here are close to or of the same order of that calculated from Fig. 6 based on the analysis of primary radical termination using Eq. (5).

Analysis of the role of solvents in modifying the initiation step

In order to analyse the role of solvents in influencing the process of initiation, the radical generation step in the presence of a solvent S is described by Eqs (11, 12)

$$I \xrightarrow{k_d} \text{pair of radicals} \quad \ldots (11)$$

$$I + S \xrightarrow{k_{ds}} \text{pair of radicals} \quad \ldots (12)$$

In that case, the overall rate of initiation R_i is expressed as:

$$R_i = 2fk_d[I] + 2f_s k_{ds}[I][S] \quad \ldots (13)$$

$$\text{or } R_i = 2fk_d K_c[DCAA][DMA] + 2f_s k_{ds} K_c[DCAA][DMA][S] \quad \ldots (14)$$

In Eqs (13) and (14), the subscript 's' refers to polymerization in the presence of a solvent (S). The overall rate of termination R_t is given by Eq. (9). Under steady state, $R_i = R_t$ and hence based on Eqs (9) and (14) and rearranging, we have:

$$\frac{2k_t}{k_p^2} \cdot \frac{R_p^2}{[DCAA][DMA][M]^2} + \frac{k_t' K_c}{k_p} \cdot \frac{R_p}{[M]}$$

$$= 2fk_d K_c + 2f_s k_{ds} K_c[S] = k_1 + k_2[S] \quad \ldots (15)$$

where $k_1 = 2fk_d K_c$ and $k_2 = 2f_s k_{ds} K_c$ (solvent modified initiation kinetic parameter).

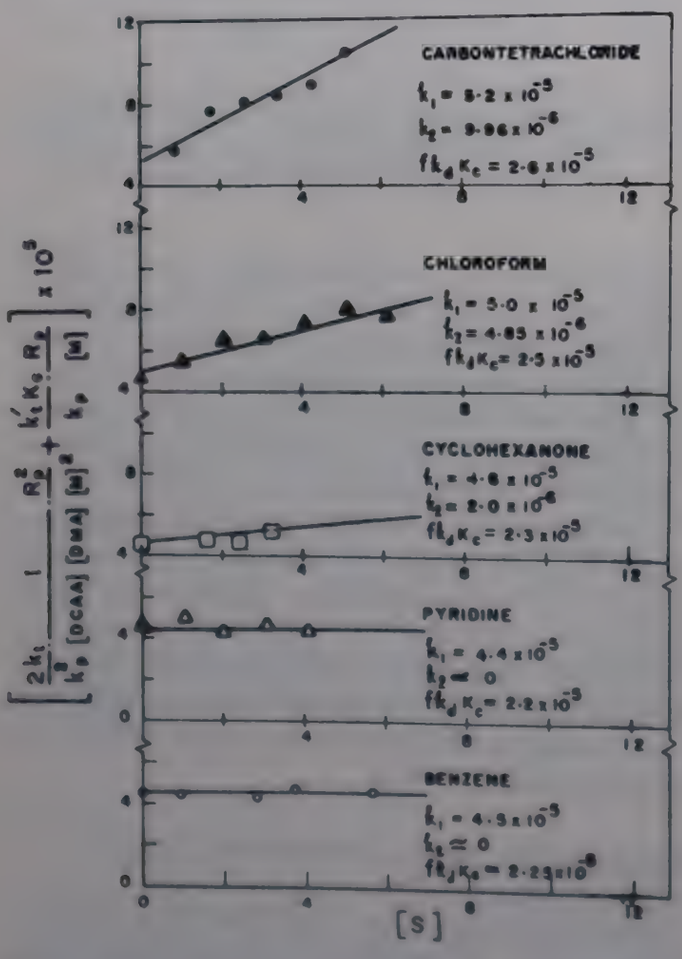

Fig. 8—Analysis of the role of different solvents (S) in photopolymerization of MMA at 40°C using DCAA-DMA combination as photoinitiator. Plot of $[2k_t R_p^2/k_p^2[DCAA][DMA][M]^2 + k_t' K_c R_p/k_p[M]]$ versus [S].

Using the value of the parameter $k_t' K_c/k_p$ as 3.54 $dm^3\ mol^{-1}$ as obtained from Fig. 7 and the R_p values at different [S] for a fixed value of [I], ($[DCAA][DMA] = 10 \times 10^{-4}\ mol^2\ dm^{-6}$), at 40°C, a plot of left hand side of Eq. (15) versus [S] was drawn for each of the solvent systems studied, Fig. 8. Linear plots with negligible slopes are obtained (i.e. $k_2 \approx 0$) for polymerizations in presence of benzene and pyridine which suggest that these two solvents have little influence on the initiation or radical generation step in the (DCAA-DMA) induced photopolymerization. On the other hand, for polymerization in the presence of cyclohexanone, and the chloromethanes such linear plots give significant positive slopes. Cyclohexanone, chloroform and carbon tetrachloride play active roles in influencing the initiation process, the k_2 values given by the slopes are $2.0 \times 10^{-6}\ dm^3\ mol^{-1}\ s^{-1}$, $4.85 \times 10^{-6}\ dm^3\ mol^{-1}\ s^{-1}$ and $9.96 \times 10^{-6}\ dm^3\ mol^{-1}\ s^{-1}$ respectively. The values of the parameter $fk_d K_c$ calculated from the intercept of each plot, made to examine the role of the respective solvents, are close and they average out to about $2.37 \times 10^{-5}\ dm^3\ mol^{-1}\ s^{-1}$. The average value of $fk_d K_c$ obtained from Fig. 8 is mostly in good agreement with those obtained from Fig. 6 based on Eq. (5) and from Fig. 7 based on Eq. (10).

References

1 Akimova Z I, Tsarevskaya M N & Fakilov Y U, *Zh obshch Khim*, 44 (1974) 1613.
2 Ghosh P & Mukherjee G S, *Eur Polym J*, 22 (1986) 103.
3 Ghosh P, Mitra P S & Banerjee A N, *J polym Sci, Polym Chem* Ed, 11 (1973) 2021.
4 Ghosh P & Banerjee A N, *J polym Sci, Polym Chem* Ed, 12 (1974) 375.
5 Riddik J A & Bunger W B, *Techniques of chemistry*, Vol. II. *Organic solvents (Physical properties and methods of preparation)* (Wiley Interscience, New York), 1970.
6 For T G, Kinsinger J B, Mason H F & Schuele E M, *Polymer*, 3 (1962) 71.
7 Ghosh P & Chakraborty S, *J polym Sci, Polym Chem* Ed, 13 (1975) 1531.
8 Ghosh P & Mitra P S, *J polym Sci, Polym Chem* Ed, 15 (1977) 1743.
9 Ghosh P & Mukherjee N, *Eur polym J*, 19 (1983) 493.
10 Ghosh P, Jana S & Biswas S, *J polym Sci, Polym Chem* Ed, 21 (1983) 3347.
11 Ghosh P, Biswas S & Niyogi U, *J polym Sci, Polym Chem* Ed, 24 (1986) 1053.
12 Benson S N & North A M, *J Am chem Soc*, 81 (1959) 1339.
13 Ghosh P & Chowdhury D K, *J polym Materials*, 1 (1984) 82.
14 Palit S R & Ghosh P, *Microchem Tech*, 2 (1961) 663.
15 Palit S R & Ghosh P, *J polym Sci*, 58 (1962) 1225.
16 Ghosh P & Mukhopadhyay G, *J polym Sci, Polym Chem* Ed, 17 (1979) 583.
17 Deb P C, *Eur polym J*, 11 (1975) 31.

Indian Journal of Chemistry
Vol. 31A, February 1992, pp. 77-82

Studies on interaction of cationic dye with bacterial acidic polysaccharide†

A Mitra & A K Chakraborty*
Department of Chemistry, Tripura University, Agartala, Tripura 799 004

Received 22 March 1991; revised 19 August 1991; accepted 10 October 1991

Interaction of acidic capsular polysaccharide isolated from *Klebsiella* K17 with cationic dye pinacyanol chloride has been investigated by spectral measurements, and thermodynamic parameters of the interaction evaluated. The polymer induces metachromasy in the cationic dye and a blue-shift from 600 nm to 500 nm in the visible absorption spectrum of the dye is observed. The spectral changes have been studied during interaction of the dye cations with the polyanions at different polymer/dye molar ratios. The polyanion-dye compound is formed with polymer/dye stoichiometry of 1:1, indicating formation of stacking conformation. The values of thermodynamic constants, enthalpy of complex formation ($\Delta H = -7.02$ kcal mol^{-1}), entropy change ($\Delta S = -6.80$ cal mol^{-1} deg^{-1}) and free energy change (ΔG at 307 K $= -4.98$ kcal mol^{-1}) indicate chromotropic character of the polymer in inducing metachromasy in the cationic dye pinacyanol chloride. Interaction of the polymer with acridine orange dye has also been studied by fluorescence measurements.

Many gram-positive and gram-negative bacteria produce extracellular polysaccharides which surround the bacterium as a capsule. The most interesting and important feature of the capsular polysaccharide is its antigenic character. The highly specific interaction of the antigen with the combining sites on the antibody suggests that the specific antibody conformation dictates conformation of the antigens. Our interest is to understand these conformational characteristics of the antigenic materials in solutions.

Studies on metachromasy of various classes of acidic polysaccharides like polycarboxylates, polysulphates, mucopolysaccharides and different synthetic polyanions with different cationic dyes are available in literature[1-3]. But such investigations on bacterial polysaccharides are rarely made. The present study forms a part of our programme of investigating chromotropic character of the capsular polysaccharides from different strains of *Klebsiella* and *Esch. coli* inducing metachromasy in cationic dyes[4-6].

Materials and Methods

The serological test strain of *Klebsilla* serotype K 17 was obtained from Max-Planck Institute for Immunobiology, Freiburg, West Germany. The strain was checked for agglutination in Difco type-specific antisera. A culture of the strain was grown in nutrient agar medium in big agar plates, harvested, dried, and capsular polysaccharide isolated by phenol-water-Cetavlon method[7]. The polysaccharide was solubilized in phenol-water and the cell-wall lipopolysaccharide was separated by ultracentrifugation. The acidic capsular polysaccharide was isolated from the supernatant by fractional (0.25 ~ 0.06 *M* NaCl) precipitation with Cetavlon. The final product was dialysed against distilled water and lyophilized.

The polysaccharide was hydrolysed with 0.5 *M* H_2SO_4 (20 h, 100°), and the monosaccharides were identified by paper chromatography (Whatman No. 1 paper), using (i) ethyl acetate-pyridine-water (4:1:1) and (ii) ethyl acetate-glacial acetic acid-formic acid-water (18:3:1:4).

Neutral sugars were estimated by GLC of the alditol acetates[8], using a Shimadzu gas chromatograph-GC 16A. Uronic acid was determined colorimetrically[9] in the unhydrolysed product.

Pinacyanol chloride [1-ethyl-2-[3-(1-ethyl-2(1*H*)-quinolylidene)-propenyl] quinolinium chloride] and acridine orange were purchased from Sigma Chemicals Co., USA. Pinacyanol chloride was used as such. However, acridine orange (double salt as $ZnCl_2$) was purified before use.

A stock solution of the dye was prepared in doubly distilled water and kept in dark at 4°C. The stock solution was always prepared afresh though it could be used for a week.

Absorbance of the solution was measured at 400-700 nm employing a Molton Roy spectrophotome-

†Presented at the XVth International Carbohydrate Symposium, 1990, held at Yokohama, Japan.

ter. Concentrations fo the dye and polymer solutions were within the range of 10^{-3}-$10^{-5}M$. Aqueous solution of pinacyanol chloride (1 ml, $1.003\times10^{-5}M$) was added to various volumes of $1.00\times10^{-3}M$ aqueous solution of *Klebsiella* K17 polysaccharide, and total volume of the mixture was made upto 10 ml by adding required volume of distilled water in each case.

Fluorescence of acridine orange dye solution ($1.00\times10^{-5}M$) was measured using a Shimadzu-RF 5000 spectrofluorophotometer. The solutions were excited at 430 nm and fluorescence intensity was measured at 522 nm. Required volume of polymer solution was thoroughly mixed with the dye solution to measure fluorescence spectra at different polymer/dye molar ratios.

Determination of stoichiometry

Stoichiometry of the dye-polymer compound was determined by isolating the metachromatic compound according to the method of MacIntosh[10]. To aliquots of dye solution (10 ml each, $1.003\times10^{-5}M$), increasing amounts of the polymer solution (0.2-2.0 ml, $1.00\times10^{-4}M$) were added, and the contents were thoroughly mixed. An aliquot (10 ml) of the mixture was shaken with petroleum ether (5 ml) for 10 min, the coloured aqueous layer was separated and the colourless organic layer discarded. The process was repeated thrice. The metachromatic dye-polymer compound was thus removed; uncomplexed dye was insoluble in the organic layer. Concentration of free dye was estimated colorimetrically in the aqueous layer. Concentrations of complexed dye were plotted against the moles of polymer added, and stoichiometry of polymer and dye in the metachromatic dye-polymer compound was determined from the point of intersection of the linear curves.

Stoichiometry was also determined by centrifugation method[3]. When the metachromatic solution was centrifuged at 23,000g (11,000 rpm) for 30 min, the dye-polymer compound was sedimented. The supernatant was analysed colorimetrically for the free dye and stoichiometry was then graphically determined.

Reversal of metachromasy[11,12]

The reversal of metachromasy was investigated by measuring absorbance of metachromatic solution (polymer/dye molar ratio, 5.0) at the metachromatic band (μ-band, 500 nm) of the spectra and also at the monomeric band (α-band, 600 nm) of the pure dye solution upon addition of different co-solvents like 1-propanol, ethanol, methanol and urea in increasing amounts (alcohols, 0 ~ 70%; urea, 0 ~ 8 *M*).

Spectrophotometric titration

For carrying out spectrophotometric titration[13], increasing amounts of polymer solution (0.1 ~ 1.0 ml, $1.00\times10^{-4}M$) were added to a fixed volume of the dye solution (0.5 ml, $1.003\times10^{-4}M$) and total volume of the mixture was made upto 10 ml by adding water. Absorbance of the mixtures were measured at the monomeric band (α-band, 600 nm) of the pinacyanol chloride dye solution after thorough mixing. Absorbance versus polymer solution added was plotted, and from the point of intersection of the two linear lines, volume of the polymer soution required for equivalence of the anionic groups of the polymer and the dye cations was measured.

Spectrofluorometric titration

Spectrofluorometric titrations[14] were carried out by adding polymer solution in increasing quantities to a fixed volume of acridine orange solution ($1.00\times10^{-5}M$). The solutions were first excited at 430 nm, and fluorescence intensity measured at 522 nm upon addition of polymer. End point of titration was determined graphically as was done in spectrophotometric titration.

Results and Discussion

Klebsiella K 17 capsular polysaccharide is a heteroglycan consisting of repeating units that contain D-glucose, D-glucuronic acid and L-rhamnose in approximate molar ratio of 1:1:3. The pentasaccharide repeating unit[15] is represented by structure (**1**):

The cationic dye pinacyanol chloride (**2**) belongs to cyanine group of dyes.

Absorption spectra of the pure dye solution and the mixtures containing *Klebsiella* K17 polymer at different polymer/dye molar ratios (P/D = 0 ~ 80)

→4)-β-D-Glcp-(1→2)-α-L-Rhap-(1→4)-α-D-GlcAp-(1→3)-β-L-Rhap(1→

3 ↑ 1

α-L-Rhap

1

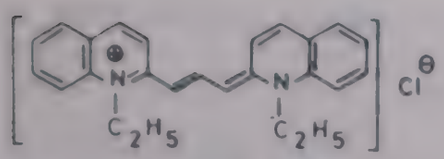

PINACYANOL CHLORIDE

2

are shown in Fig. 1. An aqueous solution of the dye ($1.003 \times 10^{-5} M$) showed two peaks at 600 nm (α-band) and 545 nm (β-band) corresponding to monomeric and dimeric forms of the dye molecule respectively. Upon addition of polymer, intensities of both α and β-bands decreased and a new band (μ-band) appeared at shorter wavelength, indicating metachromasy. At P/D = 10, a distinct μ-band appeared at 500 nm. On further increase of P/D value, the spectral behaviour changed significantly, and the μ-band became stronger with complete disappearance of β-band at 545 nm and α-band at 600 nm. The metachromatic blue shift of 100 nm indicated induction of strong metachromasy in the cationic dye by the polymer.

Stoichiometry of the polymer-dye compound was determined by the isolation method[10] and also by centrifugation method[3]. The results are presented in Fig. 2. Both the methods yielded identical results. It was observed that the metachromatic compound was formed at polyanion: dye cation of 1:1. The results were in good agreement with the reported values[16,17] for interaction of dyes like pinacyanol chloride and acridine orange with synthetic polyanions. The 1:1 stoichiometry of the metachromatic compound indicated that every potential anionic site of the polymer was associated with the dye cation resulting in stacking conformation[3]. It has been suggested that the dye cations are held sufficiently close to the surface of the polyanions to allow them to interact and form aggregates similar to those that were supposedly responsible for the metachromatic behaviour in concentrated dye solutions[18]. Aggregation of such rigid and planar dyes like methylene blue, acridine orange, pinacyanol chloride, etc. on anionic polymers is expected to lead to the formation of a card pack stacking[19] of the individual dye monomers on the surface of the polyanion so that the allowed transition gives rise to a blue-shifted metachromasy.

Figure 3 represents the results of metachromatic titration. Aqueous solution of the cationic dye pinacyanol chloride was titrated spectrophotometrically by adding *Klebsiella* K17 polymer solution. It was observed that intensity of absorbance of the α-band decreased linearly when increasing amount of the polymer solution was added to a fixed volume of the

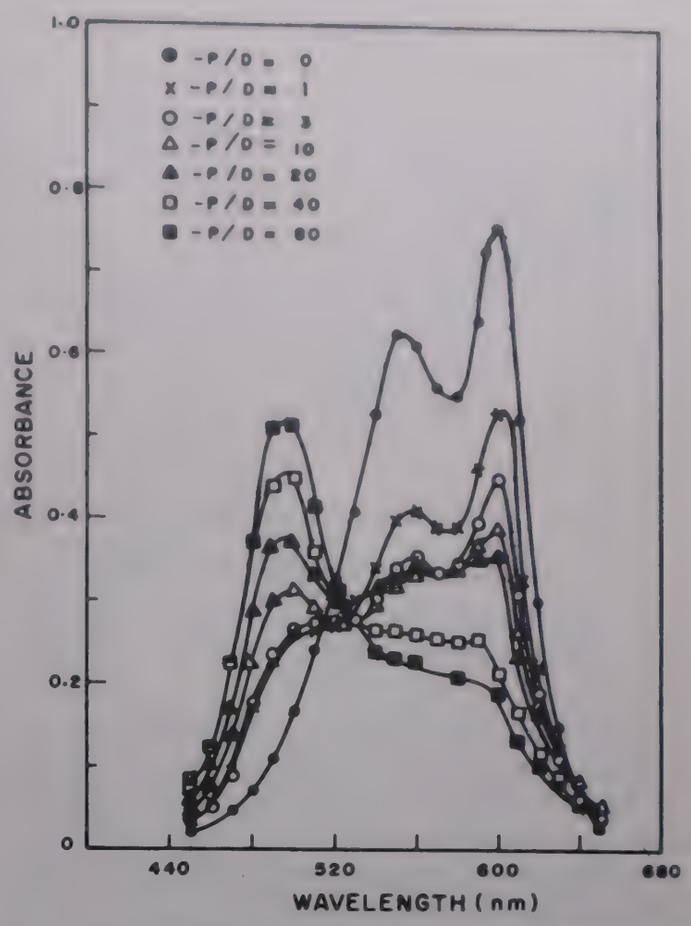

Fig. 1—Absorption spectra of metachromatic solutions; *Klebsiella* K17 polymer/pinacyanol chloride dye at different P/D molar ratios (dye conc., $1.003 \times 10^{-5} M$).

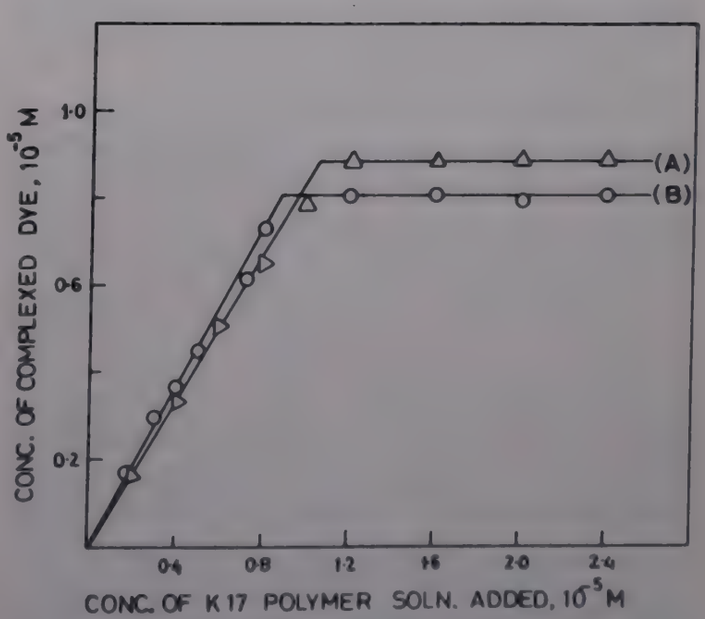

Fig. 2—Stoichiometry of polymer/dye in metachromatic compound obtained by the interaction of pinacyanol chloride dye with *Klebsiella* K17 polymer. [A. MacIntosh method and B. centrifugation method].

dye solution until it became constant. The point of intersection of the linear curves indicated neutralisation point. The stoichiometry of the polyanion-dye compound at the neutralisation point was found to

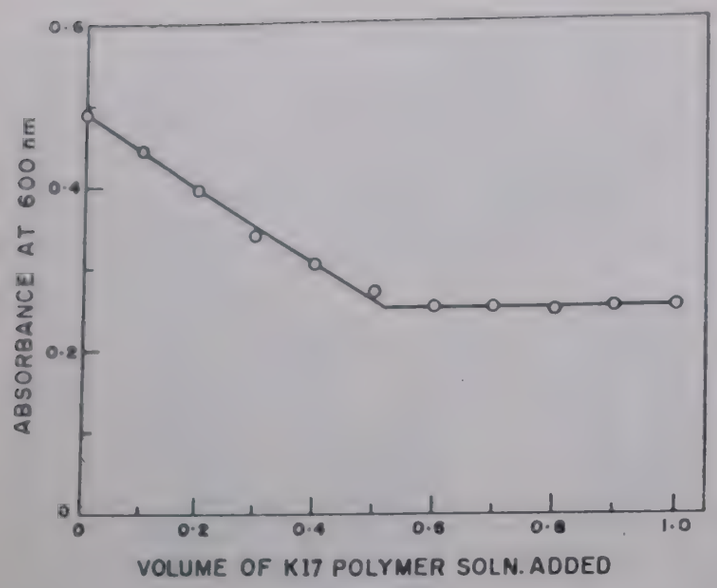

Fig. 3—Metachromatic titration of 0.5 ml of 1.003×10^{-5} *M* pinacyanol chloride dye solution with 1×10^{-5} *M Klebsiella* K17 polymer solution.

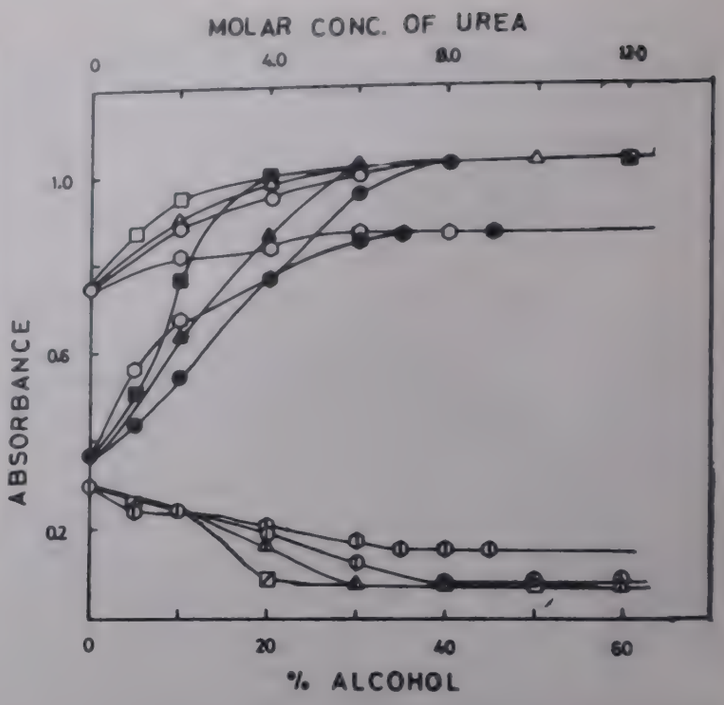

Fig. 4—Reversal of metachromasy in *Klebsiella* K17 polymer/pinacyanol chloride dye upon addition of alcohol and urea [dye conc., 1.003×10^{-5} *M* and P/D = 5].

be 1.02:1.00 which was almost identical to that obtained by isolation and centrifugation methods (Fig. 2). This technique of spectrophotometric titration can be conveniently used to determine either concentration of the polymer sample of known molecular weight or anionic group content of the polyanionic sample of unknown structure in a relatively dilute solution. The equivalent weight of *Klebsiella* K 17 polysaccharide calculated from the results of metachromatic titration was found to be 778 and this was very close to the value 794 obtained from the known structure of the repeating unit.

Results of reversal of metachromasy are shown in Figs 4 and 5. Absorbances at 600 nm (α-band) and 500 nm (μ-band) were measured upon addition of different co-solvents like 1-propanol, ethanol, methanol, and urea to the pure dye solution and also to the dye-polymer mixture (P/D = 5). Absorbance of the metachromatic solution (at 600 nm) increased with increase in alcohol or urea concentration and finally reached a constant value corresponding to that of pure dye solution, indicating complete destruction of the metachromatic compound. Minimum concentration of the co-solvent required for complete reversal of metachromasy was different for different co-solvents, *viz*. 40%, 30% and 20% respectively for methanol, ethanol and 1-propanol. About 7 *M* urea solution was sufficient for complete reversal of metachromasy. Lower curves of Fig. 4 indicated that absorbance at 500 nm decreased gradually and reached constant value at the same corresponding co-solvent concentration. Absorption spectra of metachromatic solution and reversal of metachromasy by 40% methanol are shown in Fig. 5. At this methanol concentration, the pure dye solution gave

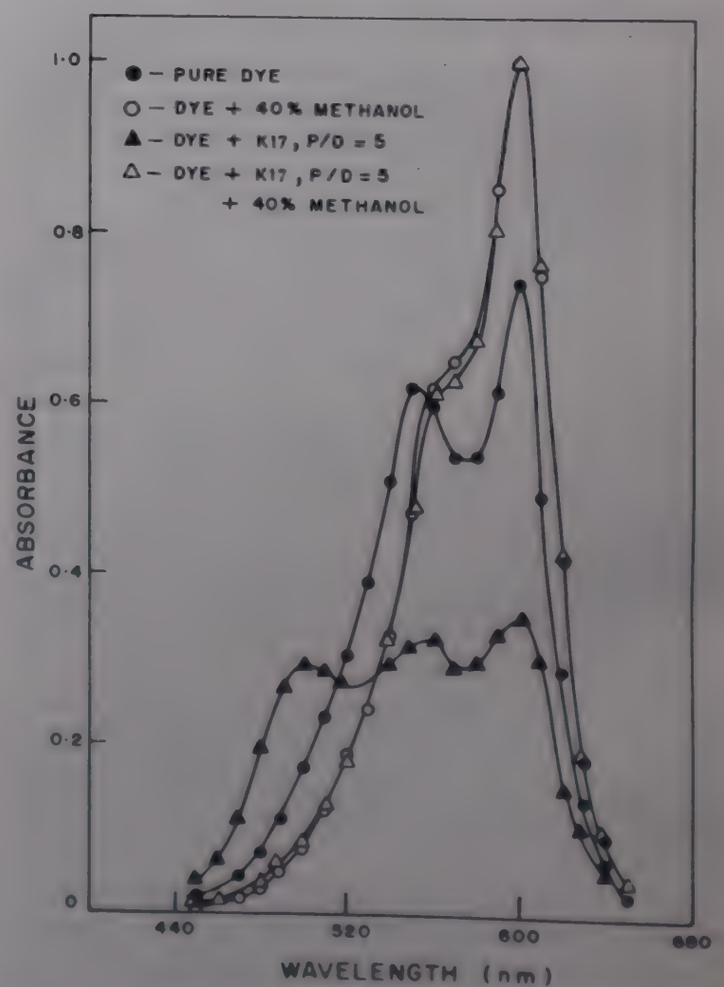

Fig. 5—Absorption spectra of metachromatic solution of *Klebsiella* K17 polymer pinacyanol chloride dye at P/D = 5, and reversal of metachromasy upon addition of 40% methanol at dye conc. 1.003×10^{-5} *M*

a spectrum showing an intense peak at 600 nm. The dimeric β-band of the aqueous dye solution almost completely disappeared. It also appeared that the metachromatic band (μ-band) at 500 nm of the dye-polymer mixture (P/D = 5) disappeared and the spectrum became identical to that of pure dye solution. Progressive destruction of metachromatic compound by alcohols and urea might be attributed to the cleavage of hydrophobic bonds by alcohols and urea in the induction process of metachromasy, leading to the dimerization of the dye as well as metachromatic compound formation. The efficiencies of various alcohols in disrupting matachromasy followed the order: methanol < ethanol < 1-propanol, indicating that reversal became quicker with increasing hydrophobic character of alcohol.

In order to determine thermodynamic parameters of the dye-polymer interaction, absorbance of the pure dye solution (A_0) and that of dye-polymer mixture (A) at μ-band (500 nm) were measured at five different temperatures in the range 31° to 49° ± 0.1°C for different sets of solutions containing varying amounts of polymer (C_S) in a fixed volume of dye solution (C_D). The values of $C_D.C_S/(A-A_O)$ were plotted against C_S when linear relationship was obtained at all the five different temperatures. The results are shown in Fig. 6. From the slope and intercept of the linear relationship, equilibrium constant or interaction constant (K_c) was calculated at each temperature using the following equation[19]:

$$\frac{C_D C_S}{(A-A_O)} = \frac{1}{K_c.L(E_{DS}-E_D)} + \frac{C_S}{(E_{DS}-E_D)L}$$

By plotting log K_c against $1/T$, change in enthalpy of complex formation (ΔH) was calculated from the slope of the linear plot obtained according to van't Hoff equation. Free energy change (ΔG) was obtained from the expression $\Delta G = -RT\ln K_c$ at all the four temperatures. Finally, entropy change (ΔS) was obtained by plotting ΔG values against T according to thermodynamic expression, $\Delta G = \Delta H - T\Delta S$. The slope of the linear plot yielded ΔS. The results are given in Table 1. The value of K_c decreased with increase in temperature and ΔH value of -7.02 kcalmol^{-1} was quite reasonable for such interaction. The negative vlaue of ΔG (-4.98 kcalmol^{-1}) at 307 K was also within the range of a reversible biological process. The negative entropy change, $\Delta S = -6.80$ calmol^{-1}deg^{-1} was also not unreasonable as it indicated more ordered state of the ions due to aggregation. Such negative entropy changes were also reported earlier[2] in the induction of metachromasy in cationic dye, Azure A, by heparin in solution. All these thermodynamic parameters, evaluated on the assumption of simple equilibrium: $D + S \rightleftharpoons DS$ ($K_c = [DS]/[D][S]$) suggested that there was interaction between anionic sites of the polyanion and the dye counterions, resulting in induction of metachromasy.

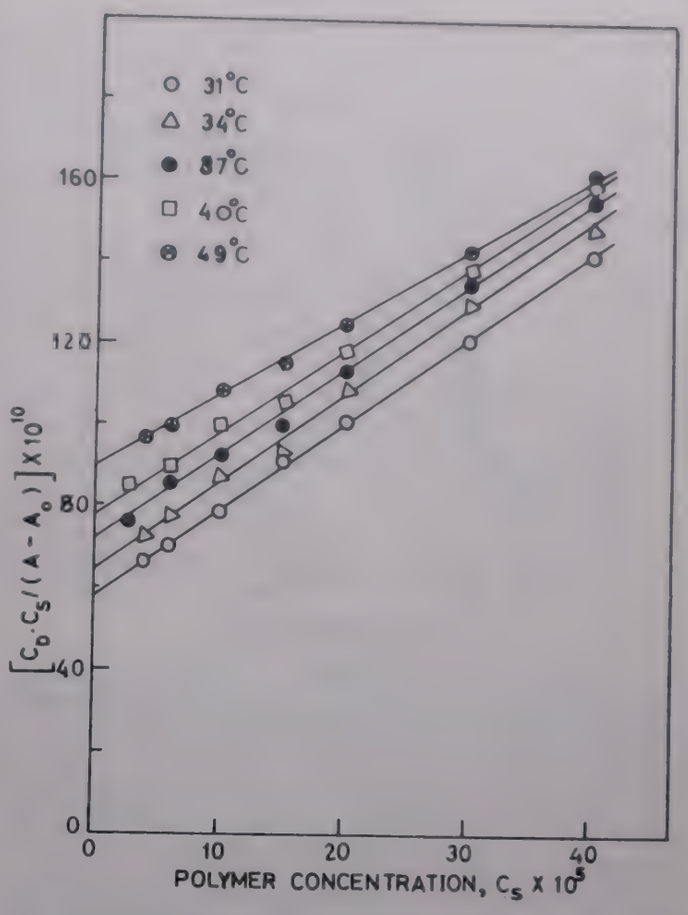

Fig. 6—Plots of function of $C_D.C_S/(A-A_0)$ against C_S in *Klebsiella* K17 polymer-pinacyanol chloride interaction at different temperatures [C_D = conc. of dye in mole/litre, C_S = conc. of polymer in mole/litre (1 mole of polymer referred to the mass of the repeating unit), A_0 = absorbance of initial dye solution, A = absorbance of dye/polymer complex at 500 nm].

Table 1—Thermodynamic parameters for interaction between pinacyanol chloride dye and *Klebsiella* K17 polymer

Temp (K)	K_c	ΔG (Kcal mol^{-1})	ΔH (Kcal mol^{-1})	ΔS (cal mol^{-1} deg^{-1})
304	3707	−4.997		
307	3308	−4.976		
310	2917	−4.947	−7.02	−6.80
313	2628	−4.929		
322	1944	−4.877		

Fluorescence spectral studies were carried out with the fluorescent dye acridine orange which is also a cationic dye. Emission spectra of the dye in the presence and absence of *Klebsiella* K17 polymer are shown in Fig. 7. When the dye solution was excited at 430 nm and emission spectral values were

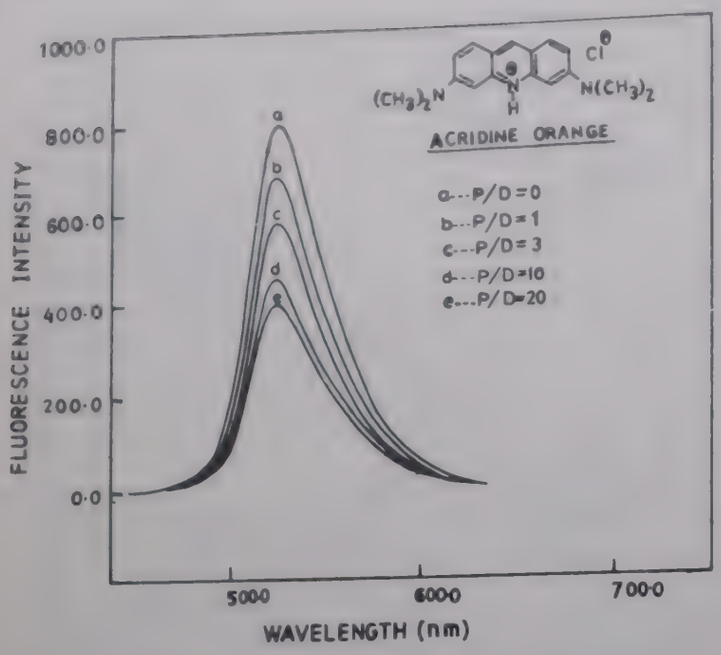

Fig. 7—Emission spectraof acridine orange in presence and absence of *Klebsiella* K17 polymer at different polymer/dye molar ratios; dye conc., $1 \times 10^{-5} M$ [$\lambda_{em} = 522$ nm and $\lambda_{ex} = 430$ nm.]

recorded, the maximum emission peak was observed at 522 nm (λ_{em}). Upon addition of polymer solution to the dye solution, quenching of fluorescence was observed in the dye-polymer mixture (Fig. 7).

The results of fluorescence were also treated with Stero-Volmer equation[20] to study the interaction phenomenon between the dye and polymer molecules in solution. In Stern-Volmer equation, $\phi_f^0 / \phi_f = 1 + K_{SV}[Q]$, ϕ_f^0 is the fluorescence intensity of dye solution and ϕ_f is that of dye-polymer mixture, and [Q] is the concentration of the quencher. In our studies [Q] indicates the molar concentration of the polymer; K_{SV} is known as Stern-Volmer constant. The linear plot of ϕ_f^0/ϕ_f versus polymer concentration indicated that Stern-Volmer equation was satisfied.

The results of spectrofluorometric titration show that when increasing amounts of polymer solution (0-2ml, $1 \times 10^{-5} M$) were added to a dilute solution of dye (1ml, $1 \times 10^{-5} M$), fluorescence intensity decreased gradually, showing quenching of dye due to interaction with the added polymer. The intensity progressively dropped till the amounts of the dye cations and the polyanion were equivalent. After the equivalence point, no significant change in the intensity was observed. Equivalent weight of the polymer was calculated at the equivalence point and it was found to be 794. This method can also be used to estimate the amount of an anionic polymer of known structure in a very dilute solution.

From the results as discussed above, chromotropic character of *Klebsiella* K 17 polysaccharide in inducing blue-shifted metachromasy in cationic dye pinacyanol chloride and quenching of fluorescence in acridine orange, was established.

Acknowledgement

The work was supported by the Department of Science and Technology, Government of India, and one of the authors (AM) acknowledges receipt of a Junior Research Fellowship during the work.

References

1 Stone A L & Bradley D F, *Biochim Biophys Acta*, 148 (1967) 172.
2 Young M D, Philips G D & Balazs E A, *Biochim Biophys Acta*, 141 (1967) 374.
3 Pal M K & Schubert M, *J Histochem Cytochem*, 9 (1961) 673.
4 Chakrabarti A, Nath R K & Chakraborty A K, *Spectrochim Acta*, 45A (1989) 981.
5 Chakrabarti A, Nath R K & Chakraborty A K, *Indian J Biochem Biophys*, 24 (1987) 229.
6 Chakrabarti A, Nath R K & Chakraborty A K, *Indian J biochem Biophys*, 26 (1989) 74.
7 Westphal O & Jann K, *Methods carbohydr Chem*, 5 (1965) 83.
8 Sawardeker J S, Sloneker J H & Jeanes A, *Anal Chem*, 12 (1965) 1602.
9 Bitter T & Muir M H, *Anal Biochem*, 4 (1962) 330.
10 MacIntosh F C, *Biochem J*, 35 (1941) 776.
11 Gummow B D & Roberts G A F, *Makromol Chem*, 186 (1985) 1245.
12 Pal M K & Schubert M, *J Am chem Soc*, 84 (1962) 4384.
13 Gummow B D & Roberts G A F, *Makromol Chem*, 186 (1985) 1239.
14 Pal M K, Ghosh J K & Das S, *Indian J Biochem Biophys*, 26 (1989) 311.
15 Dutton G G S & Folkman T E, *Carbohydr Res*, 80 (1980) 147.
16 Pal M K & Ghosh B K, *Makromol Chem*, 181 (1980) 1459.
17 Pal M K & Schubert M, *J phys Chem*, 65 (1961) 872.
18 Michaelis L, *J phys Chem*, 54 (1959) 5.
19 Rose N J & Drago R S, *J Am chem Soc*, 81 (1959) 6138.
20 Basu S, Gupta A K & Rohatgi-Mukherjee K K, *J Indian chem Soc*, 59 (1982) 578.

Indian Journal of Chemistry
Vol. 31A, February 1992, pp. 83-85

Thionine-triethylamine interactions in mixed solvents

K S Sidhu*, Satbir Singh & Anil Kumar
Department of Chemistry, Panjabi University, Patiala 147 002

Received 9 September 1991; revised and accepted 28 October 1991

Addition of triethylamine (TEA) to thionine (Th^+) solutions in CH_3CN-H_2O (9:1, v/v) and CH_3OH-H_2O (9:1, v/v) solvents leads to shift in absorption maxima from 597 nm to 500 nm and from 600 nm to 515 nm respectively. The spectral changes with various TEA concentrations have isosbestic points at 533 nm and 544 nm. Various types of interactions have been analysed to show that the charge transfer initiated redox disproportionation of the dye does not explain the observed data and the interaction in fact involves 1:1 complexation of the lewis acid/base type with $K = 2.60 \times 10^2$ $mol^{-1}dm^3$ in CH_3CN/H_2O and 0.33×10^2 $mol^{-1}dm^3$ in CH_3OH/H_2O solvent.

Several reports have appeared on the replacement of a normal blue colour of the solution of phenothiazine dyes such as methylene blue (MB^+) and new methylene blue (NMB^+) by a weak pink colour on the addition of amines, phosphines or arsines in polar aprotic solvents[1-4]. Addition of polar protic solvents to the mixtures has been reported to result in the immediate, but not total, reconversion to the original colour. However, in our opinion no satisfactory explanation has been offered for such a reversible change. McKay[1] suggested the formation of Lewis acid(dye)/base (amine) complexes in MB^+ solutions in the presence of strongly basic amines ($pK_b < 5$) and observed that the absorption bands of red form of the dyes in amines have low molar absorption coefficients which was consistent with the interaction of anion at the terminal group in the dye ion whereby one resonant structure of high dipole moment is stabilized at the expense of another equivalent structure. Sheafer and Zimmermann[2] suggested that the colour change is due to a base induced redox disproportionation resulting in the formation of leuco-MB^+ and an oxidised imino form. Hydrolysis of the imino form can demethylate the dye to afford a new coloured species, the basic tautomer of trimethylethionine, whose absorption is blue shifted relative to MB^+. Blue form is regenerated on protonation of the pink dye by an acid or other weak proton donor.

Similar interaction of NMB^+ with triethylamine (TEA) in dry acetonitrile has been explained by a charge transfer initiated redox disproportionation mechanism. However, the results do not completely conform to this mechanism. The dye is not fully converted to the red product at lower amine concentrations, which requires the establishment of some kind of equilibrium to arrive at an acceptable mechanism for such colour changes. The present investigation has been carried out on the interaction of another thiazine dye, thionine (Th^+), with TEA in mixed solvents in order to further analyse the observations and arrive at an acceptable mechanism.

Materials and Methods

Th^+ (Aldrich, USA) was purified by repeated crystallisations from ethanol and its purity was checked on the basis of its UV/visible spectrum in water (Doubly distilled). TEA (Ranbaxy, A.R.) was used as such. Solvents acetonitrile (CH_3CN) and methanol (CH_3OH) were purified by distillation. Stock solutions of the dye were prepared in blackened volumetric flasks. Various spectra were recorded in closed quartz cells (1 cm) with the help of a double beam spectrophotometer (U.V. − 190, Shimadzu, Japan). The absorbance measurements were within the Beer's law limit.

Results and Discussion

Addition of TEA to Th^+ solutions in CH_3CN/H_2O (9:1, v/v) and CH_3OH/H_2O (9:1, v/v) solvents results in blue shift in the absorption maxima from 597 to 500 nm and 600 to 515 nm. The spectral changes with varying TEA concentrations have isosbestic points at 533 and 544 nm respectively for CH_3CN/H_2O and CH_3OH/H_2O solvents as shown in Figs 1 and 2. The charge transfer initiated redox disproportionation mechanism suggested for such spectral shifts in similar systems[2,3] and observed results necessitate the consideration of the processes as given in Scheme 1 for Th^+ and TEA interactions.

On the basis of steady state approximation, Scheme 1 involving equilibrium between steps 1 and 2 (K) and steps 4 and 5 (K'), yields,

$$k_3 KK'/2(k_4 - K'k_5) \times [Th^+][TEA] = [I]^2 \quad \ldots (1)$$

In the event of direct formation of ThH and I from the complex [$Th^+ - - TEA$] without the intervention of $Th^\cdot$ and TEA^+, steady state treatment yields,

$$\sqrt{K'K}[Th^+][TEA] = [I] \quad \ldots (2)$$

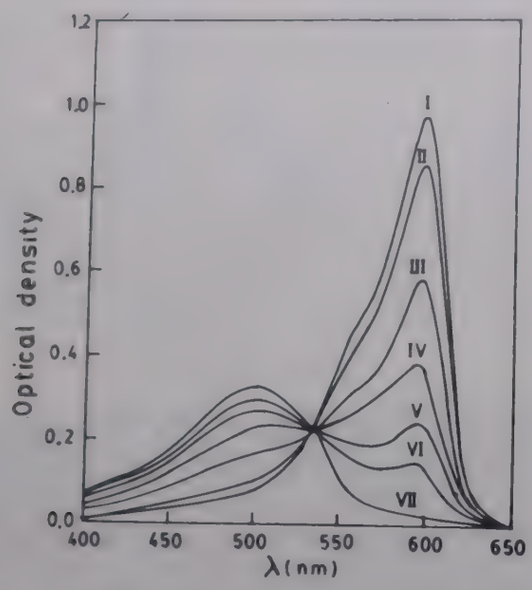

Fig. 1—Spectra of Th^+ at different TEA concentrations {Solvent = CH_3CN/H_2O (9:1, v/v); $[Th^+] = 1.42 \times 10^{-5}$ mol dm^{-3}; curve I for [TEA] = 0 mol dm^{-3}, curve II for [TEA] = 0.0001 mol dm^{-3}, curve III for [TEA] = 0.001 mol dm^{-3}, curve IV for [TEA] = 0.005 mol dm^{-3}, curve V for [TEA] = 0.01 mol dm^{-3}, curve VI for [TEA] = 0.05 mol dm^{-3} and curve VII for [TEA] = 0.1, 0.5, 1.0 and 2.0 mol dm^{-3}}

$$Th^+ + TEA \underset{2}{\overset{1}{\rightleftharpoons}} [Th^+ - - TEA]$$

$$[Th^+ - - TEA] \xrightarrow{3} Th^\cdot + TEA^+$$

$$2\,Th^\cdot \rightleftharpoons ThH + 1\ Imine\ (pink)$$

ThH = leuco-thionine

Imine = 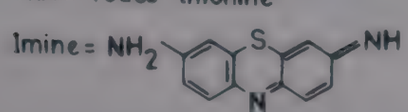

SCHEME 1

Equation (1) predicts a linear plot of [TEA] versus $[I]^2$ at constant $[Th^+]$ with zero intercept while equation (2) predicts linear relatioship between [TEA] and [I]. Such linearities are not observed and hence the observed data rule out the possibility of such chemical interactions in this system.

Here McKay's explanation of lewis acid (dye)/base (amine) complex formation appears to hold good. TEA is a good electron donor and a large number of examples of charge transfer complex formation between TEA and compounds similar to these dyes are known[5-9]. Such interactions have also been reported in Th^+-Fe(II) systems[10,11]. Generally, 1:1 and 1:2 complexes are formed. For the present system the interactions can be:

$$Th^+ + TEA \rightleftharpoons [Th^+ - - TEA],\ 1{:}1\ \text{complex}$$
$$Th^+ + 2\,TEA \rightleftharpoons [TEA - - Th^+ - - TEA],\ 1{:}2\ \text{complex}$$
$$2Th^+ + TEA \rightleftharpoons [Th^+ - - TEA - - Th],\ 2{:}1\ \text{complex}$$

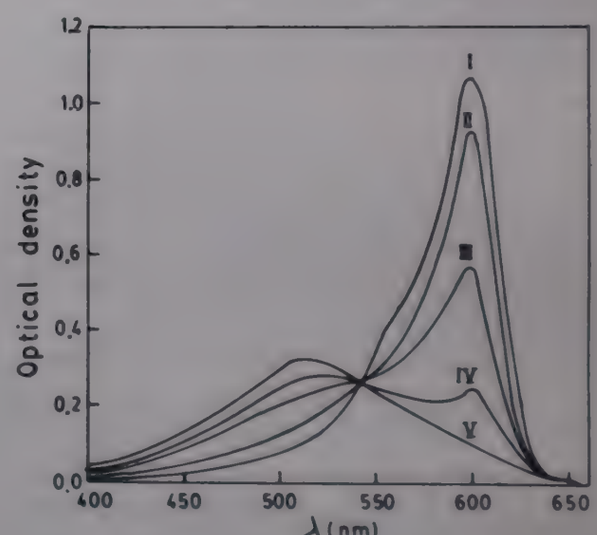

Fig. 2—Spectra of Th^+ at different TEA concentrations. {Solvent = CH_3OH/H_2O (9:1, v/v); $[Th^+] = 1.42 \times 10^{-5}$ mol dm^{-3}; curve I for [TEA] = 0 mol dm^{-3}, curve II for [TEA] = 0.005 mol dm^{-3}. Curve III for [TEA] = 0.05 mol dm^{-3}, curve IV for [TEA] = 0.5 mol dm^{-3} and curve V for [TEA] = 5 mol dm^{-3}.}

Table 1—Calculated values of equilibrium constants for complexation between Th^+ and TEA

Sr. No.	[TEA] (mol dm^{-3})	$K_{1:1} \times 10^{-2}$ (mol dm^{-3})$^{-1}$		$K_{1:2} \times 10^{-4}$ (mol dm^{-3})$^{-2}$		$K_{2:1} \times 10^{-7}$ (mol dm^{-3})$^{-2}$	
		a	b	a	b	a	b
1	5×10^{-3}	2.32	0.31	5.78	0.75	4.71	0.61
2	1×10^{-2}	3.04	—	3.04	—	8.20	—
3	5×10^{-2}	2.30	0.38	0.47	0.62	6.20	1.06
4	1×10^{-1}	2.89	—	0.23	—	3.74	—
5	5×10^{-1}	—	0.30	—	0.08	—	0.48
6	5.00	—	0.34	—	0.02	—	0.08
	Average	2.64	0.33	—	—	—	—

a = CH_3CN/H_2O (9:1, v/v)
b = CH_3OH/H_2O (9:1, v/v)

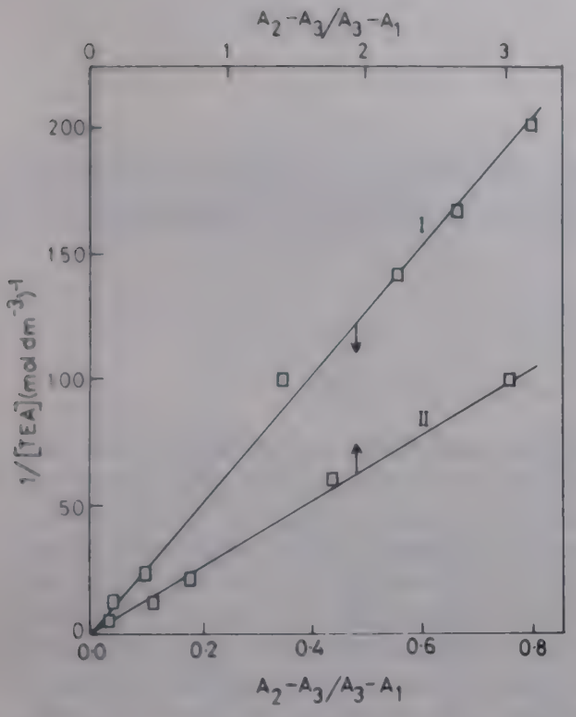

Fig. 3—Plots of results from Eq. (3). [Plot I for Fig. 1 and plot II for Fig. 2]

Equilibrium constants for each of the above possibilities were calculated at various [TEA]'s at constant $[Th^+]$ and these are given in Table 1. The data clearly fit the 1:1 complex case.

The isosbestic points at 533 nm and 544 nm (c.f. Figs 1 and 2) correspond to equal molar absorption coefficients for Th^+ and the complex at these wavelengths. It is apparent that the total concentration of Th^+ and the complex is constant for all the curves and this argument leads to a simple relationship for 1:1 complexation[12,13],

$$1/[TEA] = K \times [Th^+]/[COMPLEX]$$

$$= K \times A_2 - A_3/A_3 - A_1 \quad \ldots (3)$$

where A_1, A_2 and A_3 are the absorbances of Th^+ in the absence of TEA, complex (Th^+ in the presence of excess TEA) and mixture solution at 597 nm and 600 nm for CH_3CN/H_2O and CH_3OH/H_2O respectively. Plots of $1/[TEA]$ versus $A_2 - A_3/A_3 - A_1$ are shown in Fig. 3. These are good straight lines with zero intercept. The slopes of straight lines give $K = 260\,mol^{-1}dm^3$ and $33\,mol^{-1}dm^3$ for CH_3CN/H_2O and CH_3OH/H_2O solvents respectively, which is in good agreement with the results of Table 1. The present analysis and data thus support the formation of 1:1 complex.

Acknowledgement

Financial assistance from the UGC, New Delhi to one of the authors is gratefully acknowledged.

References

1 McKay R B, *Nature*, 210 (1966) 296.

2 Shaefer P C & Zimmermann W D, *Nature*, 220 (1968) 66.

3 Eaton D F, *Dye sensitized photopolymerisation*, in Advances in photochemistry (Interscience Publishers-John Wiley and Sons, New York) 13 (1986) 469.

4 Rust J B, *U S Patent* 3, 573 (1969) 922.

5 Girgis M M, Yanni A S & Khalil Z H, *Indian J Chem*, 29A (1990) 138.

6 Dwivedi P C, Sharma N, Rathi R S & Pandey S D, *Indian J Chem*, 29A (1990) 381.

7 Itoha K, Tajma Y, Tenbata M & Dialchi Y, *Diagaku Kenkyu Nenpo*, 18, (1987) 17.

8 Achar B N & Krishnaswamy M V, *Indian J Chem*, 29A (1990) 480.

9 Roy M, Mukherjee A K & Seal B K, *Indian J Chem*, 29A (1990) 205.

10 Singal G S & Rabinowitch E, *J phys Chem*, 71 (1968) 3347.

11 Ainsworth S, *J phys Chem*, 64 (1960) 715.

12 Alan Vincent, *Education in Chem*, 27 (1990) 107.

13 Long J R & Drago R S, *J chem Educ*, 59 (1982) 1037.

Indian Journal of Chemistry
Vol. 31A, February 1992, pp. 86-90

Kinetics of hydrogen evolution reaction on bright platinum electrode in aqueous dimethylformamide solutions by cyclic voltammetry

Subrata K. Ray, Jayati Datta & Kiron K Kundu*

Physical Chemistry Laboratories, Jadavpur University, Calcutta 700 032, India

Received 6 May 1991; revised 17 October 1991; accepted 15 November 1991

Kinetic behaviour of hydrogen evolution reaction (HER) has been studied on bright platinum electrode in aqueous mixtures of 0, 25, 50, 75, 90 and 100 wt% N,N-dimethylformamide (DMF) from both HCl and $HClO_4$ solutions by cyclic voltammetry under varying sweep rates [500-1 mVs^{-1}] in the cathodic potential region of 0-1000 mV. The cyclic voltammograms are characterized by single cathodic and the corresponding anodic peaks and are found to be quasi-reversible in nature. The relevant kinetic parameters like the diffusion coefficient (D_R) of the reductant and the rate constant (k_s) (based on apparent area of the electrode) have been derived using the formulations of Shain and Nicholson. The values of D_R and k_s in aq. DMF mixtures decrease from that in pure water due to possible increased protophilicity of DMF-water mixtures which hinders the solvated H^+ ions to approach the electrode surface for undergoing HER.

As a part of our studies on electrocatalytic behaviour of different electrodes with a view to developing a desirable reversible hydrogen electrode (RHE) suitable in some aquo-organic solvents, in a previous paper[1] we have reported the kinetics of hydrogen evolution reaction (HER) on a bright platinum (Pt) electrode in aqueous mixtures of ACN from both HCl and $HClO_4$ solutions using cyclic voltammetry. With a view to examining the feasibility of RHE in aqueous DMF mixtures similar studies have now been extended to the aq.DMF mixtures of different compositions with HCl and $HClO_4$ (~ 0.001 mol dm^{-3}) serving as the electrolytes and 0.1 mol dm^{-3} $NaClO_4$ as the supporting electrolyte. The kinetic parameters have been evaluated employing Nicholson's formulations[2] applicable to the quasi-reversible systems as observed in the present study. The observed kinetic parameters have been interpreted in terms of the relative difficulties of diffusion of solvated H^+ species from bulk to the electrode surface and the subsequent fast charge transfer across the interface forming adsorbed H atoms followed by desorption of the formed hydrogen molecules in the gaseous state.

Materials and Methods

Dimethylformamide (DMF; AR, SD) was dried over neutral aluminium oxide (Sisco Res. Lab., India) for a few days followed by fractional distillation under reduced pressure, collecting the middle fractions only. Hydrochloric acid and $HClO_4$ (both E. Merck) were used for preparing electrolyte solutions. The supporting electrolyte $NaClO_4$ (E. Merck) was dried *in vacuo*.

The working acid solutions (conc. range 1 to 8×10^{-3} mol dm^{-3}) containing $NaClO_4$ (0.1 mol dm^{-3}) were prepared in aq.DMF mixtures containing 0, 25, 50, 75, 90 weight %DMF. In pure DMF however tetraethylammonium perchlorate (GFS Chemicals, USA) was used as the supporting electrolyte. Water content resulting from 1 to 8×10^{-3} mol dm^{-3} HCl or $HClO_4$ solution was taken to be negligibly small. Working solutions were purged with pure N_2 gas presaturated with the respective solvent for about 20 min to remove dissolved oxygen. The cell used was of conventional type[3] with three-electrode assembly in one compartment. A bright Pt-foil [4 cm^2 geometric area (A)] and a bright Pt-wire (A = 0.2 cm^2), both pretreated by usual procedures[4], were used as the counter electrode and the working electrode respectively. The reference electrode employed was a doubly jacketted aqueous saturated calomel electrode[3], SCE(w) (Fischer, E 6 A).

Measurements were made employing a set up consisting of a Standard Potentiostat (Wenking, model VSG 72) and a Houston Omnigraphic (model 2000) x-y recorder. The potential range employed was from 0 to − 1 V and the voltage sweep rates (v) used were in the range of 0.5 to 0.002 Vs^{-1}.

In view of the fact that the products of the cathodic reduction of H^+ ions are M-H and thence H_2 molecules, and some of which are likely to get desorbed, the constancy of E_p as well as $i_{p,c}/i_{p,a}$ values

Table 1—Cyclic voltammetric parameters, E_p (mV) and i_p (mA cm^{-2}) of HER on bright Pt under different scan rates and the evolved D (cm^{2}s^{-1}) of H_3O^+ and the rate constant k_s (cms^{-1}) in some aqueous mixtures of DMF at 25°C

		DMF (wt%)													
		Water		25		50		75		90		95	99	Pure DMF	
Scan rate (Vs^{-1})	Parameter	HCl 3.71 mM	$HClO_4$ 3.58 mM	HCl 2.46 mM	$HClO_4$ 6.58 mM	HCl 2.33 mM	$HClO_4$ 6.35 mM	HCl 3.23 mM	$HClO_4$ 7.70 mM	HCl 5.52 mM	$HClO_4$ 5.87 mM	HCl 5.89 mM	$HClO_4$ 6.18 mM	HCl 5.94 mM	$HClO_4$ 6.65 mM
0.5	$-E_p$	495	495			550			525			540			
	i_p	5.21	5.02			1.24			2.61			1.14			
0.4	$-E_p$	485								525	460	522		570	
	i_p	4.96								0.89	0.88	1.0		1.76	
0.3	$-E_p$	480	485	515	575	520	625	590	510	515	450	513	450	555	440
	i_p	4.54	4.31	1.65	3.17	1.07	1.79	0.85	2.10	0.85	0.74	0.88	1.37	1.61	1.79
0.2	$-E_p$	475	480	505	565	510	615	570	505	500	440	508	440	530	435
	i_p	4.04	3.61	1.40	2.61	0.87	1.46	0.71	1.80	0.72	0.57	0.72	1.12	1.18	1.49
0.1	$-E_p$		470	500	550	500	605	550	495	485	430	494	435	510	430
	i_p		2.96	1.01	2.02	0.62	1.07	0.53	1.26	0.55	0.38	0.54	0.81	0.99	0.98
0.05	$-E_p$	460	470	500	545	495	600	525	485	470	425	476	430	485	425
	i_p	2.33	2.54	0.74	1.51	0.43	0.79	0.36	0.92	0.38	0.31	0.39	0.62	0.71	0.67
0.03	$-E_p$	455	465	500	545	495		515	485	465	410	471	425	475	420
	i_p	1.91	2.09	0.56	1.21	0.36		0.28	0.75	0.29	0.29	0.30	0.56	0.60	0.65
0.02	$-E_p$	455	465	500	545	495	600	505	485	460	410	462	420	460	420
	i_p	1.68	1.99	0.48	1.03	0.29	0.62	0.22	0.62	0.23	0.28	0.24	0.45	0.47	0.52
0.01	$-E_p$	455	460	500	545		600	490	485	450		448	420	450	420
	i_p	1.32	1.40	0.38	0.82		0.49	0.15	0.44	0.15		0.16	0.33	0.33	0.40
0.005	$-E_p$		460					480	485	450		425	420	440	420
	i_p		1.12					0.09	0.38	0.10		0.13	0.24	0.26	0.36
0.003	$-E_p$		460					480				405			
	i_p		1.01					0.06				0.1			
0.002	$-E_p$		460					480				405		440	
	i_p		0.91					0.04				0.08		0.20	
	$D_{H^+} \times 10^6$	23.9	32.8	3.1	2.1	1.2	0.7	0.1	0.4	0.2	0.2	0.2	0.3	0.6	0.4
	$k_s \times 10^3$	5.3	9.3	4.8	3.1	2.5	1.8	0.4	1.4	0.3	0.6	0.2	0.8	0.5	0.9

with scan rates was not maintained in these cases. But the approximate constancy of $E_{p,c}$ values at the lower scan rates especially below 20-10 mVs^{-1} could be taken as examples of quasi-reversible character in all the compositions.

Results

Figure 1 represents some typical cyclic voltammograms (CVG s) at different scan rates for the electrochemical process: $H^+_{solv} + e^-(M) = (1/2)H_2(g)$ as observed on M = bright Pt surface in different DMF-water mixtures. The CVG s are characterized by single cathodic peak with peak potential $E_{p.c}$ and the corresponding anodic peak with peak potential $E_{p.a}$ in all the solvents in the potential range of 0 to −1000 mV indicating that HER follows an identical mechanism in each case. Table 1 presents the cyclic voltammetric parameters like $E_{p.c}$ and the corresponding cathodic peak currents $i_{p.c}$ at different scan rates in different DMF-water mixtures. The constancy of $E_{p.c}$ with scan rates at low sweep rates $< 20\ mVs^{-1}$ and their reasonable variation at higher scan rates are indicative of the quasi-reversible nature of CVG s in all aq.DMF mixtures.

At low sweep rates where reversibility persists, the values of diffusion coefficients (D_R) of the reductant $(H^+)_{solv}$ were derived from the slopes of the linear plots of $i_{p.c}$ versus $v^{1/2}$ as expected from Shain and Nicholson's expression[1,2], for reversible peak $(i_{p.c})_{rev}$ on the apparent area (see Eq. 1).

$$(i_{p.c})_{rev} = 0.269 n^{3/2} C_R D_R^{1/2} v^{1/2} \quad \ldots(1)$$

In Eq. 1 the various terms have their usual significance. Typical i_p versus $v^{1/2}$ plots for HER in differ-

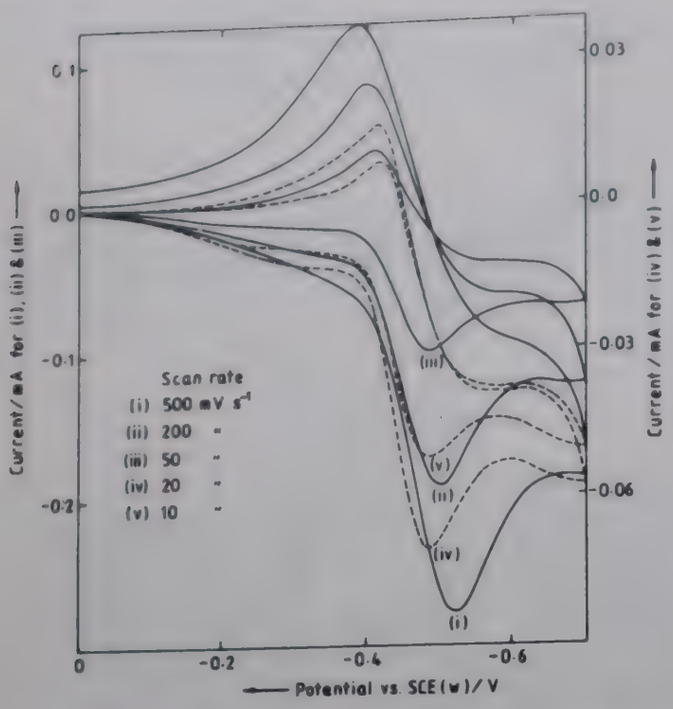

Fig. 1—Typical cyclic voltammograms at different scan rates of HER with $HClO_4$ solution in 75 wt% DMF on a bright platinum electrode at 25°C

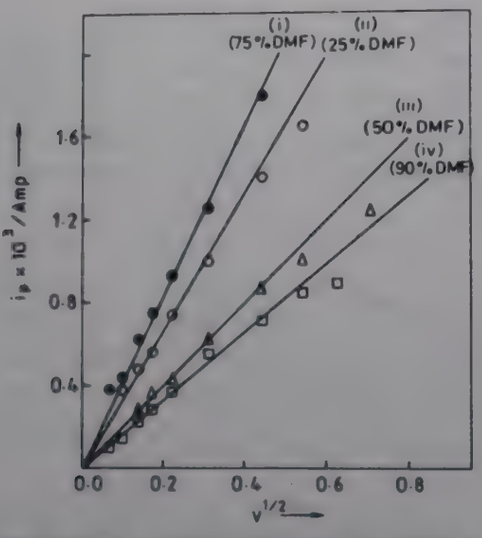

Fig. 2—Some typical i_p versus $v^{1/2}$ plots for HER in aqueous DMF mixtures for $HClO_4$ (i) and HCl [(ii), (iii) and (iv)] at 25°C

ent aq.DMF mixtures are presented in Fig. 2 and D_R values are presented in Table 1.

The values of rate constant (k_s) of the reaction on the unit apparent area of Pt surface were obtained, as before[1], using Shain and Nicholson's expression[2] for the reversible and irreversible peak potentials

$$(E_{p,c})_{rev} = E_{1/2} - 1.1RT/nF \quad \ldots(2)$$

$$(E_{p,c})_{irrev} = E_{1/2} - b[0.52 - (1/2)\log b/D_R - \log k_s] - (b/2)\log v \quad \ldots(3)$$

where $E_{1/2}$ is the half-wave potential of redox reaction and 'b' is the Tafel slope being equal to $RT/\alpha nF$

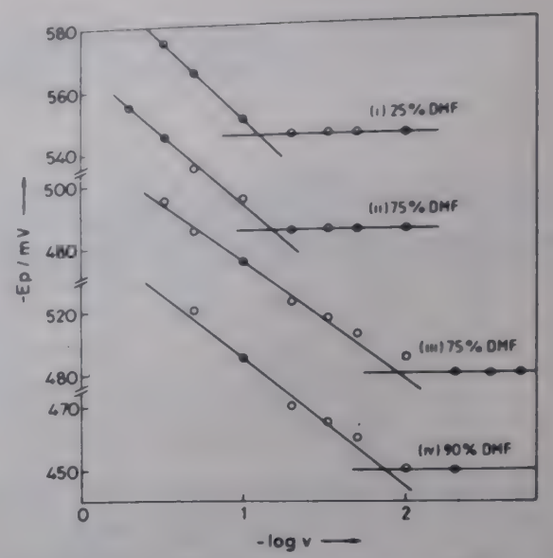

Fig. 3—Some typical $-E_p$ vs $-\log v$ plots for HER on bright Pt in aqueous DMF mixtures for $HClO_4$[(i) and (ii)] and HCl[(iii) and (iv)] at 25°C

where α is the transfer coefficient. Some typical plots of E_p vs log v are presented in Fig. 3. The values of (b) were obtained from the slopes of the observed linear plots in Fig. 3 in the irreversible region. The desired values of rate constant k_s were evaluated as before[1] by combining Eqs (2) and (3) at sweep rate $v = v_c$ where transformation from reversible behaviour to the irreversible one occurred, i.e. from the point of intersection of the plots of $E_{p,c}$ versus log v in reversible and irreversible region so that

$$E_{1/2} - 1.1RT/nF = E_{1/2} - b[0.52 - (1/2)\log(b/D_R) - \log(k_s)] - (b/2)\log v_c \quad \ldots(4)$$

The k_s values were therefore obtained using Eq. (5)

$$\log(k_s) = 0.52 - (1/2)\log(b/D_R) + (1/2)\log v_c - 1.1RT/bnF \quad \ldots(5)$$

The values of k_s so obtained are presented in Table 1.

Discussion

From Table 1 it appears that D_R values in various aq.DMF mixtures decrease by about an order as compared with that in water, which is found to be more or less in agreement with the literature value[5]. The profiles of D_R as well as k_s versus solvent composition are compared with those of ACN-water mixtures reported earlier[1] in Fig. 4. It appears that while D_R values in DMF-water mixtures decrease sharply at low percentage of DMF, it levels off at higher content of DMF. The same in ACN-water mixtures however decrease more or less monotonically. Seemingly, the diffusion of H^+_{solv} in aqueous DMF mixtures is hindered by the possible formation of large sized solvated H^+, i.e. (H^+_{solv}), due to

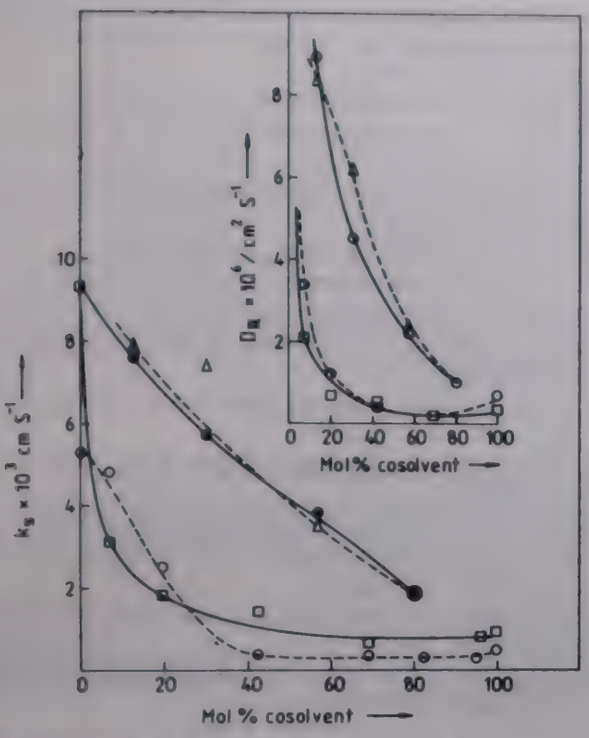

Fig. 4—Variation of k_s and D_R (inset) values with composition for HER in aqueous mixtures of DMF [⊙ HCl and □ $HClO_4$] and ACN [Δ HCl and ⊕ $HClO_4$] at 25°C

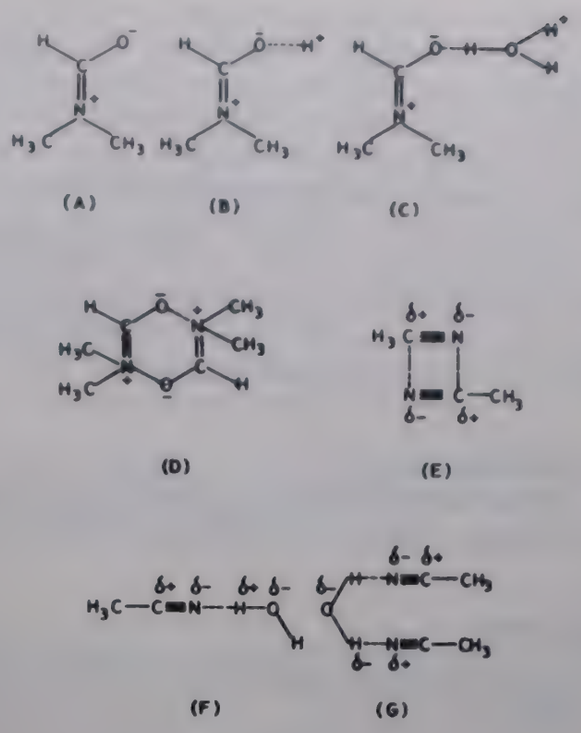

larger protophilicity[6] of DMF molecules having the possible zwitterionic form (A) which helps formation of the hydrates[7,8] either (B) or (C) in its aqueous mixtures. The increased basicity of aqueous DMF mixtures is also evident from the observed negative magnitudes of transfer free energies of H^+, $\Delta G_t^0(H^+)$[9,10]. The observed levelling off of D_R-composition profiles in aq.DMF mixtures having higher DMF percentage is seemingly due to the superimposed effects of the gradual desolvation of $(H^+)_{solv}$ because of increased aproticity of the solvents which arises from the possible formation of $(DMF)_2$ clusters (D). This is evident not only from the upward trend of $\Delta G_t^0(i)$-composition profile of H^+ (refs 9, 10) but also from the sharp rise of $\Delta G_t^0(i)$ of the anions like Cl^-, Br^-, I^- (ref. 10) and OH^- (ref. 11).

In the case of ACN-water mixtures, despite intrinsic protophobicity of ACN molecules because of the possible formation of $(ACN)_2$ dimers like (E), the possible formation of H-bonded ACN-H_2O(F) and $(ACN)_2$-H_2O(G) complexes in its aqueous mixtures, H^+ is likely to be solvatd by the O centres with negative formal charges of the complexes (F) and (G) which are seemingly responsible for the observed monotonic decrement of D_R values with increase in the proportion of ACN in aq.ACN. The effect of aproticity due to the $(ACN)_2$ aggregates (E) on D_R values does not however seem to be that significant as in the case of DMF-water mixtures. The values of rate constant (k_s) in Table 1 and the k_s-composition profiles in Fig. 4 also suggest that these are having more or less similar trends as that of D_R values in the respective solvent systems. The rate of HER which is fairly facile in pure H_2O, becomes increasingly sluggish with increase in the proportions of both the cosolvents. As is expected for quasi-reversible reactions, this behaviour of k_s may be attributed partly to the behaviour of D_R and subsequent quantum tunnelling[12] of the reductant (H^+) and partly to the effectively free uncovered fraction $(1-\theta_s)$ of the Pt electrode, where θ_s is the fraction of the surface covered by the solvent molecules, besides the intrinsic catalytic activity of Pt. Since the polarisability (α_s) and dipole moment (μ_s) of the solvent molecules are likely to guide θ_s (ref. 13) values and their values for the three solvent molecules H_2O, ACN and DMF are 1.44, 4.41 and 7.90 Å^3 (ref. 13) and 1.86, 3.44, 3.86 D (ref. 14) respectively, it is expected that θ_s values will have the order H_2O > ACN > DMF.

Since the intrinsic catalytic activity of the common Pt electrode surface is independent of solvent, it remains the same in all the solvents. Also, the solvated radii of the reductant $(H^+)_{solv}$ dictating the diffusion coefficient and the capability of quantum tunnelling for the charge transfer reaction across the interface in these solvents are of the same order. So, it appears that the rate constant k_s for HER in the aqueous DMF and ACN mixtures are in accord with what is expected from the relative solvation of the reductant $(H^+)_{solv}$ as well as the relative $(1-\theta_s)$ values in these solvents. The difference in D_R or k_s values resulting from HCl and $HClO_4$ solutions in

each of the cosolvent may be taken to be fairly small and hence seemingly insignificant. The apparent differences in k_s values in aqueous DMF may possibly be due to the effect of larger specific adsorption of Cl^- as compared to that of ClO_4^-, if any, in these aquo-organic solvent systems as in pure water[12].

Thus the present results show that as in the case of aqueous mixtures of ACN, the electrocatalytic activity of bright Pt decreases in aqueous DMF mixtures also and it cannot be used as RHE in pure DMF as well as in its aqueous mixtures.

Acknowledgement

Thanks are due to the CSIR, New Delhi for financial assistance under an EMR-II Research Scheme.

References

1 Ray S K, Talukdar H & Kundu K K, *Bull Electro Chem*, 6(5) (1990) 557.

2 Gileadi E, Kirowa-Eisner E and Pencner J, *Interfacial electrochemistry—an experimental approach* (Addison-Wesley Massachusetts) (1975).

3 Gritzner G, *J electroanal Chem*, 144 (1983) 259.

4 *Reference electrodes*, edited by D J G Ives & C Janz (Academic Press, London) (1961).

5 Atkins P W, *Physical chemistry* (Oxford University Press, Oxford) (1988) p. 836.

6 Kolthoff I M, *Pure appl Chem*, 25 (1971) 305.

7 Rohdewald P & Moldner M, *J phys Chem*, 77 (1973) 373.

8 Davisser C & Somsen G, *Z phys Chem*, 92 (1974) 159.

9 Smits R, Massart D L, Julliard J & Morel J P, *Electrochim Acta*, 21 (1976) 431.

10 Das K, Das A K & Kundu K K, *Electrochimica Acta*, 26 (1981) 479.

11 Mandal U, Bhattacharya S & Kundu K K, *Indian J Chem*, 24A (1985) 191.

12 *Modern electrochemistry* by J O'M Bockris & A K N Reddy, vol 2 Chap 10 (Plenum Press, New York) (1970) and the relevant references therein.

13 Bhattacharya S & Kundu K K, *Bull chem Soc Japan*, 67 (1990) 1489.

14 Engberts J B F N in *Water—a comprehensive treatise* edited by F Franks, vol 6 (1976) p 151.

Indian Journal of Chemistry
Vol. 31A, February 1992, pp. 91-96

Kinetics and mechanism of oxidation of thiocyanate ion with peroxomonophosphoric acid

Dilip Kumar Mishra, T Peter Amala Dhas, Pankaj Bhatnagar & Y K Gupta*
Department of Chemistry, University of Rajasthan, Jaipur, India

Received 9 July 1991; revised 7 October 1991, accepted 28 November 1991

Thiocyanate and peroxomonophosphoric acid (pmpa) react to give H_3PO_4 and HCN in the *p*H range 3.67 to 10.6. Kinetics of the reaction has been studied in acid perchlorate, acetate, phosphate and borate buffer media. The different rate laws have been deduced and suitable mechanism proposed.

A few kinetics studies on the oxidation of organic compounds[1] with peroxomonophosphoric acid (pmpa) and still fewer on inorganic compounds[2-4] have shown that there is nucleophilic attack of the reducing substance on the peroxide linkage. However, in the case of oxidation of As(III)[5], the same behaviour is true upto *p*H 3 and thereafter the trend is reversed. In addition to this a tautomeric equilibrium involving an active form of H_3PO_5 has been recently reported[3], analogous to active forms[6] of H_3PO_2 and H_3PO_3. Thus, it is obvious that some more oxidation studies on inorganic compounds should be carried out to know the mechanism. Thiocyanate ion having two atoms of different electronegativities undergoing oxidation, seemed to be appropriate for the study. Its oxidation itself evinces interest since most of the oxidation studies have been made with one electron oxidants[7-9] yielding a free radical SCN and then thiocyanogen which undergoes hydrolysis to give the products.

Materials and Methods

Solutions of pmpa were prepared afresh by the hydrolysis of peroxodiphosphate in $HClO_4$ (0.5 mol dm^{-3}) at 45° for about 1.5 hr and standardised iodometrically. Solutions of lithium perchlorate were prepared by neutralising $HClO_4$ (70%, E. Merck) with lithium carbonate (BDH, AR) to *p*H 6.8. Aqueous solutions of potassium thiocyanate (BDH, AR) were standardised by Volhard's method. All other chemicals were either BDH analaR or E. Merck GR quality and were used as such. All solutions were prepared in doubly distilled water, the second distillation being from potassium tetraoxomanganate(VII).

Kinetic procedure

The reaction was initiated by adding a known volume of pmpa to a thermally equilibrated (± 0.1°C) mixture containing thiocyanate, perchloric acid or buffers (acetate, borate or phosphate) and other reagents of desired concentrations. The kinetics were followed by withdrawing aliquots (5.0 cm^3) at regular time intervals and determining [pmpa] iodometrically.

Thiocyanogen though said to react with iodide, undergoes quick hydrolysis in the system and hence does not interfere at the time of iodometric determination.

Initial rates were calculated from the plots of [pmpa] versus time by the plane mirror method. Second order plots were also constructed wherever conditions permitted. The results were reproducible to $\pm$ 5%.

Results

Stoichiometry—These experiments were conducted with excess [pmpa] and the latter was determined iodometrically after about three hours. Excess thiocyanate could not be taken since it could not be determined in the presence of phosphate which is the product from pmpa. Sulphate was tested qualitatively only. Cyanide was determined by Ni^{2+} by the method of Huditz and Flaschka[10], but $\Delta[SCN^-]/\Delta[CN^-]$ was always larger than 1 and less than 1.5. This error may have been caused by the escape of HCN from the reaction mixture. All these results show that the reaction occurs as in Eq. (1).

$$3H_3PO_5 + SCN^- + H_2O = 3H_3PO_4 + SO_4^{2-} + HCN + H^+ \quad \ldots (1)$$

Incidentally all redox reaction of SCN^- so far studied give $\Delta[\text{oxidant}]/\Delta[SCN^-] \approx 6$ for one-electron oxidants and the same products.

[pmpa] and [thiocyanate] dependence

[pmpa] was varied from 4.7×10^{-4} to 9.4×10^{-3} mol dm^{-3}. $[SCN^-]$ was varied from 3.2×10^{-4} to 3.2×10^{-3} mol dm^{-3}. These results shown in Table 1 indicate that the orders in each of them is one. The second order rate constants calculated from the initial rates and found from the log $[pmpa]/[SCN^-]$ versus time plots are in good agreement.

Hydrogen ion dependence

$[HClO_4]$ was varied in the range 0005-0.80 mol dm^{-3}, with acetate buffers for *p*H range 3.67-4.70, with phosphate buffers for *p*H range 6.2-7.4, and with borate buffers for *p*H range 8.41-10.97 at constant ionic strength of 1.0 mol dm^{-3} adjusted with lithium perchlorate. The results given in Table 2 show that the rate is independent of $[H^+]$ in the acetate and borate buffers, but in perchloric acid solutions, it increases, attains a maximum and then decreases. In phosphate buffers (*p*H 6.2 to 7.4) rate decreases.

Effect of added Cu(II), Fe(III), phosphate and sulphate ions

Added [Cu(II)] in the range 5.0×10^{-6} to 11.0×10^{-4} mol dm^{-3}, [Fe(III)] in the range 1.0×10^{-6} to 2.0×10^{-5} mol dm^{-3}, phosphate and sulphate in the range 1.0×10^{-4} to 1.0×10^{-3} mol dm^{-3} have no effect on the rate.

Effect of ionic strength

Ionic strength was varied with the help of $LiClO_4$ in the range 0.1 mol dm^{-3} to 1.0 mol dm^{-3}, but without any effect on the rate.

Discussion

The reaction appears to be a simple bimolecular one and the only interest arises from H^+ depend-

Table 1—Second order rate constants (k_0) of pmpa-SCN^- reaction at 30° and I = 1.0 mol dm^{-3}

10^3 [pmpa] (mol dm^{-3})	10^3 $[SCN^-]$ (mol dm^{-3})	k_0 from the second order plots (mol dm^{-3} s^{-1})	*p*H	10^5 (i.r.) (mol dm^3 s^{-1})	(k_0 from the initial rates (i.r.)/[pmpa] $[SCN^-]$
0.47	1.00	4.9	4.47	0.22	4.68
0.94	1.00	5.1	4.47	0.45	4.78
1.88	1.00	4.9	4.47	0.96	5.10
3.76	1.00	4.9	4.47	1.75	4.65
5.64	1.00	5.0	4.47	2.75	4.87
7.52	1.00	4.7	4.47	3.83	5.09
9.40	1.00	5.0	4.47	4.67	4.97
4.70	0.32	4.9	4.47	0.70	4.65
4.70	0.96	4.8	4.47	2.20	4.87
4.70	1.60	5.0	4.47	3.50	4.68
4.70	2.40	4.8	4.47	5.67	5.02
4.70	3.20	5.0	4.47	7.00	4.65
		Av. 4.9 ± 0.09			4.83 ± 0.16
0.90	0.20	14	0.01*	0.25	13.9
0.90	0.50	13	0.01*	0.60	13.3
0.90	1.00	14	0.01*	1.17	13.0
0.90	2.00	15	0.01*	2.53	14.0
0.90	3.00	14	0.01*	3.87	14.3
0.45	0.20	13	0.01*	0.13	14.4
0.15	0.20	15	0.01*	0.042	14.0
		Av. 14 ± 0.5			13.8 ± 0.4

*$HClO_4$ concentration

Table 2—Hydrogen ion dependence of rate in the pmpa-SCN^- reaction at 30° and $I = 1.0$ mol dm^{-3}

$[pmpa] = 9.0 \times 10^{-4}$ mol dm^{-3}, $[SCN^-]_T = 2.0 \times 10^{-4}$ mol dm^{-3}

$10^2[H^+]$ (mol dm^{-3})	0.5	1.0	2.5	5.0	7.5	10.0	15.0	17.5
10^6 (i.r.) (mol dm^{-3} s^{-1})	1.4	2.5	5.0	6.7	8.0	9.0	10.1	10.4
$10^2[H^+]$ (mol dm^{-3})	20.0	30.0	40.0	50.0	60.0	80.0		
10^6 (i.r.) (mol dm^{-3} s^{-1})	10.3	9.7	8.7	7.7	7.1	6.0		

$[pmpa] = 4.25 \times 10^{-3}$ mol dm^{-3}, $[SCN^-]_T = 1.0 \times 10^{-3}$ mol dm^{-3}

*p*H	3.67	3.95	4.05	4.28	4.70
10^5 (i.r.) (mol dm^{-3} s^{-1})	2.0	2.1	2.1	2.0	2.1

$[pmpa] = 2.01 \times 10^{-3}$ mol dm^{-3}, $[SCN^-]_T = 1.0 \times 10^{-3}$ mol dm^{-3}

*p*H	6.2	6.4	7.0	7.4
10^6 (i.r.) (mol dm^{-3} s^{-1})	7.3	5.6	3.8	3.4

$[pmpa] = 2.12 \times 10^{-3}$ mol dm^{-3}, $[SCN^-]_T = 5.0 \times 10^{-4}$ mol dm^{-3}

*p*H	8.41	8.85	9.84	10.64	10.97
10^6 (i.r.) (mol dm^{-3} s^{-1})	1.6	1.6	1.6	1.6	1.6

ence of the rate. The three acid dissociation constants of H_3PO_5 are reported to be $K_d^1 = 8.9 \times 10^{-2}$ mol dm^{-3}, $K_d^2 = 3.16 \times 10^{-6}$ mol dm^{-3} and $K_d^3 = 1.6 \times 10^{-13}$ mol dm^{-3} at 25° and $I = 0.15$ mol dm^{-3} by Battaglia and Edwards[11]. There is some uncertainty about the first acid dissociation constant. It is reported to be 0.3 in a review article[12] and 0.34 at 35° by Mahapatro and coworkers[13]. There is uncertainty about the value of K_d^2 also. HSCN in general is considered to be a strong acid, but its acid dissociation constant has been variously reported[9,14-17] between 0.02 to 100 at 25°. Our results of H^+-dependence show that if a maximum in a plot of rate versus $[H^+]$ occurs between $[H^+] = 0.15$ and 0.2 mol dm^{-3}, K_d should be less than 1.

In acetate buffers the two likely species of pmpa and thiocyanate are $H_2PO_5^-$ and SCN^- respectively. However, in acid perchlorate solutions pmpa would exist as H_3PO_5 and $H_2PO_5^-$ and thiocyanate would exist as HSCN and SCN^-. Since with the increase in $[H^+]$, the rate increases, attains a maximum and then decreases, protonated form of one acid and deprotonated form of the other must be reactive. Thus either H_3PO_5 and SCN^-, or $H_2PO_5^-$ and HSCN are reactive, and kinetically it would not be possible to distinguish between the two. Other less significant pairs of reactants are also possible. However, since in acetate buffers $H_2PO_5^-$ and SCN^- are reactive, and SCN^- acts as a nucleophile, H_3PO_5 and SCN^- appear to be the main reactive pair in acid perchlorate solutions. In borate buffers the predominant species would be HPO_5^{2-} and SCN^-. Following general mechanism in Scheme 1 may be proposed for the reaction in the entire range of $[H^+]$ studied.

$$HSCN \overset{K_d}{\rightleftharpoons} SCN^- + H^+ \quad \ldots (2)$$

$$H_3PO_5 \overset{K_d^1}{\rightleftharpoons} H_2PO_5^- + H^+ \quad \ldots (3)$$

$$H_2PO_5^- \overset{K_d^2}{\rightleftharpoons} HPO_5^{2-} + H^+ \quad \ldots (4)$$

$$H_3PO_5 + SCN^- \overset{k_1}{\rightarrow} \text{Products} \quad \ldots (5)$$

$$H_2PO_5^- + SCN^- \overset{k_2}{\rightarrow} \text{Products} \quad \ldots (6)$$

$$HPO_4^{2-} + SCN^- \xrightarrow{k_1} \text{Products} \quad \ldots (7)$$

Scheme 1

The general rate law is given by Eq. (8)

$$-d[\text{pmpa}]/dt = \frac{K_d(k_1[H^+]^2 + k_2K_d^1[H^+] + k_3K_d^1K_d^2)[\text{pmpa}][SCN^-]_T}{([H^+]^2 + K_d^1[H^+] + K_d^1K_d^2)(K_d + [H^+])} \quad \ldots (8)$$

In borate buffers (pH 8.41 to 10.97) the denominator would reduce to $K_d^1K_d^2$ and only the third term in the numerator significantly contributes to the rate, and hence rate law (8) reduces to (9)

$$-d[\text{pmpa}]/dt = k_3[\text{pmpa}][SCN^-]_T \quad \ldots (9)$$

The value of k_3 has been found to be 1.5 mol^{-1} dm^3 s^{-1} at 30°. In acetate buffers (pH 3.67 to 4.70) the denominator reduces to $K_d^1[H^+]$ and only second term of the numerator would contribute significantly to the rate. Hence rate law is reduced to (10).

$$-d[\text{pmpa}]/dt = k_2[\text{pmpa}][SCN^-]_T \quad \ldots (10)$$

The value of k_2 was found to be 4.85 mol^{-1} dm^3 s^{-1} at 30°. Since the rate is not constant in the pH range 6.2-7.4, the rate law (8) is likely to be reduced to (11)

$$-d[\text{pmpa}]/dt = (k_2[H^+] + k_3K_d^2)/([H^+] + K_d^2) \quad \ldots (11)$$

but we cannot verify it quantitatively since K_d^2 at $I = 1.0$ mol dm^{-3} is not known. Since there is uncertainty about the values of both K_d and K_d^1, no suitable plot for H^+ dependence can be made in acid perchlorate solutions. In any case rate law (8) would reduce to (12) in acid perchlorate solutions.

$$-d[\text{pmpa}]/dt = \frac{K_d(k_1[H^+] + k_2K_d^1)[\text{pmpa}][SCN^-]_T}{([H^+] + K_d^1)(K_d + [H^+])} \quad \ldots (12)$$

If we assume $K_d = 1.0$ mol dm^{-3} and $K_d^1 = 0.1$ mol dm^{-3} and make a plot of rate $\times([H^+] + K_d^1)(K_d + [H^+])$ versus $[H^+]$, we obtain a curve with insignificant intercept on the rate-axis. Hence $k_2K_d^1$ appears to be insignificant as compared to $k_1[H^+]$ and the rate law (12) is further reduced to (13) in acid perchlorate solutions.

$$-d[\text{pmpa}]/dt = \frac{K_dk_1[H^+][\text{pmpa}][SCN^-]_T}{([H^+] + K_d^1)(K_d + [H^+])} \quad \ldots (13)$$

The value of K_d, K_d^1 and k_1 can be calculated from the slopes and intercepts of the linear plots of $(\text{rate})^{-1}$ versus $[H^+]^{-1}$ and $(\text{rate})^{-1}$ versus $[H^+]$ in the low and high [acid] ranges respectively. These are given in Figs 1 and 2. k_1 was found to be 92 mol^{-1} dm^3 s^{-1} at 30° and $I = 1.0$ mol dm^{-3}. For K_d and K_d^1, a pair of values were obtained i.e., either 0.53 and 0.05, or 0.05 and 0.53. Since a large number of systems seem to give results in accordance with a value for K_d larger than 1 and since K_d^1 has been determined spectrophotometrically to be 0.1, HSCN should be stronger of the two acids. Hence it is logical to assign the value of 0.53 to K_d and 0.05 to K_d^1.

Since $k_1[H^+] \gg k_2K_d^1$ in acid perchlorate solutions, k_1/k_2 should be more than 10. Similarly in acetate buffers $k_2K_d^1 \gg k_1[H^+]$, k_1/k_2 should not be larger than 100. The value of 92 obtained falls in the expected range. If equation (13) is differentiated with respect to $[H^+]$, it predicts a maximum at $[H^+] = 0.166$ mol dm^{-3}. From Table 2 it is obvious that the maximum is at $[HClO_4]$ between 0.15 and 0.20 mol dm^{-3}. Thus the results seem to be in accord with rate law (13) in acid perchlorate solutions, and in accord with the rate law (8) in general. A plot of rate $\times([H^+] + K_d)([H^+] + K_d^1)$ versus $[H^+]$ using $K_d = 0.53$ and $K_d^1 = 0.05$ is linear (Fig. 3) passing through the origin and yielding a value of 93 mol^{-1} dm^3 s^{-1} for k_1.

The reactivity of pmpa increases with the increase in protonation since it acts as an electrophile. The same behaviour has been found in the oxidations of nitrite[4], iodide[18], hydrazine[3], anilines[19] and aromatic amines[20]. In general k_1 is about 100 times larger than k_2. The role of pmpa in the oxidation of thiocyanate and iodide is more clearcut since HI and

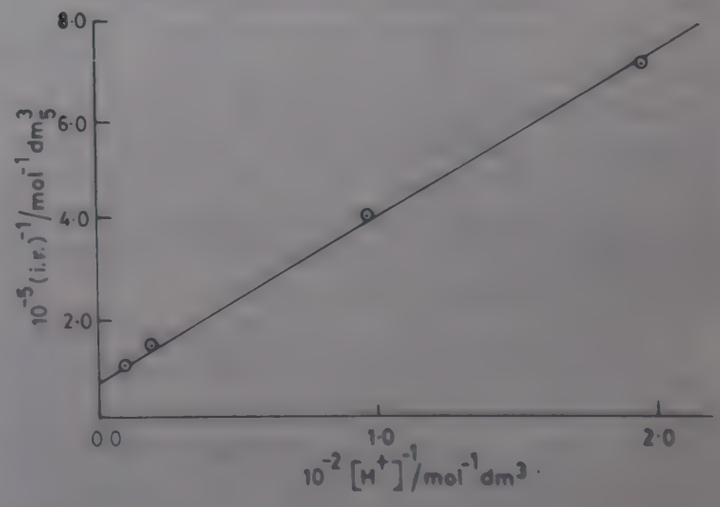

Fig. 1—A plot of $(\text{i.r.})^{-1}$ versus $[H^+]^{-1}$ ($[SCN^-] = 2.0 \times 10^{-4}$ mol dm^{-3}; $[\text{pmpa}] = 9.0 \times 10^{-4}$ mol dm^{-3}; $I = 1.0$ mol dm^{-3}; temp = 30°C)

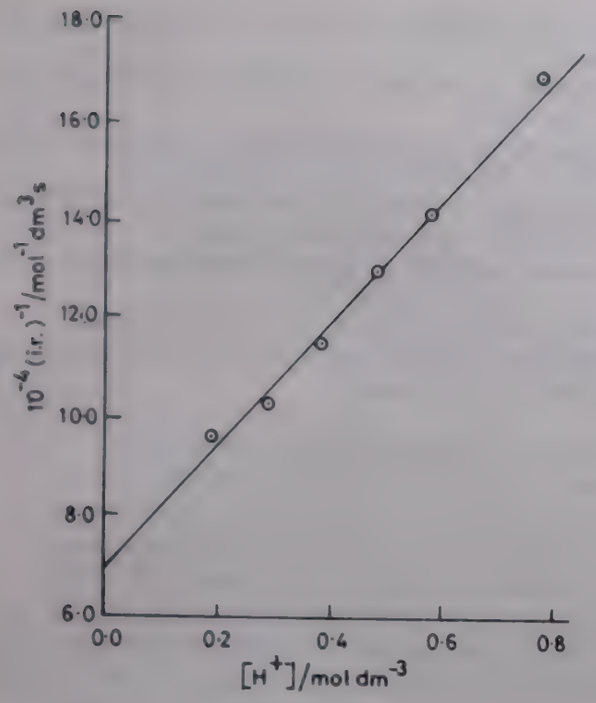

Fig. 2—A plot of (i.r.)$^{-1}$ versus [H$^+$] ([SCN$^-$] = 2.0×10^{-4} mol dm^{-3}; [pmpa] = 9.0×10^{-4} mol dm^{-3}; I = 1.0 mol dm^{-3}; temp = 30°C)

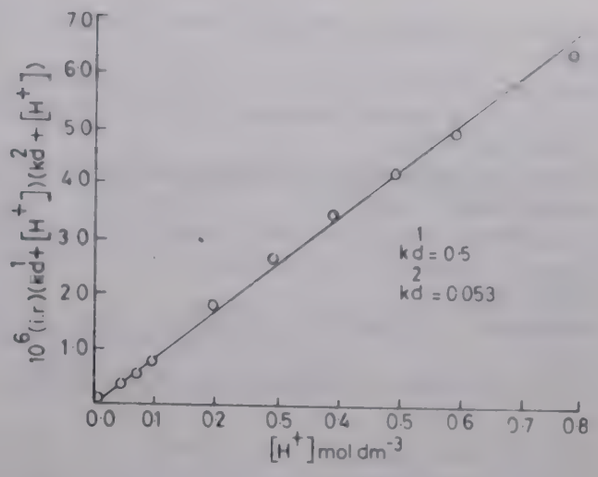

Fig. 3—A plot of (i.r.) (K_d^1 + [H$^+$]) (K_d^2 + [H$^+$]) versus [H$^+$] ([SCN$^-$] = 2.0×10^{-4} mol dm^{-3}; [pmpa] = 9.0×10^{-4} mol dm^{-3}; I = 1.0 mol dm^{-3}; temp = 30°C)

HSCN are strong acids and the latter would predominantly exist as anions.

In all oxidations of thiocyanate, the products of oxidation have been reported to be SO_4^{2-}, and HCN, and in general SCN and $(SCN)_2$ have been considered to be the intermediates. In all oxidations of thiocyanate, hydrolysis of thiocyanogen has been reported except the oxidation by Cr(VI)[16] where such intermediate species have not been reported, but the final products are the same. All one electron oxidants like Fe(III)[21], Mn(III)[22], Os(VIII)[7] and Ir(IV)[8], are reported to yield free radical SCN in the rate determining step since the order in oxidant is always one. In case of two electron oxidants like Tl(III)[23] and H_3PO_5, SCN is not likely to be the intermediate of any stability since even if it is formed, it will react with another reactive species or free radical Tl(II) or $H_2PO_5^-$ and any intermediate of consequence seems to be $(SCN)_2$. Thus SCN^- seems to undergo two electron oxidation with Tl(III) and H_3PO_5 and in all probability SCN^+ species is likely to be formed as shown in (14). The cation SCN^+ may then react with SCN^- to form thiocyanogen. This is analogous to the formation of I^+ and subsequent combination with I^- to form iodine. Thiocyanate is likely to behave

$$H_3PO_5 + SCN^- + 2H^+ \xrightarrow{\text{slow}} H_3PO_4 + SCN^+ + H_2O \quad \ldots (14)$$

$$Tl(III) + SCN^- \xrightarrow{\text{slow}} Tl(I) + SCN^+ \quad \ldots (15)$$

$$SCN^+ + SCN^- \xrightarrow{\text{fast}} (SCN)_2 \quad \ldots (16)$$

like this since it is regarded to be a pseudo halide or halogenide. The other bases Cl^-, ClO_4^-, NO_3^-, F^- etc. can combine with SCN^+ to form thiocyanogen chloride, perchlorate, nitrate and fluoride respectively. This is not impossible since thiocyanogen monochloride[24] and thiocyanogen monocyanide[25] have been reported in the past. However, if these compounds also undergo hydrolysis readily, their formation cannot be proved. The stoichiometry of the reaction does not change even in the presence of large concentration of these salts and hence such thiocyanogen compounds, if formed, are not stable.

References

1 Panigrahi G P & coworkers, *Bull Chem Soc, Japan*, 54 (1981) 250; *Reaction Kinet Catalysis Lett*, 21 (1982) 283; *Bull chem Soc Kinet*, 12 (1980) 491.

2 Keshwani P, Goyal M R & Gupta Y K, *J chem Soc Dalton Trans*, (1983) 1831.

3 Peter Amala Dhas T, Mittal R K & Gupta Y K, *Int J chem Kinet*, 23 (1991).

4 Keshwani P & Gupta Y K, *Indian J Chem*, 22A (1983) 763; Panigrahi G P & coworkers, *Int J chem Kinet*, 15 (1983) 989.

5 Panigrahi G P & Nayak R N, *Indian J Chem*, 22 (1983) 239.

6 Mitchell A D, *J chem Soc*, 117 (1920) 1322; 119 (1921) 1266; 121 (1922) 1624; 123 (1923) 629; Griffith R O, McKeown A & Taylor R P, *Trans Faraday Soc*, 36 (1940) 752; Griffith R O & McKeown A, *Trans Faraday Soc*, 30 (1934) 530.

7 Nord G, Pederson B & Farve O, *Inorg Chem*, 17 (1978) 2233.

8 Stanbury D M, Wilmarth W K, Khalaf S, Po H N & Byrd J E, *Inorg Chem*, 19 (1980) 2715.

9 Ng F T T & Henry P M, *Can J Chem*, 53 (1975) 3319.

10 Huditz F & Flaschka H, *Fresenius Z Anal Chem*, 136 (1952) 185.
11 Battaglia C J & Edwards J O, *Inorg Chem*, 4 (1965) 552.
12 Edwards J O, *Peroxide reaction mechanism* (Interscience, London) 1962, p. 42.
13 Dharma Rao S ch, Panda A K & Mahapatro S N, *J chem Soc, Perkin Trans II*, (1983) 769.
14 Special Publication, *J chem Soc, London*, 1964, Vol. 1, p. 17.
15 Morgan T, Stedman G & Whincup P A E, *J chem Soc*, (1965) 4813.
16 Muirhead K A & Haight (Jr) G P, *Inorg Chem*, 12 (1973) 1116.
17 Lin C T & Beattie J K, *J Am chem Soc*, 94 (1972) 3011.
18 Secco F & Venturini M, *J chem Soc, Dalton Trans*, (1976) 1410.
19 Panda A K, Mahapatro S N & Panigrahi G P, *J org Chem*, 46 (1981) 4000.
20 Ogata Y, Tomizawa K & Morikawa T, *J org Chem*, 44 (1979) 352.
21 Betts R H & Dainton F S, *J Am chem Soc*, 75 (1953) 5721.
22 Davies G, *Inorg Chem*, 11 (1972) 2488.
23 Gupta Y K, Kumar D, Seema Jain & Gupta K S, *J chem Soc, Dalton Trans*, (1990) 1915.
24 Kaufmann H P & Liepe J, *Ber*, 57B (1924) 923.
25 Audreith L F & Browne A W, *J Am chem Soc*, 52 (1930) 2799.

Indian Journal of Chemistry
Vol. 31A, February 1992, pp. 97-101

Kinetics of oxidation of some monosaccharides by pyridinium chlorochromate (PCC)†

Raj K Dhar‡
Indian Institute of Technology, Hauz Khas, New Delhi 110 016

Received 28 June 1991; revised and accepted 27 November 1991

The oxidation kinetics of glucose, considered as a model compound for reducing sugars, with pyridinium chlorochromate in perchloric acid medium has revealed a linear correlation between the observed rate constant k_{obs} and [glucose], [H^+]. A comparison of D-glucose oxidation with its various C-1 and C-2 substituted derivatives shows that inductive, steric and shielding effects may all be important which explains the reactivity as 2-deoxy-D-glucose > D-glucose > 1-*o*-methyl-α-D-glucopyranoside > 2-amino-2-deoxy-D-glucose hydrochloride. A comparison between α and β-anomers of some monosaccharides reveals that β-anomer is oxidised faster than α-anomers. Further, activation energy and thermodynamic parameters have been evaluated for D-glucose oxidation and mechanism consistent with experimental observation is attempted.

In carbohydrate chemistry, D-glucose plays an important role because it is the unit of which starch, cellulose and glycogen are made up. In view of this, studies on oxidation of D-glucose and other monosaccharides have been given a great deal of attention[1-12]. Surprisingly, there has been no systematic oxidation studies carried out to examine the effect of substituents on C-1 and C-2 position of D-glucose. Hence, the present study is undertaken. For this oxidation study, PCC as the Cr oxidant was chosen in view of its ease of preparation[11], high stability[12] and because of the fact that it is a mild and selective oxidant for a wide range of substrates[12,13]. Attempt has also been made to compare the oxidation rates of α and β-anomers of some sugars which further substantiates the mechanism of oxidation.

Materials and Methods

Perchloric acid (Merck GR) was used for preparing solutions of different acid concentrations. Deuterium oxide (BARC, India) was of 99.5% purity. All sugars used for kinetic studies were of highest purity grade, procured either from Sigma Chemicals or E. Merck. These were used without further purification after drying *in vacuo* for at least 4 hr and the solutions of these sugars were made always fresh in deionized water, by direct weighing.

Pyridinium chlorochromate (PCC)

Chromium trioxide (100 g, 0.7 mol) was rapidly added with stirring to 6 N hydrochloric acid (184 ml, 1.7 mol). After 5 min the homogeneous solution was cooled to 0°C and pyridine (79.1 g, 1 mol) was carefully added over 15 min. Recooling to 0°C gave a yellow-orange solid which was collected on a sintered glass filter and dried *in vacuo* for 2-3 hr (yield 150.5 g, 78%). UV-visible spectrum of PCC showed λ_{max} at 350 nm in pure water and in acidic medium.

Kinetic measurement

All kinetic measurements were carried out at 350 nm, in a thermostated cell compartment of Pye-Unicam SP-500 or SP-700 spectrophotometer instrument. The rate constants k_0, k_2 and activation energy (E_a) were obtained using standard programmes of regression analysis by ICL 2960 computer.

Tests for intermediate radicals were carried out through initiation of polymerisation of purified acrylonitrile in a nitrogen atmosphere under typical kinetic conditions for all sugars. No polymerisation was observed.

Product analysis of D-glucose was carried out under typical kinetic conditions. The products were identified by paper chromatography in comparison with the oxidation products of D-glucose by bromine and nitric acid separately[14]. A solvent system of 1-butanol-acetic acid-water (4:1:5) was used and detection was carried out with the alkaline silver nitrate. Paper chromatography of the syrup obtained from the oxidation of D-glucose with PCC indicated the presence of gluconic acid. This is in

† Dedicated to Prof. Herbert C. Brown on his 80th birthday

‡ Present address: Chemistry Department, Louisiana State University (LSU), Baton Rouge, La 70808 USA.

Table 1—Values of observed rate constants, $k_0 \times 10^5$ s^{-1}, for the oxidation of D-glucose by pyridinium chlorochromate (PCC)
I = 1 mol dm^{-3}, [PCC] = 1.4×10^{-3} mol dm^{-3}

Temp. (°C)	[D-glucose] × 10^2 mol dm^{-3}	[$HClO_4$], mol dm^{-3}			
		0.25	0.50	0.75	1.00
23	2	1.00	3.35	5.05	7.31
	4	2.36	6.08	10.00	19.60
	6	3.80	7.46	13.33	32.80
	8	4.60	9.93	19.10	34.50
	10	5.73	14.50	23.80	46.30
	20	13.60	27.50	40.80	92.50
33.5	2	2.34	6.11	14.80	24.60
	4	5.50	12.50	30.56	48.60
	6	7.26	18.80	43.00	76.00
	8	8.70	26.10	58.31	106.0
	10	9.43	32.10	62.70	117.0
	20	18.20	62.10	126.0	227.0
43.5	2	4.78	10.61	32.60	40.50
	4	9.89	21.20	61.60	82.30
	6	11.90	45.80	108.0	132.0
	8	14.40	48.10	137.0	194.0
	10	17.10	59.90	154.0	247.0
	20	31.50	147.0	266.0	516.0
53.5	2	5.70	—	64.48	86.30
	4	12.70	75.10	98.63	147.0
	6	20.83	88.50	123.2	209.0
	8	25.20	101.5	160.0	290.6
	10	39.90	122.0	247.0	366.4
	20	58.10	250.0	462.0	644.8

Table 2—Bimolecular rate constants $k_2 \times 10^3$ (dm^3 mol^{-1} s^{-1}) for the oxidation of D-glucose by PCC
[Ionic strength = 1 mol dm^{-3}]

Temp. (K)	[$HClO_4$], mol dm^{-3}			
	0.25	0.50	0.75	1.00
296.15	0.69	1.35	1.98	4.71
306.65	0.83	3.10	6.03	11.15
316.65	1.41	7.53	12.73	26.78
326.65	2.93	10.88	22.96	31.30

agreement with the observation that the aldonic acid invariably remains in equilibrium with corresponding γ and δ-lactones in acidic medium[14,15]. D-glucose oxidation also indicated the presence of formic acid and arabinose. Formic acid was tested by initially treating the oxidized product with Zn/HCl followed by addition of chromotropic acid which gave positive test for formaldehyde, thus, confirming the presence of formic acid[16]. Arabinose was confirmed by hydrazone formation and co-TLC of the hydrazone[17] with an authentic sample of arabinose.

Table 3—Values of the activation parameters for the oxidation of D-glucose by PCC at 1 mol dm^{-3} ionic strength

[$HClO_4$] (mol dm^{-3})	E_a (kJ mol^{-1})	$\Delta H^{\ddagger}$ (kJ mol^{-1})	$\Delta S^{\ddagger}$ (e.u.)	$\Delta G^{\ddagger}$ (kJ mol^{-1})
0.25	38.14	35.42	−42.74	93.84
0.50	57.26	54.54	−26.14	90.28
0.75	65.07	62.35	−18.96	88.24
1.00	52.90	50.18	−27.24	87.41

rates of oxidation were found to increse with increase in [H^+], the slopes of the plots of overall bimolecular rate constants, log k_2 versus log [H^+] at four

Results and Discussion

An inspection of the observed rate constants (k_0) shows that the k_0 values rise markedly with increase in [D-glucose] (Table 1). The plots of k_0 against [D-glucose] were linear passing through the origin thereby confirming first order dependence in [D-glucose]. The bimolecular rate constants have been calculated from the slopes of these lines and are given in Table 2 at four different temperatures. The rates of oxidation were found to increase with increase in [H^+], the slopes of the plots of overall bimolecular rate constants, log k_2 versus log [H^+] at four different temperatures were approximately 1, showing thereby first order dependence in [acid]. The order in oxidant is one as revealed by the linearity of log (a/a − x) versus time plot passing through the origin. These observations lead to the rate law (1):

$$\frac{-d[\text{PCC}]}{dt} = k[\text{D-glucose}][\text{PCC}][\text{H}^+] \qquad \ldots (1)$$

The oxidation of D-glucose has been carried out at four different temperatures, viz. 296, 306, 316 and 326 K. The activation parameters were calculated from the linear plots of log k_2 versus T^{-1}. Activation energies and the related thermodynamic parameters are listed in Table 3. The values of activation energy for D-glucose oxidation lie between 38.14 and 52.90 kJ mol^{-1}. Constancy of $\Delta G^{\ddagger}$ (90 ± 3 kJ mol^{-1}) suggests that there is a mutual compensation effect of $\Delta H^{\ddagger}$ and $\Delta S^{\ddagger}$. A comparison of previous studies[10] on oxidation of D-glucose demonstrates that pyridinium flurochromate (PFC) is faster oxidizing agent than PCC with lower activation energy.

The rates of oxidation of D-glucose were determined both in water and in deuterium oxide. The rate k_{D_2O}/k_{H_2O} was found to be 3. Comparison of

Table 4—Comparison of oxidation rates of α- and β-anomers [PCC] = 1.30×10^{-3} mol dm^{-3}, [H] = 4 mol dm^{-3}, T = 22°C, I = 5.6 mol dm^{-3}

Anomers	k_2 (dm^3 mol s^{-1})
α-D-Glucopyranoside	1.565
β-D-Glucopyranoside	1.738
1-o-Methyl-α-D-glucopyranoside	0.507
1-o-Methyl-β-D-glucopyranoside	0.699

acid base equilibrium in water and in deuterium oxide indicates that for any proton catalyzed reaction one should expect a solvent isotopic effect[18] k_{D_2O}/k_{H_2O} about to 2.5. The observed high value of 3 in the present study may not be due to participation of second proton in the oxidation as no deviation has been observed in the first order dependence in [H$^+$]. Two acid-catalyzed processes may be assumed, one being the acid-catalyzed mutarotation and the other protonation of the anomer or the protonation of the PFC species. It is likely that protonation of PFC species is the dominant factor. This is reflected in the energy of activation (Table 3) and increase in rate constant with increase in ionic strength (Values of $10^3 k_0$ are 0.046, 0.191, 0.510, 0.806 and 2.93 s^{-1} at ionic strengths of 1.0, 2.0, 2.5, 3.0 and 4.0 mol dm^{-3} respectively under the conditions D-glucose = 0.02 mol dm^{-3}, [PCC] = 1.6×10^{-3} mol dm^{-3} and temp = 28°C).

PCC effects the oxidation of D-glucose to mostly gluconic acid besides formic acid and arabinose as the products of oxidation. Oxidation of these products under the kinetic conditions is insignificant, since, all the kinetics were carried out under pseudo-first order conditions.

In aqueous acidic solutions, D(+)-glucose predominantly exists in equilibrium between pyranose forms with free aldehyde form as the intermediate, beside furanoid forms[19], which are too low in concentrations to make any impact towards competing for oxidation with above intermediates. The pyranoid form being more stable constitutes more than 99% of the total [D-glucose]. Further, attempt to compare the oxidation rates of individual anomers (α and β) under the present kinetic condition were not successful suggesting that rate of mutarotation is many times greater than the rate of oxidation under normal kinetic conditions. Hence, the rate of oxidation of these epimers was measured at higher [H$^+$] and at higher ionic strength. Under these conditions, the oxidation rates are considerably fast. The conditions under which kinetic measurements were carried out, only 30% completion of the reaction for these pure epimers was noticed in less than 100 seconds from the start of the reaction. It is presumed that even in this short time of kinetic measurement, these epimers must have mutarotated to a certain degree. Nevertheless, comparison of oxidation rates of individual anomers at higher ionic strength (Table 4) revealed that β-anomer is oxidised faster, though comparison for mutual oxidation rates is small ($\beta/\alpha = 1.11$ for α and β-D-glucopyranoside and $\beta/\alpha = 1.37$ for 1-o-methyl-α- and β-D-glucopyranoside), yet it gives justification for β-anomer being oxidised faster in preference to α-anomer. The slightly higher rates of β-D-anomer could be explained on the basis of $\Delta 2$ effect of Reeves[20], where on axial hydroxyl group on C-2 bisects the oxygen valences of C-1, such an arrangement results in the maximum repulsion of the oxygen atom, thus facilitating the approach of PCC.

The reaction is presumed to follow a direct hydride ion transfer of the axial-anomeric H of the β-pyranose. The hydride ion transfer can occur in two ways: (1) direct hydride ion transfer, (2) via ester formation. Both these paths lead to the formation of gluconic acid (Scheme 1). In acidic solution, gluconic acid invariably remains in equilibrium between γ- and δ-lactones. This hydride ion transfer is similar to the oxidation of alcohols by PCC[21].

The formation of arabinose and formic acid leads to a mechanism (Scheme 2) which shows involvement of C-1 and C-2 hydroxyl groups. However, there was no intermediate complex formation seen either kinetically or spectrophotometrically in the present investigations. But the product identification suggests that there may be an intermediate complex formation involving C-1 and C-2 hydroxyl groups similar to the oxidation of cyclohexanediol[22]. The intermediate complex breaks leading to the formation of 4-o-formyl-D-arabinose which, however, in protic solvent cannot be stable and, therefore, immediately hydrolyses to formic acid and arabinose. 4-o-Formyl-D-arabinose can be identified by NMR in aprotic solvent as the oxidised product[23].

Oxidation of D-glucose by PCC (Schemes 1 and 2) is presumed to go via ionic mechanism since the reaction mixture failed to induce polymerisation of acrylonitrile. The positive salt effect suggests the involvement of cation-cation and cation-dipole interactions. It is believed that this reaction involves ion-dipole type interaction, dipole being the sugar and ion being the protonated PCC, since unprotonated aldose is more nucleophilic than protonated aldose[23].

Further, a comparison of D-glucose oxidation with those of various C-1 and C-2 substituted D-glucose derivatives has been carried out. The plots of k_0

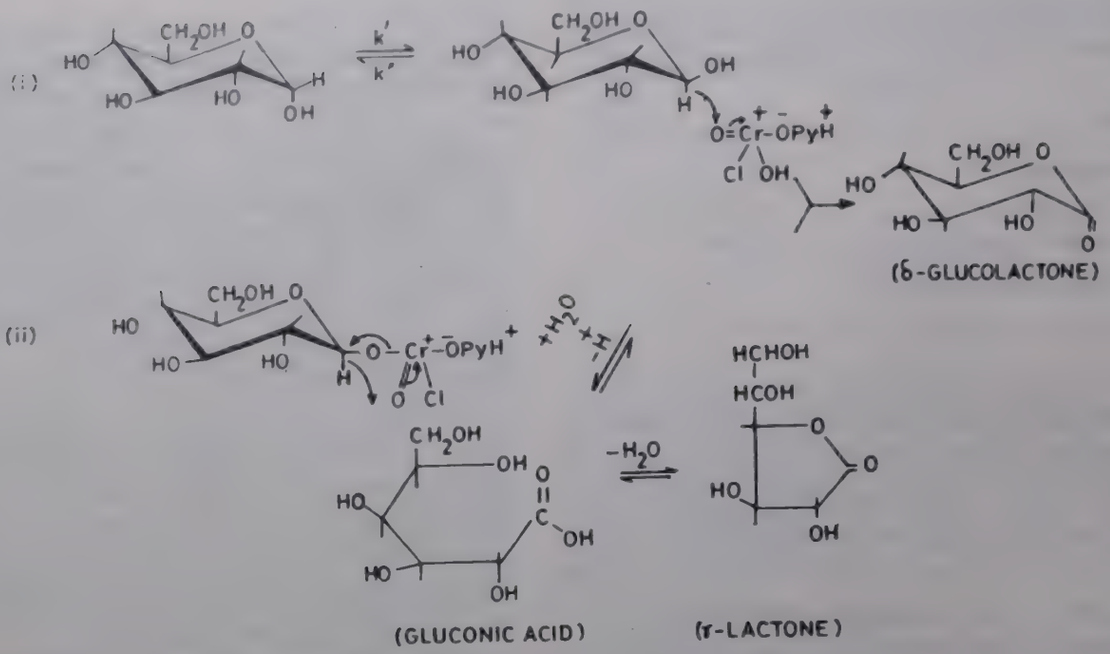

Scheme 1

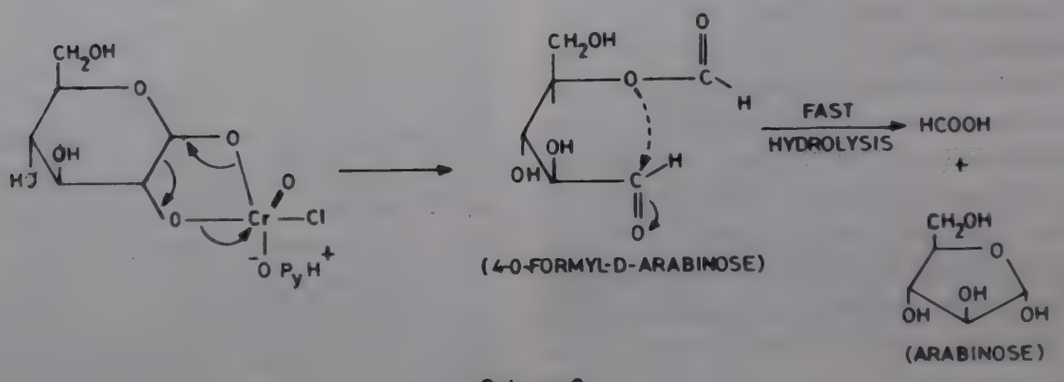

Scheme 2

Table 5—Comparison of oxidation rates of D-glucose with various C_1 or C_2-substituted derivatives of D-glucose
[PCC] = 1.40×10^{-3} mol dm^{-3}, I = 1 mol dm^{-3}, [$HClO_4$] = 1 mol dm^{-3}, temp = 26°C

[Sugars] (mol dm^{-3})	$k_0 \times 10^4$ (s^{-1})				$k_2 \times 10^2$ (dm^3 mol^{-1} s^{-1})	Relative rate
	0.01	0.02	0.03	0.04		
D-Glucose	0.726	1.361	2.240	2.850	0.725 ± 0.025	1.00
2-Deoxy-D-glucose	0.903	1.920	2.820	3.64	0.911 ± 0.022	1.25
1-α-Methyl-α-D-glucopyranoside	0.261	0.626	0.971	1.320	0.352 ± 0.002	0.48
2-Amino-2-deoxy-D-glucose HCl	0.142	0.301	0.401	0.502	0.118 ± 0.007	0.16

against the concentration of various substituted D-glucose derivatives were linear passing through the origin (Fig. 1), thus confirming first order dependence in these [sugars]. A mutual comparison of oxidation rates of these sugars demonstrated: 2-deoxy-D-glucose > D-glucose > 1-α-methyl-α-D-glucopyranoside > 2-amino-2-deoxy-D-glucose hydrochloride (Table 5). It could be that, inductive, steric, and shielding effects are all important and difficult to separate from each other. It is not clear whether effect is electronic or steric since substituents modify conformational stability. 2-Amino-2-deoxy-D-glucose hydrochloride is oxidised very slowly because of the shielding effect of the ammonium group in acidic solution and the effect of ammonium group is related to the distance from the oxygen atom. However, the same trend has been observed also in case of acid catalysed hydrolysis of glycosides[24]. The enhanced rate of oxidation of 2-deoxy-D-glucose may be due to two effects: (1) the removal of OH group at C-2 which would enhance the rate of interaction of PCC with the C-1 H transfer (as hydride ion) and (2)

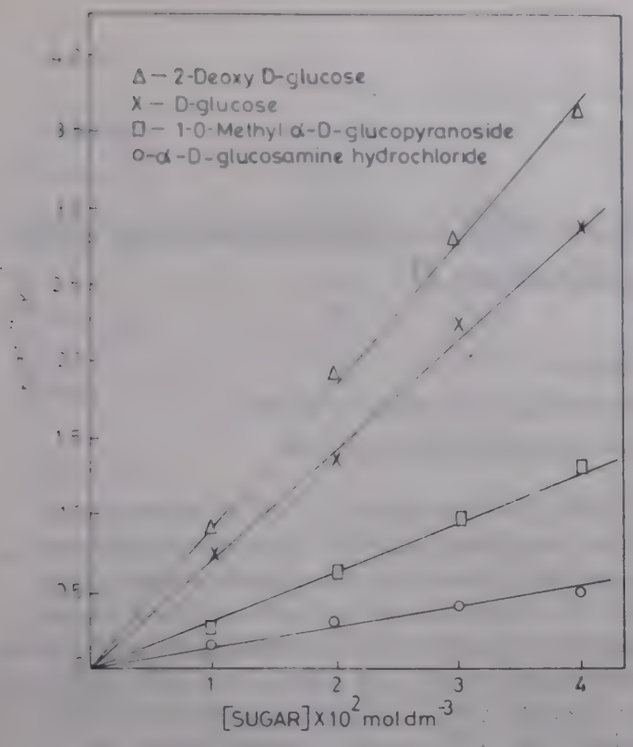

Fig. 1—Plots of k_{obs} versus [sugar] at 26°C

probably the absence of OH group would remove the restriction on rotation and thereby leading to a conformational stability with the PCC interaction.

Acknowledgement

The author is grateful to IIT, New Delhi for the award of a senior research fellowship. Helpful discussions with Prof. R. Varadarajan, Chemistry Department, IIT New Delhi, are duly acknowledged.

References

1 Sen Gupta K K & Basu S N, *Carbohydrate Res*, 72 (1979) 139.
2 Singh S V, Saxena O C & Singh M P, *J Am chem Soc*, 92 (1970) 537.
3 Mehrotra R N & Amis E S, *J org Chem*, 39 (1974) 1788.
4 Pati S C & Panda M, *Int J chem Kinet*, II (1974) 731.
5 Mehrotra R & Kumar A, *J org Chem*, 40 (1976) 1248.
6 Pottenger C R & Johnoson D C, *J polymer Sci*, 8 (1970) 301.
7 Sen Gupta K K & Basu S N, *Carbohydrate Res*, 80 (1980) 223.
8 Sen Gupta K K & Basu S N, *Carbohydrate Res*, 86 (1980) 7.
9 Sen Gupta K K & Basu S N, *Carbohydrate Res*, 97 (1981) 1.
10 Varadarajan R & Dhar R K, *Indian J Chem*, 25A (1986) 474.
11 Corey E J & Suggs J W, *Tetrahedron Lett*, (1975) 2647.
12 Pianeatelli G, Scettri A & D'Auria, *Synthesis*, (1982) 245.
13 Herrcovici J & Antonakis K, *J chem Soc Chem Commun*, (1980) 561.
14 Capon B, *Chem Rev*, 69 (1969) 407.
15 Chandra S & Mittal R K, *Carbohydrate Res*, 19 (1971) 123.
16 Fiegl F, *Spot tests in organic chemistry* (Elsevier, Amsterdam) (1960) 368.
17 Honda S H, Kakehii K & Takiura K, *Anat Chim Acta*, 77 (1975) 125.
18 Rule & Lamer, *J Am chem Soc*, 60 (1938) 1974.
19 Wolfrom M L & Stuart R S, *Advances in carbohydrate Chemistry & Biochemistry*, 24 (1969) 13.
20 Reeves R E, *Advan carbohydrate Chem*, 6 (1951) 107.
21 Banerji K K, *Bull chem Soc Japan*, 51 (1978) 2732.
22 Huntz H L & Johnoson D C, *J org Chem*, 32 (1967) 556.
23 Perlin A S, *Can J Chem*, 42 (1964) 2365.
24 Wolfrom M L, *Advan carbohydrate Chem*, 22 (1967) 25.

Indian Journal of Chemistry
Vol. 31A, February 1992, pp. 102-105

Synthesis, characterization and cytotoxicity of (3,4-diaminobenzoic acid)-haloplatinum(II)/palladium(II)

N Jain & T S Srivastava*
Department of Chemistry, Indian Institute of Technology, Powai, Bombay 400 076

Received 24 April 1991; revised 29 July 1991; accepted 6 November 1991

The synthesis of platinum compounds of the type [Pt(daba)X_2] (where daba = 3,4-diaminobenzoic acid and X = Cl, Br, or I) and the analogous chloro and bromo compounds of Pd(II) has been carried out. These compounds have been characterized by molar conductance measurements, electronic absorption, infrared, ^{1}H NMR and X-ray photoelectron spectroscopy. The complexes are non-electrolytic in nature and have square planar geometry with two coordination positions occupied by two amino groups of 3,4-diaminobenzoic acid and remaining two positions occupied by halide ions. The sodium salts of the above compounds have been tested against P388 lymphocytic leukemia cells. [Pt(daba)Cl_2] and Pt(daba)Br_2] have I.D.$_{50}$ values less than that of *cis*platin and [Pt(daba)I_2] has I.D.$_{50}$ values comparable to that of *cis*platin.

The antitumor activity of *cis*-diamminedichloroplatinum(II) (*cis*platin) first discovered by B. Rosenberg and coworkers in 1969 has led to its use as a leading drug in cancer chemotherapy[1,2]. In order to develop more effective platinum compounds which do not have unfavourable toxicity of *cis*platin, one strategy is to prepare close analogs of *cis*platin by appropriate modification of carrier ligands and by choosing appropriate leaving ligands[3]. This approach has revealed that the strongly bound leaving ligands such as iodide, nitrite, and cyanide show no activities[4]. Recently, Carraher, Jr. and coworkers have reported a polymeric diamine platinum iodide complex (where diamine is methotrexate) which has shown good growth inhibition of 3T3 cells[5]. In this paper, we report the synthesis, characterization and cytotoxicity of [Pt(daba)X_2] and analogous Pd(II) compounds (where daba is 3,4-diaminobenzoic acid and X is Cl, Br or I). These compounds have shown the cytotoxicity against P388 lymphocytic leukemia cells. The I.D.$_{50}$ (50% growth inhibition) value of the iodo compound is comparable to that of *cis*platin[6].

Materials and Methods

[Pt(daba)Cl_2] (where daba is 3,4-diaminobenzoic acid) was prepared by the literature method[7], yield 80%. Analysis: [Found: C, 20.03; H, 2.00; N, 6.76. Calc. for $C_7H_8N_2O_2Cl_2Pt$: C, 20.08; H, 1.91; N, 6.69%].

Preparation of complexes

1. [*Pt(daba)*Br_2]

K_2PtCl_4 (207.5 mg, 0.5 mmol) was dissolved in 50 ml of distilled water and sodium bromide (1.23 g, 12 mol) was added to it. The reaction mixture was stirred for 20 min followed by addition of 3,4-diaminobenzoic acid (76.1 mg, 0.5 mmol) in methanol. The reaction mixture was further stirred for 24 h. The green solid obtained was washed with water, methanol and finally with diethyl ether. The compound was recrystallized from dimethyl sulphoxide. The crystals were filtered, washed with methanol and finally with diethyl ether. The compound was air dried and its yield was 78%. Analysis: [Found: C, 17.06, H, 1.65, N, 6.03%. Calc. for $C_7H_8N_2O_2Br_2Pt$:C, 16.56; H, 1.57; N, 5.52%].

2. [*Pt(daba)*I_2]

This compound was prepared by following the method adopted for (**1**) except that potassium iodide (1.93 g, 12 mmol) was added in place of sodium bromide. The yield was 90%. Analysis: [Found: C, 14.63; H, 1.39; N, 4.69%. Calc. for $C_7H_8N_2O_2I_2$ Pt: C, 13.97; H, 1.33; N, 4.65%].

3. [*Pd(daba)*Cl_2]

$PdCl_2$ (443.7 mg, 2.5 mmol) and sodium chloride (350.7 mg, 6 mmol) were suspended in 50 ml of distilled water. The reaction mixture was stirred for 3 h to get a clear solution. 3,4-Diaminobenzoic acid (380.3 mg, 2.5 mmol) in methanol was added to the above solution and the reaction mixture stirred for 24 h. The brown red compound obtained was filtered, washed with water, methanol and finally with diethyl ether. The compound was air dried, yield 40%. Analysis: [Found: C, 25.68; H, 2.53; N, 8.57%.

Table 1—Electronic absorption spectra of [M(daba)X_2] in DMF

Compound	Band-1	Band-2	Band-3	Band-4	Band-5	Band-6	Band-7
[Pt(daba)Cl_2]	721[a]	589	440	400	329	279	264
	(14100)[b]	(2000)	(3300)	(3400)	(7800)	(13300)	(13400)
[Pt(daba)Br_2]	720	588	441	402	334	278	265
	(6300)	(2200)	(3800)	(3800)	(9500)	(12100)	(12200)
[Pt(daba)I_2]	721	599	444	418	341	279	264
	(2100)	(2300)	(4400)	(4300)	(11100)	(13000)	(11900)
[Pd(daba)Cl_2]				400(sh)	326	275	268
				(1200)	(5600)	(7100)	(7700)
[Pd(daba)Br_2]				400(sh)	320		267
				(1400)	(5900)		(8900)

[a]λ_{max} in nm, [b]ε_{max} in l.mol^{-1} cm^{-1} is given in parentheses, [c]sh is shoulder in parentheses.

Table 2—^{1}H NMR spectral data of [M(daba)X_2] in DMSO-d_6

Compound	3,4-Diaminobenzoic Acid Protons		
	$-NH_2$	H-6	H-2,5
[Pt(daba)Cl_2]	8.40[a](br)[b]	7.20(m)	7.77(m)
	(−2.28)[c]	(−0.05)	
[Pt(daba)Br_2]	8.54(br)	7.52(m)	7.84(m)
	(−2.42)	(−0.37)	
[Pt(daba)I_2]	8.54(br)	7.54(m)	7.80(m)
	(−2.42)	(−0.39)	
[Pd(daba)Cl_2]	7.30(br)	7.30(m)	7.80(m)
	(−1.18)	(−0.15)	
[Pd(daba)Br_2]	7.20(br)	7.20(m)	7.80(m)
	(−1.08)	(−0.15)	

[a]Chemical shifts are given in δ, ppm.
[b]br is broad and m is multiplet in the parenthesis.
[c]Chemical shift difference is given in parenthesis and they are relative to free 3,4-diaminobenzoic acid. Negative sign denotes downfield shift.

Calc. for $C_7H_8N_2O_2Cl_2Pd$:C, 25.48, H, 2.42, N, 8.49%].

4. [*Pd(daba)Br*$_2$]

This compound was prepared by following the method adopted for (**3**) except that sodium bromide (617.5 mg, 6 mmol) was used in place of sodium chloride. The yield of the compound was 30%. Analysis: [Found: C, 20.28, H, 1.99; N, 7.30%. Calc. for $C_7H_8N_2O_2Br_2Pd$:C, 20.07; H, 1.91; N, 6.69%].

The methods used for the physical measurements and cytotoxic studies have been described elsewhere[6,8,9].

Results and Discussion

Three platinum(II) compounds of the general formula [Pt(daba)X_2] and two analogous chloro and bromo compounds of Pd(II) have been prepared. The molar conductance values in DMF obtained for [Pt(daba)X_2] and [Pd(daba)X_2] are in the range of 3 to 18 cm^2 ohm^{-1} mol^{-1} which are suggestive of their non-electrolytic nature.

The infrared spectra (600-4000 cm^{-1}) of the above compounds in nujol mull and KBr pellets have been recorded. The N−H bending vibration in these compounds is located in the region 1540-1560 cm^{-1} which is at lower position as compared to that in the free 3,4-diaminobenzoic acid. In addition, the C=O stretching vibration of carboxylic acid group in the metal chelates has been observed in the region 1720-1730 cm^{-1} which indicates the presence of uncoordinated carboxylic acid group[11,12].

The electronic absorption spectra (λ_{max}, ε_{max} values) of the above compounds in DMF are listed in Table 1. The band 1 is assigned to charge-transfer transition from platinum *d* orbitals to π^* orbital of 3,4-diaminobenzoic acid. The band shift of 15 to 20 nm towards blue region is observed on increasing the polarity of solvents from dimethyl sulphoxide to methanol[13]. The bands 2,3,4 and 5 are tentatively assigned to d-d+ π-π^* transitions. The bands 6 and 7 are due to π-π^* and n-π^* transitions of the benzene ring and −COOH group of 3,4-diaminobenzoic acid respectively. These bands show red and blue shifts respectively, with increasing polarity of solvents from dimethyl sulphoxide to methanol.

The ^{1}H NMR spectra of 3,4-diaminobenzoic acid and their Pt(II) and Pd(II) complexes in (DMSO-d_6) were measured on a 100 MHz FT NMR spectrometer (Table 2). The ^{1}H NMR spectrum of 3,4-diaminobenzoic acid shows a broad peak at δ 6.22 ppm due to protons as indicated by its disappearance after D_2O exchange. In the free ligand spectrum, a doublet at 6.56 ppm is assigned to H-5 proton, and a doublet of a doublet at 7.15 ppm is assigned to

Table 3—X-ray photoelectron spectral data of $[M(daba)X_2]$

Compound	Pt($4d_{5/2}$)	N($1s_{1/2}$)	Cl($2p_{3/2}$)	Br($2p_{1/2,3/2}$)	I($3d_{5/2}$)	Pd($3d_{5/2}$)
$[Pt(daba)Cl_2]$	310.6[a]	400.1	198.3			
$[Pt(daba)Br_2]$	314.1	403.7		183.3		
$[Pt(daba)I_2]$	321.7	405.7			623.2	
					636.6	
						344.3
$[Pd(daba)Cl_2]$		401.0	200.6			338.9
						342.7
$[Pd(daba)Br_2]$		399.6		181.6		337.4
				188.2		

[a]Binding energies are given in eV.

H-6 proton. The ^1H NMR spectra of Pt(II) and Pd(II) complexes show the downfield shifts of NH_2 protons and H-2, H-5 and H-6 protons as compared to the free liand[14] values. This suggests that bonding of 3,4-diaminobenzoic acid to metal is through both the nitrogen atoms of the amino groups (Structure I). The carboxylic acid group of 3,4-diaminobenzoic acid in the above compounds is uncoordinated because the C−O stretching vibration of carboxylic acid is present between 1720 and 1730 cm^{-1} in the metal chelates[11].

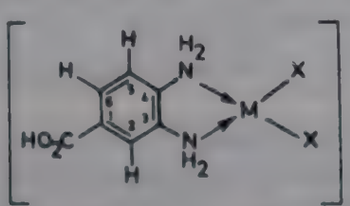

$[M(daba)X_2]$ M = Pd(II) or Pt(II)

(I)

The X-ray photoelectron spectral data of the above compounds are summarized in Table 3. The measured Pt($4d_{5/2}$) binding energies of the $[Pt(daba)X_2]$ increase in the order Cl→Br→I. The increase in binding energy of Pt($4d_{5/2}$) in the $[Pt(daba)X_2]$ may be correlated in terms of electronegativity difference between the platinum and halogen atom and in terms of platinum to ligand π-bonding[15-17]. In the platinum complexes, the latter mechanism seems to be of significance. This is expected to increase the overall positive charge on platinum due to increase in platinum-halogen π-binding in the order Cl→Br→I. On the other hand, the measured Pd($4d_{5/2}$) binding energies of $[Pd(daba)X_2]$ decrease as Cl→Br, which are in accord with the decreasing electronegativity of halogens Cl>Br>I. The N($1s$) binding energy of $M(daba)X_2$ shifts towards the higher energy as the anion changes from Cl→Br→I. This observation is the result of increase in metal halogen π-bonding in the order Cl→Br→I. The lower energies of Cl($2p_{3/2}$ Br($3p_{1/2,3/2}$) and I($3d_{5/2}$) in the above compounds (see Table 2) as compared to the corresponding value of free halide ions [Cl($2p_{3/2}$) (200 eV), Br($3p_{1/2,3/2}$) (189.0 eV) and I($3d_{5/2}$) (620.0 eV)] suggest that there is electron drift towards halogens in the platinum compounds[19].

Solutions of $[M(daba)X_2]$ in 1% sodium bicarbonate solution were initially tested against P388 lymphocytic leukemia cells using concentrations of 1,20 and 100 μg/ml[6,9]. Those compounds showing I.D.$_{50}$ (50% inhibitory dose) values less than 20 μg/mol were further tested at varying concentrations of 1 to 20 μg/ml. The I.D.$_{50}$ values obtained for $[Pt(daba)Cl_2]$, $[Pt(daba)Br_2]$ and $[Pt(daba)I_2]$ are 9.5, 9.4 and 18.2 μmol/litre respectively. The I.D.$_{50}$ values obtained for $[Pt(daba)Cl_2]$, $[Pt(daba)Br_2]$ are less than that of *cis*platin (I.D.$_{50}$ = 17 μmol/litre) whereas I.D.$_{50}$ value of $[Pt(daba)I_2]$ is comparable to that of *cis*platin. The chloride and bromide ions as leaving ligands in the $[Pt(daba)Cl_2]$ and $[Pt(daba)Br_2]$ complexes seem to be lost inside the cancer cells with the formation of $[Pt(daba)(H_2O)(OH)]^+$ because the leaving ligands in the above complexes have intermediate liability of Pt−Cl and Pt−Br bonds. The cytotoxicity of cancer cells is probably due to attack of $[Pt(daba)(H_2O)(OH)]^+$ on guanine and cytosine region of DNA, producing damage which is responsible for selective death of cancer cells. A similar mechanism operates for cytotoxicity of *cis*platin[20]. However, the Pt−I bonds in $[Pt(daba)I_2]$ give rise to a kinetically inert complex which is not able to give cytotoxic species like $[Pt(daba)(H_2O)(OH)]^+$ inside the cancer cells. Therefore, a different mechanism is operative for cytotoxicity of $[Pt(daba)I_2]$ than $[Pt(daba)Cl_2]$ and $[Pt(daba)Br_2]$ complexes. Thus, the iodo compounds may be looked upon as a new class of futuristic antitumor agents.

Acknowledgement

We are grateful to the CSIR, New Delhi, and DAE, India for financial supports and to Dr M P Chitnis for helping us in the cytotoxic studies.

References

1 Prestayko A W, Crooke S T & Carter S K, *Cisplatin: current status and new developments* (Academic Press, New York), 1980.

2 Hacker M P, Douple E B & Krakoff I H, *Platinum coordination complexes in cancer chemotherapy* (Martinus-Nijhoff, Boston), 1984.

3 Stern E W, in *Platinum and other metal coordination compounds in cancer chemotherapy*, edited by M Nicolini (Martinus-Nijhoff, Boston), 1988, pp 519-526.

4 Cleare M J, *Coord chem Rev*, 12 (1974) 349.

5 Siegmann D W, Brenners D & Carraher Jr C E, *Polym Mater Sci Eng*, 59 (1988) 535.

6 Kumar L, Kandasamy N R, Srivastava T S, Amonkar A J, Adwankar M K & Chitnis M P, *J inorg Biochem*, 23 (1985) 1.

7 Cornnors T A, Jones M, Ross W C J, Braddock P D, Khokhar A R & Tobe M L, *Chem Biol Interactions*, 5 (1972) 415.

8 Jain N & Srivastava T S, *Inorg chim Acta*, 128 (1987) 151.

9 Jain N, Srivastava T S, Satyamoorthy K & Chitnis M P, *J inorg Biochem*, 33 (1988) 1.

10 Geary W J, *Coord chem Rev*, 7 (1971) 81.

11 Williams D H & Fleming I, *Spectroscopic methods in organic chemistry*, 4th Edn (McGraw-Hill, London), 1987, pp 29-62.

12 Kidani Y, Asano Y & Nogi M, *Chem Pharm Bull*, 27 (1979) 2577.

13 Gidney P M, Gillard R D & Heaton B T, *J chem Soc Dalton Trans*, (1973) 132.

14 James T L, *Nuclear magnetic resonance in biochemistry* (Academic Press, New York), 1975, p. 79.

15 Jolly W L, *Coord chem Rev*, 21 (1974) 47.

16 Carlson T A, *Photoelectron and auger spectroscopy* (Plenum, New York), 1975, p. 341.

17 Watson R A, *Coord chem Rev*, 21 (1976) 63.

18 Kumar G, Blackburn J R, Albridge R G, Moddeman W E & Johnes M M, *Inorg Chem*, 11 (1972) 296.

19 Puniyani S & Srivastava T S, *Inorg chim Acta*, 131 (1987) 95.

20 Pasini A & Zunini F, *Angew Chem Int Ed Engl*, 26 (1987) 615.

Indian Journal of Chemistry
Vol. 31A, February 1992, pp. 106-109

Mixed ligand complexes of palladium(II) and platinum(II) with methionine and purines

Badar Taqui Khan* & K Murali Mohan
Department of Chemistry, University College of Science, Osmania University, Hyderabad 500 007, India
and
G Narsa Goud
Department of Chemistry, Nizam College, Osmania University, Hyderabad 500 001, India

Received 6 March 1991; revised 13 May 1991; accepted 9 July 1991

Mixed ligand complexes of Pt(II) and Pd(II) with methionine (MetH) as primary ligand and purines—adenine, guanine and hypoxanthine—as secondary ligands have been prepared by reacting *cis*-[Pd(MetH)Cl_2] (**1**) and *cis*-[Pt(MetH)Cl_2] (**2**) with adenine, guanine and hypoxanthine in 1:1 molar ratio. The complexes have been characterized on the basis of analytical, conductivity, and IR, electronic and ^{1}H NMR spectral data. In these complexes methionine is bound to the metal ion through amino nitrogen and sulphur atoms. The purines are bound to the metal ion through nitrogen (N_7) of the five-membered ring and are present in a configuration *trans* to methionine sulphur. This indicates a higher *trans* directing ability of sulphur compared to that of amino nitrogen of methionine. Conductivity data show that the complexes are 1:1 electrolytes.

The discovery of anticancer activity of certain platinum coordination compounds[1] and use of *cis*-Pt$(NH_3)_2Cl_2$ (*cis*-platin) as a drug in the treatment of several human tumours[2], have led to an upsurge in research on platinum complexes. Efforts have been directed to synthesize less toxic analogues of *cis*-platin and to study their interaction with tumours[3-6], and DNA and its constituents[7-11]. The preparation of less toxic complexes than *cis*-platin is possible by the substitution of amine ligands in these complexes by molecules found in biological systems[7,11]. Many Pt(II)-amino acid mixed ligand complexes and ternary complexes of Pd(II) and Pt(II) with amino acids and nucleosides[12-15] were also reported. Earlier we had reported[16] the interaction of *cis*-dichloroplatinum(II)-amino acid complexes with some purines, pyrimidines and nucleosides. In this paper, we report the interaction of *cis*-[Pd(MetH)Cl_2] and *cis*-[Pt(MetH)Cl_2] (MetH = methionine) with adenine, guanine and hypoxanthine.

Materials and Methods

Chromatographically pure DL-methionine and purine bases were obtained from Sigma Chemical Company (USA). Samples of palladium chloride and potassium hexachloroplatinate (AR, 98% pure) were purchased from Johnson Matthey Company (UK) and Alfa Ventron (USA) respectively. Palladium chloride was converted to potassium tetrachloropalladate(II) by heating with potassium chloride solution in 1:2 molar ratio[17]. $K_2[PtCl_6]$ was converted to potassium tetrachloroplatinate by reduction with hydrazinium hydrochloride[18]. The parent complexes, *cis*-dichloro(methionine)palladium(II), **1**[19], and *cis*-dichloro-(methionine)platinum(II), **2**[20], were prepared by published procedures.

The elemental analyses of the complexes were carried out at the Australian Mineral Development Laboratories, Australia and CDRI, Lucknow, India. The chloride present in the complexes was estimated at Indian Institute of Chemical Technology (IICT), Hyderabad, India, using a published procedure[21]. IR spectra were recorded in KBr on IR-12 Perkin-Elmer 577, 337 and Beckman spectrophotometers. The electronic spectra of the complexes were recorded on a Shimadzu UV 240 instrument at IICT, Hyderabad, India. ^{1}H NMR spectra were recorded on JEOL 100, 270 and 500 MHz instruments at the University of Hyderabad, IISc, Bangalore and TIFR, Bombay respectively. IR spectra in the region 100-600 cm^{-1} were recorded on a PE 983 spectrophotometer at RSIC, IIT, Madras, India. A digisun digital conductivity meter No. DI 909 was used to measure the conductivities of the complexes in DMSO water. The physical, analytical and conductivity data of the complexes are given in Table 1.

The mixed ligand complexes (chloro)(adenine)-

Table 1—Analytical and conductivity data of Pd(II) & Pt(II)-methionine-purine mixed ligand complexes

Complex No.	Complex (Colour)	Found (Calc.), %				Molar conductivity (mho cm^{-2} mol^{-1})
		C	H	Cl	N	
1	[Pd(MetH)Cl_2] (Yellow)					465 (H_2O) 2 (DMSO)
2	[Pt(MetH)Cl_2] (Yellow)					404 (H_2O) 10 (DMSO)
3	[Pd(MetH)(Ade)Cl]Cl.2H_2O (Yellow)	24.67 (24.12)	3.98 (4.04)		16.64 (16.87)	320 (H_2O) 36 (DMSO)
4	[Pt(MetH)(Ade)Cl]Cl (Pale yellow)	21.60 (21.71)	2.42 (2.03)	13.20 (12.88)		310 (H_2O)
5	[Pd(MetH)(Gua)Cl]Cl.2H_2O (Yellow)	23.70 (23.37)	4.20 (3.92)			350 (H_2O)
6	[Pt(MetH)(Gua)Cl]Cl (Yellow)	21.35 (21.18)	2.62 (2.84)	12.83 (12.52)		318 (H_2O)
7	[Pd(MetH)(Hypo)Cl]Cl.H_2O (Pale yellow)	24.60 (24.98)	3.37 (3.56)		13.96 (14.56)	326 (H_2O) 32 (DMSO)
8	[Pt(MetH)(Hypo)Cl]Cl.H_2O (Pale yellow)	21.32 (21.07)	2.30 (2.48)	12.70 (12.45)		295 (H_2O)

(methionine)palladium(II) chloride dihydrate (**3**), (chloro)(adenine)(methionine)platinum(II) chloride (**4**), (chloro)(guanine)(methionine)(palladium)(II) chloride hydrate (**5**), (chloro)(guanine)(methionine)platinum(II) chloride (**6**), (chloro)(hypoxanthine)(methionine)palladium(II) chloride monohydrate (**7**) and (chloro)(hypoxanthine)(methionine)platinum(II) chloride monohydrate (**8**) were prepared by reacting *cis*-(dichloro)(methionine)-palladium(II) (**1**) or *cis*-(dichloro)(methionine)-platinum(II) (**2**) with adenine/guanine/hypoxanthine in a 1:1 mole ratio in aqueous medium. When the purine was added to **1** or **2** and the contents heated on a water bath for 0.5-3.0 hr, the colour of the solution changed from yellow to light yellow. The reaction mixtures were cooled and filtered to remove unreacted traces of the parent complex and the ligand. The solution was further concentrated when pale yellow complexes **3-8** were precipitated which were washed with ethanol and dried with ether; yield, 70%.

Results and Discussion

The analytical data of the complexes (Table 1) are in agreement with the stoichiometries proposed for the complexes. The infrared spectra of the parent complexes *cis*-[Pd(MetH)Cl_2] and *cis*-[Pt(MetH)Cl_2] show strong peaks at 1705 and 1710 cm^{-1} respectively, which are characteristic of the uncoordinated carboxylic acid group of methionine[22]. Due to the hydrogen bonding interactions in these complexes, broad peaks were observed in the region 3000-3245 cm^{-1}. In the far IR region, peaks were observed at 570-592 cm^{-1} which are assigned to $\nu M-N$ mode arising due to the coordination of methionine to Pd(II) or Pt(II) through amino nitrogen. Peaks observed in the region 485-505 cm^{-1} are assigned to $\nu M-S$ which indicate coordination of ether sulphur atom of methionine. The two absorptions in the region 320-395 cm^{-1} are characteristic of *cis* configurations for the chloro ligands. These assignments are in agreement with the coordination mode of methionine with Pt(II) established by Freeman *et al.*[23,24].

The ligand adenine shows $\nu C=N+\nu C=C$ at 1335-1460 cm^{-1} while guanine and hypoxanthine show peaks due to $\nu C=N+\nu C=C$ at 1510 cm^{-1} and 1600 cm^{-1} respectively in their IR spectra. In all the mixed ligand complexes these peaks were shifted to lower frequencies indicating the involvement of one of the ring nitrogens in coordination to the metal ion[25].

In the IR spectra of the complexes **3-6** strong and broad peaks occurring in the region 1600-1710 cm^{-1} are assigned to $\nu C=O$ of the uncoordinated carboxylic acid group and NH_2 deformation modes of adenine and guanine which overlap with each other. The NH_2 groups of adenine and guanine do not participate in bonding to the metal ion under normal conditions, because the electron pair present on the nitrogen of the NH_2 is delocalized into the ring π-system and is not available for donation[26].

In the far IR spectra of mixed ligand complexes the $\nu M-N$ frequencies that arise due to the coordination

of methionine and purines are observed in the range 507-585 cm^{-1}. The peaks observed in the range 417-490 cm^{-1} are assigned to $\nu M-S$. In all the mixed ligand complexes, a single peak observed in the range 315-370 cm^{-1} is assigned to the $\nu M-Cl$ which indicates that only one chloride is present in the coordination sphere of the metal ion.

The electronic spectra of the complexes **3, 4, 5, 6, 7** and **8** show peaks at 265 nm ($\varepsilon_{max} = 9.60 \times 10^3$), 268 nm ($\varepsilon_{max} = 1.38 \times 10^4$), 248 nm ($\varepsilon_{max} = 1.32 \times 10^4$), 274 nm ($\varepsilon_{max} = 4.86 \times 10^3$), 250 nm ($\varepsilon_{max} = 2.07 \times 10^4$) and 255 nm ($\varepsilon_{max} = 9.62 \times 10^3$), respectively which can be assigned to $\pi \rightarrow \pi^*$ transitions of coordinated purine. The $\pi \rightarrow \pi^*$ transitions occur in adenine at 268 nm ($\varepsilon_{max} = 1.13 \times 10^4$) and 262 nm ($\varepsilon_{max} = 1.30 \times 10^4$). Guanine and hypoxanthine show this transition at 246 nm ($\varepsilon_{max} = 0.94 \times 10^4$) and 250 nm ($\varepsilon_{max} = 1.05 \times 10^4$) respectively.

The *d-d* transitions in Pd(II) complexes are extremely weak with ε values less than 10. Therefore, they could not be recorded with reasonable accuracy. In Pt(II) mixed ligand complexes weak *d-d* transitions occur in the region 240-280 nm.

In ^1H NMR spectrum of methionine a signal at δ 2.08 ppm is assigned to $S-CH_3$ protons while a triplet centered at δ 2.60 ppm is due to the methylene protons of the methionine. The proton present on the α-carbon atom of the methionine gives a signal at δ 3.30 ppm.

In the ^1H NMR spectra of complexes **1** and **2**, a singlet at δ 2.48 and a multiplet centered at δ 2.54 ppm are assigned to $S-CH_3$ protons. The downfield shift of the signal by 0.4 ppm and 0.46 ppm, respectively in these complexes indicates the involvement of sulphur in coordination to the metal ion. *cis*-$[Pd(MetH)Cl_2]$ showed peaks due to β-CH_2 and γ-CH_2 protons at δ 2.66 and δ 2.79 ppm, whereas the corresponding signals merged in a peak at 2.80 ppm in *cis*-$[Pt(MetH)Cl_2]$. Compared to uncoordinated methionine these signals are shifted downfield which again confirms the coordination of $S-CH_3$ group of the amino acid to the metal ion. The signal due to α-CH proton occurs at 3.55 and 4.10 ppm observed in the spectra of these complexes, respectively can be assigned to α-CH proton of methionine. These peaks are shifted downfield to the extent of 0.25 and 0.80 ppm respectively in complexes **1** and **2** indicating the coordination of NH_2 group to the metal ion.

The ^1H NMR spectrum of adenine shows a doublet at δ 8.32 and 8.20 ppm due to C_8H and C_2H protons (see structure I). The ^1H NMR spectrum of complex **3** shows a doublet at 8.46 and 8.40 ppm whereas in complex **4** these peaks appear at 8.61 and 8.56 ppm respectively. Since signals due to the C_2H and C_8H

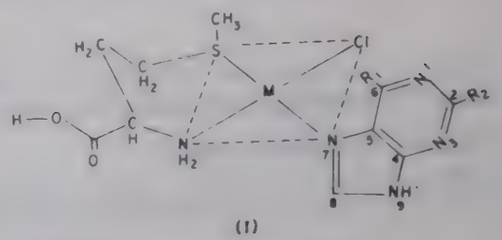

(I)

M = Pd (II) or Pt (II)
$R_1 = NH_2, R_2 = H$ Adenine
$R_1 = OH, R_2 = NH_2$ Guanine
$R_1 = OH, R_2 = H$ Hypoxanthine

protons (see structure I) are shifted downfield in complexes **3** and **4** by 0.14, 0.20 and 0.29 and 0.36 ppm respectively, it can be inferred that N_7 or N_1 of adenine is involved in coordination in these complexes[27]. In the complex **3** the signals due to α-CH, β-CH_2, γ-CH_2 and S-CH_3 are observed as a triplet at 4.10, triplets of doublets centered at 2.53 and 2.46, a triplet at 2.68 and a singlet at 2.24 ppm respectively. These signals are observed as a triplet centered at 4.28, triplets of doublets centered at 2.91 and 2.77, a triplet at 2.58 and a singlet at 2.31 ppm, respectively in complex **4**. The signal due to the proton of α-carbon is observed as a triplet because of the spin-spin coupling with β-CH_2 protons. The β-CH_2 protons show triplets of doublet due to the spin-spin coupling with adjacent α-CH and γ-CH_2 protons. The γ-CH_2 protons are observed as a triplet due to coupling with β-CH_2 protons. The $S-CH_3$ protons give a single peak.

The ^1H NMR spectrum of guanine in D_2O (basic) shows a signal at 7.68 ppm due to the C_8H protons. In the ^1H NMR spectrum of complex **6**, this signal appears at 8.78 ppm. Since this peak is shifted downfield with respect to the ligand, N_7 of the guanine is proposed as the binding site. The signals due to methionine α-CH, β-CH_2, γ-CH_2 and S-CH_3 protons are observed in the region 4.21-2.51 ppm. The signal due to the proton on the α-carbon is observed at 4.21 ppm. A triplet centered at 3.20 ppm is assigned to the γ-CH_2 protons. A doublet appearing at 2.75 and 2.63 ppm is assigned to β-CH_2 protons. The S-methyl protons are observed at 2.51 ppm.

The ^1H NMR spectrum of hypoxanthine exhibits two signals at 8.08 and 7.87 ppm respectively which are assigned to C_8H and C_2H protons. The ^1H NMR spectrum of complex **7** shows these signals at 8.33 and 7.75 respectively. Since signal due to C_8H protons is shifted more, N_7 of hypoxanthine is proposed as the coordination site. In complex **8** these signals are observed at 8.97 and 8.08 ppm respectively. As the signal due to the C_8H protons is shifted more (0.89 ppm) in comparison to that due to C_2H protons (0.21 ppm), it is proposed that N_7 of hypoxanthine is the coordination site in complex **8**. The protons of methionine give peaks in the region 4.18-2.22 ppm

and 4.11-2.21 ppm respectively in complexes **7** and **8**. Based on the above data a general structure (I) is proposed for complexes **3-8**.

In all the complexes **1-8**, both methionine and purines bind to the metal ion, Pd(II) or Pt(II), through soft donor atoms sulphur and nitrogen, since both metal ions are soft acids[28].

The reaction of purines with *cis*-[Pt(MetH)Cl_2] and *cis*-[Pd(MetH)Cl_2] is very fast, as compared to that with *cis*-[Pt(GlyH)Cl_2], *cis*-[Pt(Ala)Cl_2] and K[Pt(His)Cl_2][16]. This difference in the rates of reaction is solely due to the high *trans* directing ability of the coordinated sulphur group.

Since *trans* directing ability of coordinated sulphur in complexes **1** and **2** is greater as compared to that of coordinated nitrogen, it is proposed that purine is occupying a position *trans* to sulphur group of amino acid eventhough one more site *trans* to amino group is also available for the purine.

All these complexes show high molar conductivities in water, because of the ionization of the free COOH group in the complex. However, in DMSO some of these complexes show low conductivities (below 40 mhos cm^{-2} mol^{-1}). On the basis of the conductivity data and chloride estimation of a few complexes, it is proposed that all the complexes are 1:1 electrolytes.

Acknowledgement

Two of us (KMM and GNG) are thankful to the CSIR, New Delhi for financial support to carry out this work.

References

1 Rosenberg B, Vancamp L, Troska J E & Monsour V H, *Nature*, 222 (1965) 365.
2 (a) Rosenberg B, Vancamp L, *Cancer Res*, 30 (1970) 1977.
(b) Rozencweig M, Vonhoff D D, Salvik M & Muggia F M, *Ann intern Med*, 86 (1977) 803.
3 Cleare M J & Hydes P C, *Metal ions in biological systems*, Vol 11, Chap 1, edited by H Sigel (Marcel Dekker, New York), 1980, 4.
4 Rejdijk J, *Pure Appl Chem*,59 (1987) 181.
5 Sherman S E & Lippard S J, *Chem Rev*, 87 (1987) 1153.
6 Barnard C F J, Cleare M J & Hydes P C, *Chem Brit*, 12 (1986) 1001.
7 Hadjiliadis N & Pneumatikakis G, *J chem Soc Dalton Trans*, (1978) 1691.
8 Barton J K & Lippard S J, *Metal-nucleic acid interactions*, Vol 1, edited by T Spiro (John Wiley, New York), 1980, 32.
9 (a) Pneumatikakis G, *Inorg chim Acta*, 66 (1982) 131.
(b) Pneumatikakis G, *Inorg chim Acta*, 93 (1984) 5.
10 Ulrinch K J & Bruce M R, *Inorg chim Acta*, 80 (1983) 1.
11 Pneumatikakis G, *Polyhedron*, 3 (1984) 9.
12 (a) Lalit Kumar & Srivastava T S, *Inorg chim Acta*, 80 (1983) 47.
(b) Srivastava T S, *Inorg Biochem*, 26 (1986) 45.
13 Karselouri S, Geroutis & Hadjiliadis N, *Inorg chim Acta*, 23-25 (1987) 135.
14 Pneumatikakis G, *Polyhedron*, 3 (1984) 15.
15 Pneumatikakis G, *Inorg chim Acta*, 80 (1983) 89.
16 (a) Khan B T, Vijaya Kumari S & Narsa Goud G, *J coord Chem*, 2 (1982) 19.
(b) Narsa Goud G, Ph.D. thesis, Osmania University, Hyderabad, India, 1983.
(c) Khan B T, Narsa Goud G & Vijaya Kumari S, *Inorg chim Acta*, 80 (1983) 45.
(d) Khan B T, Murali Mohan K & Narsa Goud G, *Trans Met Chem*, 15 (1990) 407.
(e) Khan B T, Najmuddin K, shamsuddin S & Zakeeruddin S M, *Inorg chim Acta*, 170 (1990) 129.
17 Hartley F R, *The chemistry of platinum and palladium* (John Wiley, New York), 1973, 14.
18 Gurbe H L, *Hand book of preparative inorganic chemistry*, Vol 2, edited by G Brauer (Academic Press, New York), 1965, 1571.
19 Volshtein L M, Krylova L F & Mogilevkina M F, *Russ J inorg Chem*, 11 (1966) 333.
20 Volshtein L M & Mogilevkina M F, *Russ J inorg Chem*, 8 (1963) 304.
21 Steyermark A, Calancertle R & Eontrersar E M, *J Association of Analytical Chemists*, 55 (1972) 680.
22 Mcauliffe C A, *J chem Soc (A)*, 4 (1967) 641.
23 Freeman H C & Golomb M L, *Chem Commun*, (1970) 1523.
24 Appleton G, Connor T, Jeffery W & Hall R J, *Inorg Chem*, 271 (1988) 130.
25 Mikulski C M, Braccia D, Delacato D, Flemina J & Fleming D, *Inorg chim Acta*, L13 (1985) 106.
26 Marzelli L G, *Prog inorg Chem*, 23 (1977) 255.
27 (a) Terzis A, Hadjiliadis N, Rivert R & Theophanides T, *Inorg chim Acta*, 12 (1975) 25.
(b) Khan B T, Vijaya Kumari S & Narsa Goud G, *Indian J Chem*, 21A (1982) 264.
28 (a) Hartley F R, *The chemistry of platinum and palladium* (John Wiley, New York), 1973.
(b) Pearson R G, *Hard & soft acids and bases* (Dowder Hutchisen & Ross, Stronsberg, Pensylvania), 1973.

Indian Journal of Chemistry
Vol. 31A, February 1992, pp. 110-115

Syntheses of polystyrene supported chelating resin containing the schiff base derived from 3-formylsalicylic acid and *o*-hydroxybenzylamine and its copper(II), nickel(II), iron(III), zinc(II), cadmium(II), zirconium(IV), molybdenum(V and VI) and uranium(VI) complexes

A Syamal* & M M Singh
Department of Chemistry, Regional Engineering College, Kurukshetra 132 119

Received 11 February 1991; revised and accepted 10 October 1991

A series of new polystyrene-anchored coordination complexes has been synthesized by the reaction of metal complex/metal salt with the chelating resin containing the schiff base derived from *o*-hydroxybenzylamine and 3-formylsalicylic acid. The polymer supported complexes have the formulae: PS-LCu.DMF, PS-LNi.3DMF, PS-LFeCl.2DMF, PS-LZn.DMF, PS-LCd.DMF, PS-LMoOCl.DMF, PS-$LMoO_2$.DMF, PS-LUO_2.DMF and PS-$LZr(OH)_2$.2DMF (where PS-L = deprotonated polystyrene bound schiff base). The polymer supported complexes have been characterized by elemental analysis, infrared, electronic and EPR spectra and magnetic susceptibility measurements. The polymer-anchored copper(II), nickel(II), iron(III) and molybdenum(V) complexes are paramagnetic while the zinc(II), cadmium(II), molybdenum(VI), uranium(VI) and zirconium(IV) complexes are diamagnetic. The magnetic and EPR data indicate the magnetically dilute nature of the complexes. The shifts of the $\nu(C=N)$ (azomethine) and $\nu(C-O)$ (phenolic) modes have been followed to find out the donor sites of the ligand. The polymer-anchored copper(II) complex is square-planar, zinc(II) and cadmium(II) complexes are tetrahedral, nickel(II), iron(III), molybdenum(V and VI) and uranium(VI) complexes are octahedral and zirconium(IV) complex is pentagonal-bipyramidal. The structures of the complexes are comparable with the corresponding metal complexes of the non-anchored ligand.

In recent years there has been considerable research interest in the immobilisation of transition metal complexes on insoluble polymer supports[1-4]. These insoluble polymer supported complexes have the advantages over their soluble counter-parts of easy separation from the reaction mixture leading to operational flexibility, of their facile regenerability and of higher stability[5-7]. Several polystyrene supported ligands like dipyridyldiimine[8], dithiocarbamate[9], porphyrin[10], acetylacetone[11], 8-hydroxyquinoline[12] and their metal complexes have been reported. Although the schiff bases are the most versatile and thoroughly studied ligands[13,14], only a few schiff bases have been immobilised to polystyrene matrix[15-18]. In this paper the syntheses and characterization of coordination complexes of the polymer bound schiff base(I) with copper(II), nickel(II), iron(III), zinc(II), cadmium(II), molybdenum(V and VI), uranium(VI) and zirconium(IV) are described.

Materials and Methods

Chloromethylated polystyrene containing 0.0012 mol of chlorine per gram of resin and 1% cross-linked with divinylbenzene was the product of Polysciences Inc. (U.S.A.). 3-Formylsalicylic acid[19], zirconium(IV) diacetate[20], ammonium oxopentachloromolybdate(V)[21] and bis(acetylacetonato)dioxomolybdenum(VI)[22] were synthesized by following the literature procedures. Copper(II) acetate monohydrate, acetylacetone and ammonium molybdate tetrahydrate were purchased from Glaxo Laboratories. Dimethylformamide, salicylic acid, zinc(II) acetate dihydrate and nickel(II) acetate tetrahydrate were the products of S.D.'s Fine Chemicals. The polymer-anchored schiff base (I, PS-LH_2) was prepared by following the reported procedure[23]. Solvents were dried over molecular sieves.

Infrared spectra were recorded in KBr on a Beckman IR-12 spectrophotometer calibrated with polystyrene. EPR spectra were recorded at 77 K in polycrystalline solids on a Varian V4502-12 X-band EPR spectrometer with 100 kHz modulation using diphenylpicrylhydrazide as the *g*-marker. Frequency was monitored with the help of a frequency meter. The *g* values were corrected using a second order correction, $7A^2/4H_{2,3}$ for copper(II) and $17A^2/4H_{3,4}$ for molybdenum(V)[24]. Electronic spectra were recorded on a Cary model 2390 spectrophotometer attached with a reflectance arrangement. The magnetic susceptibilities were determined at room tem-

perature by the Gouy method using Hg [$Co(NCS)_4$] as the standard. A double-ended one-side sealed glass tube with zero diamagnetic susceptibility was used for better accuracy. The diamagnetic correction of the metal-ligand system was computed using the Pascal's constants following a procedure specially designed for polymer-supported complexes[25]. The magnetic susceptibilities were corrected for diamagnetism and temperature independent paramagnetism term [copper(II), 60×10^{-6} cgs units; molybdenum(V), 55×10^{-6} cgs units; nickel(II), 200×10^{-6} cgs units; iron(III), zero].

To a weighed amount (~0.15 g) of polymer-anchored complex of copper(II), nickel(II), zinc(II) or cadmium(II), acetic acid (4*N*, 20 ml) was added and the mixture was heated on a water bath for ½h for copper(II) and cadmium(II), 1h for zinc(II) and 2h for nickel(II) complex. The resin was filtered and washed with acetic acid (2*N*) followed by distilled water. Nickel was estimated in the filtrate gravimetrically as bis(dimethylglyoximato)nickel(II). Cadmium and zinc were determined complexometrically by titrating with EDTA using xylenol orange as the indicator. Copper was analysed iodometrically by titrating with a standard solution of sodium thiosulphate. The iron(III) complex was decomposed by heating the complex with HCl (6*N*, 25 ml) on a water bath for 1h. The resin was filtered and washed with 2*N* HCl followed by distilled water. Iron was determined in the filtrate by reducing it with a solution of tin(II) chloride and then titrating with a standard solution of potassium dichromate. Molybdenum(V/VI) complex was converted to MoO_3 by decomposing the complex with a few drops of conc. HNO_3 and conc. H_2SO_4 and then igniting in a muffle furnace at 500°C. MoO_3 was dissolved in a dilute solution of NaOH (6*N*) and molybdenum was analysed gravimetrically as bis(8-hydroxyquinolinato)dioxomolybdenum(VI). Uranium and zirconium were determined gravimetrically as U_3O_8 and ZrO_2 respectively after decomposing the complexes with a few drops of conc. HNO_3 and then igniting. Chlorine analysis was done by fusing the complex with NaOH pellets and Na_2O_2 in a nickel crucible and then precipitating as AgCl. Dimethylformamide was analysed by heating the complex at 160°C in an air oven for 3h. In Ni(II) complex the temperature was 170°C and in Fe(III) and Zn(II) complexes the temperature was 180°C.

The per cent reaction conversion(*P*) of the polymer-anchored complex was calculated by use of the formula:

$$P = \frac{\text{observed metal ion percentage}}{\text{calculated metal ion percentage}} \times 100$$

The calculated metal ion percentage was computed on the basis of 100% conversion from polymer-anchored ligand to polymer-anchored complex.

Synthesis of PS-LM.xDMF, where M = copper(II), nickel(II), zinc(II), cadmium(II), dioxouranium(VI) and x = 1 or 3

The polymer-anchored schiff base (0.5 g) was swelled in dimethylformamide (20 ml) for 45 min. To this a dimethylformamide solution (30-50 ml) of the appropriate metal acetate (0.001 mol) in dimethylformamide was added and the mixture was refluxed on a suspended type heating mantle for 8h while stirring magnetically and then cooled to room temperature. The solid precipitated was filtered under reduced pressure, washed with dimethylformamide, ethanol, methanol and acetone and was dried *in vacuo* at room temperature.

Synthesis of PS-LMoO$_2$.DMF

The polymer-anchored schiff base (0.5 g) was swelled in dry dimethylformamide (20 ml) for 45 min in a three-necked flask fitted with a condenser, and N_2 gas was passed through the mixture. To this a filtered dimethylformamide solution (40 ml) of $(NH_4)_2$ [$MoOCl_5$] (0.325 g, 0.001 mol) was added and the mixture was refluxed under N_2 atmosphere on a heating mantle for 5h while stirring magnetically. The mixture was cooled to room temperature, filtered under reduced pressure, washed with dimethylformamide, absolute ethanol and petroleum ether(boiling range 60-80°C). The compound was dried *in vacuo* at room temperature.

Synthesis of PS-LFeCl.2DMF

The polymer-anchored schiff base (0.5 g) was allowed to swell in dimethylformamide (20 ml) for 45 min. To this suspension, a dimethylformamide solution (40 ml) of MoO_2 (acetylacetone)$_2$ (0.33 g, 0.001 mol) was added and the mixture was refluxed on a heating mantle for 5h while stirring magnetically. The mixture was cooled to room temperature. The compound was filtered under reduced pressure, washed with dimethylformamide, ethanol and acetone and dried *in vacuo* at room temperature.

Synthesis of PS-LZr(OH)$_2$.2DMF

The polymer-anchored schiff base (1.0 g) was swelled in dimethylformamide (30 ml) for 45 min. To this a dimethylformamide solution (50 ml) of anhydrous ferric chloride (0.24 g, 0.0015 mol) was added and the mixture was refluxed for 6h while stirring magnetically, the condensor being fitted with a calcium chloride guard tube. The mixture was cooled to room temperature and the resin was fil-

tered under reduced pressure, washed with dimethylformamide, absolute ethanol and petroleum ether (boiling range 60-80°C) and dried *in vacuo* at room temperature.

Synthesis of PS-LZr(OH)$_2$.2DMF

The polymer-anchored schiff base (0.5 g) was swelled in dimethylformamide (25 ml) for 45 min. To this a freshly prepared dimethylformamide solution (40 ml) of zirconium(IV) acetate (0.001 mol, prepared *in situ*) was added and the mixture was refluxed on a heating mantle for 5h while stirring magnetically. The mixture was cooled to room temperature and the compound was filtered under reduced pressure, washed with dimethylformamide, ethanol and petroleum ether (boiling range 60-80°C). The compound was dried *in vacuo* at room temperature.

Results and Discussion

The polymer-bound chelating agent(I) is insoluble in water and common coordinating and non-coordinating solvents. Dimethylformamide is a convenient solvent for studying the metal loading property of I due to its high dielectric constant and ability to swell the polymer support and to dissolve a large number of metal salts and metal complexes. The results of the synthetic studies (Table 1) demonstrate that I is capable of chelating a variety of transition metal ions. The synthetic reactions were carried out in 1:2 molar ratio [1:1.5 in case of iron(III) complex] of polymer-bound ligand:metal salt/metal complex. The analytical data show that the polymer bound complexes have the compositions: PS-LCu.DMF, PS-LiNi.3DMF, PS-LZn.DMF, PS-LCd.DMF, PS-FeCl.2DMF, PS-LMoO$_2$.DMF, PS-LMoOCl.DMF and PS-LZr(OH)$_2$.2DMF.

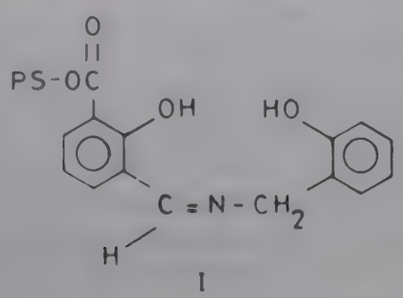

I

The metal ions are coordinated by tridentate chelating moieties anchored on the polymer and the rest of the coordination sphere is completed by DMF, O^{2-}, Cl^- or OH^-. Assuming that each metal ion is coordinated to one ligand, the metal ions were found to occupy 39 to ~100% (Table 1) of the available sites in I. It is evident from the per cent reaction conversion of the complexes that there is no apparent correlation between per cent reaction conversion and size of the metal ion. The polymer bound chelating ligand(I) is yellow in colour. As the reacton of polymer bound ligand with metal salt/metal complex proceeds, the colour of the polymer changes from yellow to cream, green or yellowish

Table 1—Analytical and magnetic susceptibility data of polymer supported complexes

Complex	Found(calc.)%			Binding capa. of resin[a] (mmol metal per gram of resin × 10^{-2})	Conversion (%)	Magnetic moment[b], BM Temp. (K)
	M	Cl	DMF			
PS-LNi.3DMF	4.3 (4.28)		16.5 (15.97)	73.3	98	3.02 (302)
PS-LCu.DMF	2.4 (2.42)		2.95 (2.79)	37.8	46	1.87 (289)
PS-LFeCl.2DMF	2.2 (2.19)	1.5 (1.38)	6.0 (5.71)	39.4	51	6.01 (298)
PS-LZn.DMF	4.7 (4.67)		5.2 (5.45)	71.9	86	Diamag.
PS-LCd.DMF	4.1 (4.13)		2.8 (2.68)	36.5	46	Diamag.
PS-LMoOCl.DMF	3.2 (3.20)	1.2 (1.18)	2.6 (2.44)	33.3	43	1.65 (300)
PS-LMoO$_2$.DMF	6.0 (5.99)		4.7 (4.55)	62.5	79	Diamag.
PS-LZr(OH)$_2$.2DMF	6.75 (6.82)		10.9 (10.81)	74.6	99	Diamag.
PS-LUO$_2$.DMF	6.6 (6.59)		2.3 (2.02)	27.3	39	Diamag.

(a) Calculated from the observed value of metal percentage in the polymer-anchored complex.
(b) Calculated using the relation $\mu_{eff} = 2.83 \times \chi_M^{corr} \times T)^{1/2}$ B.M.

brown depending on the metal ion. The colour of the polymer-anchored complexes does not change even after prolonged washing with dimethylformamide, methanol, ethanol and petroleum ether. The metal ions can be easily stripped from the polymer-anchored complexes by dilute acids with little effect on the ability to regenerate the polymer-anchored complexes. Regeneration studies indicated that after six complete cycles, about 90% of the ligand sites were still available for complexation. The polymer-anchored complexes lose the coordinated dimethylformamide completely on heating in air.

The infrared spectrum of the schiff base derived from salicylaldehyde and *o*-hydroxybenzylamine exhibits a band at 1655 cm^{-1} characteristic of $\nu(C=N)$ (azomethine)[26]. The polymer bound schiff base(I) exhibits the $\nu(C=N)$ (azomethine) at 1645 cm^{-1} (Table 2). This band shifts to lower energy by 5-20 cm^{-1} in the infrared spectra of the polymer-anchored complexes indicating the nitrogen coordination of the schiff base(I)[27]. The $\nu(C-O)$ (phenolic) occurs at 1550 cm^{-1} in the schiff base(I) and this band moves to higher energy by 5-10 cm^{-1} in the polymer-anchored complexes. This is indicative of the phenolic oxygen coordination of the schiff base(I). In the non-anchored schiff base the $\nu(C-O)$ (phenolic) occurs at 1540 cm^{-1}. The IR data preclude the presence of a dimetallic structure and indicate a monometallic structure as in the event of a dimetallic structure the $\nu(C-O)$ (phenolic) is expected to shift to higher energy by >10 cm^{-1} (ref. 28). The absence of $\nu(OH)$ in the complexes indicates the deprotonation of both the phenolic hydroxyl groups. Thus, the IR data indicate the ONO donor tridentate behaviour of I.

Dimethylformamide exhibits the $\nu(C=O)$ at 1680 cm^{-1} which shifts to lower energy by 20-45 cm^{-1} in the complexes indicating the oxygen coordination of DMF[29].

PS-$LMoO_2$.DMF exhibits the ν_s (OMoO) and ν_{as} (OMoO) at 930 and 862 cm^{-1} respectively which occur in the usual range (ν_s, 892-964 cm^{-1}; ν_{as}, 840-925 cm^{-1}) observed for the majority of Mo(VI) complexes[30]. The appearance of these bands indicates a *cis*-MoO_2 structure as only the ν_{as} (OMoO) is expected in case of *trans*-MoO_2 structure since the ν_s (OMoO) is IR-inactive. The IR data rule out the presence of a chain structure ...Mo=O ...Mo=O ... in which $\nu(Mo=O)$ is expected[14] to occur at <850 cm^{-1}. PS-LMoOCl.DMF shows $\nu(Mo=O)$ at 945 cm^{-1} which occurs in the usual range (900-1007 cm^{-1}) observed for the majority of Mo(V) complexes[14]. PS-LUO_2.DMF exhibits ν_{as}(OUO) at 905 cm^{-1} which occurs in the usual range (870-950 cm^{-1}) observed for the majority of *trans*-UO_2 complexes[31]. The force constant (f_{U-O}) was calculated according to the method given by McGlynn *et al.*[32] and the value obtained (6.80 mdyne/Å) is in the expected range. The U−O bond distance was calculated using Jones' equation[33]: $R_{U-O}=1.08f^{-1/3}+1.17$ and the value was found to be 1.74 Å which is in the usual range (1.60-1.92 Å) reported for the majority of U(VI) complexes. PS-$LZr(OH)_2$.2DMF exhibits a band at 1115 cm^{-1} due to the δ(Zr-OH)[34].

The complexes PS-LCu.DMF and PS-LMoOCl.DMF record magnetic moments of 1.87 and 1.65 BM respectively characteristic of magnetically dilute Cu(II) and Mo(V) complexes[14,35]. It is of interest to note that the Cu(II) and Mo(V) complexes of the schiff base derived from salicylaldehyde and *o*-hydroxybenzylamine are dimetallic and are involved in antiferromagnetic exchange[14,27]. The presence of bulky diamagnetic polymer backbone has prevented the M−M interaction in polymer-anchored complexes and has resulted in the formation of magnetically dilute complexes. The ESR spectra of the complexes described later also support the magnetically dilute nature of the complexes. PS-LFeCl.2DMF and PS-LNi.3DMF exhibit magnetic moments of 6.01 and 3.02 B.M. respectively which are in the normal range expected for magnetically dilute octahedral complexes of Fe(III) and Ni(II)[36]. PS-LZn.DMF, PS-LCd.DMF, PS-$LMoO_2$.DMF, PS-$LZr(OH)_2$.2DMF and PS-LUO_2.DMF are diamagnetic as expected for d^0, d^{10} and f^0 systems. A tetrahedral structure for Zn(II) and Cd(II) complexes, octahedral structure for Mo(VI) and U(VI) complexes and pentagonal-bipyramidal structure for the Zr(IV) complex are suggested. The structures of the complexes are compar-

Table 2—Infrared spectral data of polymer supported ligand and complexes[a]

Complex/ligand	$\nu(C=N)$	$\nu(C-O)$ (phenolic)	$\nu(C=O)$ (DMF)
PS-LH_2	1645	1550	—
PS-LNi.3DMF	1635	1555	1635
PS-LCu.DMF	1625	1560	1655
PS-LFeCl.2DMF	1635	1560	1650
PS-LCd.DMF	1630	1560	1645
PS-LZn.DMF	1635	1560	1645
PS-LMoOCl.DMF	1640	1560	1650
PS-$LMoO_2$.DMF	1630	1555	1650
PS-$LZr(OH)_2$.2DMF	1630	1560	1655
PS-LUO_2.DMF	1625	1560	1660

[a]All IR bands are in cm^{-1}.

able with those of the corresponding complexes of non-anchored ligand[14,37,38].

The polymer-anchored complexes are insoluble in water and common organic solvents and this precluded the recording of their solution electronic spectra. The complexes also do not form a good mull with nujol and hence nujol mull spectra could not be recorded. Hence, the reflectance spectra of the complexes were recorded. The electronic spectrum of PS-LCu.DMF exhibits a band at 17700 cm^{-1}, characteristic of $CuNO_3$ coordination sphere[37]. The complex does not exhibit a band at 8000-10000 cm^{-1} which precludes the presence of a tetrahedral structure[39]. PS-LNi.3DMF exhibits bands at 8300, 15100 and 25000 cm^{-1} due to the $^3A_{2g} \rightarrow {}^3T_{2g}$ (ν_1), $^3A_{2g} \rightarrow {}^3T_{1g}(F)$ (ν_2) and $^3A_{2g} \rightarrow {}^3T_{1g}(P)$ (ν_3) transitions respectively in an octahedral field. The $\nu_2:\nu_1$ ratio of PS-LNi.3DMF is 1.82 which lies in the usual range (1.6-1.82) reported for the majority of octahedral Ni(II) complexes[40]. The spectral parameters of the Ni(II) complex calculated by following the method of Lever[41] are as follows: $Dq = 830$ cm^{-1}, $B' = 884$ cm^{-1}, $\beta = B'/B = 0.83$, $\beta^0 = 17\%$. The reduction of the Racah parameter from the free ion value of 1056 cm^{-1} and β^0 value of 17% indicate the presence of strong covalent interaction of the metal ion with the ligand[40]. PS-LMoOCl.DMF shows two bands at 12250 and 17400 cm^{-1} due to the $^2B_2 \rightarrow {}^2E$ and $^2B_2 \rightarrow {}^2A_1$ transitions respectively[30]. The band due to the $^2B_2 \rightarrow {}^2B_1$ transition, which occurs around 19600 cm^{-1} was not observed and it is probably covered underneath the intense $^2B_2 \rightarrow {}^2A_1$ transition.

In the polymer-anchored complexes the bulky diamagnetic polymer backbone forces the metal centres to remain considerably separated and as a result dipolar broadening is reduced to a minimum. The complexes exhibit reasonably good EPR spectra in polycrystalline solids in the absence of a host coordination complex diluent. PS-LCu.DMF shows two g values ($g_\parallel = 2.23$, $g_\perp = 2.08$) indicating the presence of a tetragonal type symmetry about the Cu(II) ion[42]. The EPR parameters are as follows: $A_\parallel^{Cu} = 180 \times 10^{-4}$ cm^{-1}, $A_\perp^{Cu} = 45 \times 10^{-4}$ cm^{-1}. The EPR data indicate that $g_\perp < g_\parallel$ and $A_\perp < A_\parallel$ which are according to the expectations. $g_\parallel$ is normally < 2.3 for covalent environments and is ≥ 2.3 for ionic environments[43]. The $g_\parallel$ value of the Cu(II) complex identifies it as a covalent type complex. G was calculated using the relation[43], $G = (g_\parallel - 2.002)/(g_\perp - 2.002)$. The Cu(II) complex exhibits a G value of 2.92 which identifies the ligand as a strong field ligand; strong field ligands are known to exhibit the G value < 4.0. The in-plane covalence parameter, α_{Cu}^2 was calculated using the relation[43]

$$\alpha_{Cu}^2 = (g_\parallel - 2.002) + \frac{3}{7}(g_\perp - 2.002) - \frac{A_\parallel}{0.036} + 0.04$$

The overlap integral (S) is related to α as follows[43]:

$$\alpha^2 - 2S\alpha\alpha' + (\alpha')^2 = 1$$

S has a value of 0.076 for oxygen donor atoms and 0.093 for nitrogen donor atoms. The Cu(II) complex contains NO_3 coordination sphere and, hence, an S value of 0.080 was calculated for NO_3 donors from the above values and this was used for the calculation of α_{Cu}^2. The copper(II) complex exhibits α_{Cu}^2 value of 0.80 which indicates the covalent nature of the complex. The bonding in a complex is regarded more covalent if the α_{Cu}^2 value is smaller; $\alpha_{Cu}^2 = 1.0$ indicates complete ionic bonding and $\alpha_{Cu}^2 = 0.5$ suggests complete covalent bonding. The bonding in a complex is considered more covalent if the $(\alpha')^2$ value is larger; $(\alpha')^2 = 0$ indicates complete ionic bonding. The $(\alpha')^2$ value of 0.27 in the Cu(II) complex identifies it as a covalent complex. The parameter κP_d is the Fermi contact contribution to the coupling and P_d is the dipolar contribution. P_d was calculated using the relation[44]: $P_d = (A_\perp - A_\parallel)/0.78$. κ was calculated using the relation: $\kappa = -(A_\parallel/P_d) - 0.48$. The Cu(II) complex exhibits the P_d and κ values of 1.73×10^{-2} cm^{-1} and 0.50 respectively. The reduction of the P_d value from the free ion value of 3.5×10^{-2} cm^{-1} is indicative of the presence of covalent bonding in the complex[44]. The positive value of κ predicts $A_\parallel > A_\perp$ and the same was observed. The Cu(II) complex exhibits the Fermi contact contribution (A) value of 8.65×10^{-3} cm^{-1}.

The Mo(V) complex exhibits the following EPR parameters: $g_\parallel = 1.92$, $g_\perp = 1.96$, $g_{av} = 1.95$, $A_\parallel^{Mo} = 83 \times 10^{-4}$ cm^{-1} and $A_\perp^{Mo} = 24 \times 10^{-4}$ cm^{-1}. The EPR data indicate that $g_\parallel < g_\perp$ and $A_\perp < A_\parallel$ which are according to expectations. The spectral shape, g and A values of the Mo(V) complex are comparable to those of a monometallic complex [MoO(salicylaldehyde-*o*-aminophenol)$Cl \cdot CH_3OH$] ($g_\parallel = 1.923$, $g_\perp = 1.947$, $g_{av} = 1.939$, $A_\parallel^{Mo} = 82.6 \times 10^{-4}$ cm^{-1}, $A_\perp^{Mo} = 36.8 \times 10^{-4}$ cm^{-1})[45]. This similarity suggests that the stereochemistry and electronic structure in these systems are identical. The absence of $\Delta M_S = 2$ line around 1500 gauss in the EPR spectra of the present Cu(II) and Mo(V) complexes rules out the presence of M – M interaction. A rough calculation indicates that the metal ions are situated on the phenyl rings (of polystyrene) which are seven to eight styrene units apart when the per cent conversion is 100% and the styrene units are more than eight when the per cent conversion is < 100%. Thus a magnetically dilute environment around the metal ions is main-

tained since the pathway for M − M interaction is reduced. But the polymer is 1% crosslinked with the polymer chains overlapped and twisted and this may bring some reactive groups closer leading to M − M interaction which was undetectable by the EPR method. The Ni(II) complex exhibits single line EPR spectrum with g_{av} value of 2.03 which is characteristic of octahedral Ni(II) complexes[24].

Acknowledgement

The authors are grateful to the Department of Atomic Energy (Govt. of India), Bombay for financial support of the work.

References

1 Kartz M R & Hendricker D G, *Polymer*, 27 (1986) 1641.
2 Suzuki T M, Yokoyama T, Matsunga H & Kimura T, *Bull chem Soc Japan*, 55 (1986) 865.
3 Davies J A & Sood A, *Asian J Chem*, 1 (1989) 1.
4 Kurimura Y & Takato K, *J chem Soc Faraday Trans-I*, 84 (1988) 841.
5 Akelah A & Sherrington D C, *Chem Rev*, 81 (1981) 557.
6 Pillai V N R, *Synthesis*, (1980) 1.
7 Akelah A, Abbasi M M & Awad M K H, *Indian J Chem*, 25A (1986) 923.
8 Melby R S, *J Am chem Soc*, 97 (1975) 4044.
9 Suzuki T M & Yokoyama T, *Polyhedron*, 2 (1983) 127.
10 Pederson C J & Frensdroff H K, *Angew Chem Int Edn Engl*, 11 (1972) 16.
11 Bhaduri S, Khawaja H & Khanwalkar V, *J chem Soc Dalton Trans-I*, (1982) 445.
12 Park S Y & Sung H, *Pollimo*, 6 (1982) 323; *Chem Abstr*, 97 (1982) 216859.
13 Holm R H, Everett (Jr) G W & Chakravorty A, *Prog inorg Chem*, 7 (1966) 83; Dey K, *J scient ind Res*, 33 (1974) 76.
14 Syamal A & Maurya M R, *Coord chem Rev*, 95 (1989) 183.
15 Akelah A, Masoud M S & Kandil S S, *Indian J Chem*, 25A (1986) 918; Brostert K & Klagner D, *Ger Offen DE*, (1987) 3611421; *Chem Abstr*, 108 (1988) 187452.
16 Laverty J J & Gardlund Z G, *Polym Sci, Part A-1*, 9 (1971) 243.
17 Topich J, *Inorg Chem*, 21 (1982) 2079.
18 Chen X & Y Wu, *Yingyong Huaxue*, 6 (1989) 13; *Chem Abstr*, 111 (1989) 8252; Leiser K H, *Ger Offen DE*, (1980) 3019159; *Chem Abstr*, 96 (1982) 53207.
19 Duff J C & Bills E J, *J chem Soc*, (1932) 1987.
20 Syamal A & Maurya M R, *Indian J Chem*, 24A (1985) 836.
21 Syamal A & Maurya M R, *Inorg Synth*, 26 (1989) 36.
22 Chin C J, McDonald J W & Newton W E, *Inorg Chem*, 15 (1976) 2612.
23 Syamal A & Singh M M, *J polym Materials*, 6 (1989) 175.
24 Goodman B A & Raynor J B, *Advan inorg chem Radiochem*, 13 (1973) 135.
25 Syamal A & Singh M M, *Transition Met Chem*, (in press).
26 Syamal A, Ahmed S & Kumar D, *Indian J Chem*, 28A (1989) 783.
27 Teyssi P & Charrette J J, *Spectrochim Acta*, 19 (1963) 1407.
28 Sinn E & Harris C M, *Coord chem Rev*, 4 (1969) 391.
29 Krishnamurty S S & Soundarajan S, *J inorg nucl Chem*, 28 (1966) 1689.
30 Steifel E I, *Prog inorg Chem*, 22 (1977) 1.
31 Tokii T, Muto Y, Kato M, Imai K & Jonassen H B, *J inorg nucl Chem*, 34 (1972) 3377; Hsieh A T, Sheahan R M & West B O, *Aust J Chem*, 28 (1975) 885; Shankar G, Premkumar R R & Ramalingam S K, *Polyhedron*, 5 (1986) 991.
32 McGlynn S P, Smith J K & Neely W C, *J chem Phys*, 35 (1961) 105.
33 Jones L H, *Spectrochim Acta*, 10 (1958) 395; 11 (1959) 409.
34 Kharitanov Y Y, Zaitsev L M, Bochkarer G S & Evastafeva O P, *Russ J inorg Chem*, 7 (1964) 1617.
35 Syamal A, *Coord chem Rev*, 16 (1975) 309.
36 Cotton F A & Wilkinson G, *Advanced inorganic chemistry*, 3rd Edition (Wiley Eastern Pvt Ltd, New Delhi) 1985, 867.
37 Syamal A & Kale K S, *Transition Met Chem*, 4 (1979) 298.
38 Syamal A & Kumar D, *Synth React inorg met org Chem*, 10 (1980) 63; Syamal A, Ahmed S & Kumar D, *Indian J Chem*, 28A (1989) 783; Syamal A & Gupta B K, *Indian J Chem*, 21A (1982) 83; *J Indian chem Soc*, 59 (1982) 697; *Acta Cien Indica*, 8C (1982) 107; Hsieh A T T, Sheahan R M & West B O, *Aust J Chem*, 28 (1975) 885.
39 Foster D & Goodgame D M L, *J chem Soc*, (1964) 2796; *Inorg Chem*, 4 (1965) 823.
40 Syamal A, *Chem Educ*, 4 (1987) 33.
41 Lever A B P, *Inorganic electronic spectroscopy* (Elsevier, Amsterdem), 2nd Edition, 1984..
42 Gersman H R & Neiman R, *J chem Phys*, 36 (1962) 3221.
43 Kivelson D & Neiman R, *J chem Phys*, 35 (1961) 149.
44 Drago R S, *Physical methods in chemistry*, 2nd Edition (W B Saunders Company, London) 1976, 487.
45 Taylor R D, Todd P C, Chasteen N D & Spence J T, *Inorg Chem*, 18 (1979) 44.

Indian Journal of Chemistry
Vol. 31A, February 1992, pp. 116-119

Solvent extraction equilibria of palladium(II) complex with 5,8-diethyl-7-hydroxydodecan-6-one oxime in some organic diluents

B Siladitya, K Sen & S P Bag*
Department of Chemistry, Jadavpur University, Calcutta 700 032, India

Received 13 June 1991; revised 3 October 1991; accepted 22 November 1991

The extraction equilibrium behaviour of palladium(II) from aqueous chloride solution with 5,8-diethyl-7-hydroxydodecan-6-one oxime (LIX 63) in seven organic solvents has been studied. The overall extraction equilibrium is represented by the expression:

$$Pd^{2} + 2\,HL_{(o)} \overset{K_{ex}}{\rightleftharpoons} PdL_{2(o)} + 2H^{+}$$

The distribution constant (K_{DR}) of LIX 63, determined between the organic solvents and water, increases in the order: *n*-heptane < *n*-hexane < carbon tetrachloride < benzene < dichloromethane < toluene < chloroform. The extraction equilibrium constant (K_{ex}) is found to be independent of the solvent. Acid dissociation constant of the reagent LIX 63 is determined from 70% (vol/vol) ethanol-water medium and the overall extraction is predicted to be independent of the nature of solvent.

The successful commercial development of high molecular weight hydroxy oxime series of copper-selective extractants[1,2] has led to much interest in the chemistry of transition metal-hydroxy oxime systems. Equilibrium behaviour as well as kinetics of the extraction of copper(II) with 5,8-diethyl-7-hydroxydodecan-6-one oxime (LIX 63) in chloroform has been reported[3].

The existing methods of hydrometallurgical extraction of platinum group metals often present difficulties due to the slow rate of formation of the extractable complexes from aqueous chloride medium[4]. However, because of the strong tendency of palladium to form chloro complexes in aqueous solutions, its extraction with LIX 63 seems to be interesting because of the higher selectivity with respect to the base metals and platinum and also for the higher acidity that it can tolerate for the complete extraction.

Materials and Methods

Absorbances were recorded using a Shimadzu Graphicord UV 240 spectrophotometer. All *p*H measurements were made with a Systronics 335 digital *p*H meter, calibrated daily with buffer solutions of *p*H 2.00, 4.00 and 7.00. A box type Sambros reciprocating shaker with a shaking speed of 200 oscillations per minute was used to equilibrate the aqueous and organic phases, whenever needed.

A stock solution of palladium (5.65×10^{-2} *M*) was prepared by dissolving palladium(II) chloride (Johnson-Mathey, 99.9% purity) in 1 *M* hydrochloric acid. It was standardised gravimetrically by dimethyl glyoxime. 5,8-Diethyl-7-hydroxydodecan-6-one oxime, commercially available as LIX 63, was kindly supplied by Henkel Corporation, Tucson, Arizona in the undiluted form. All other reagents used were of AR grade. Organic diluents used for the extraction studies were distilled twice and were presaturated with water whenever required.

Extraction procedure for determination of K_{DR}

For determination of the distribution constants (K_{DR}) of the extractant (LIX 63) in different solvents, known amounts of the extractant in 25 ml of the diluent were equilibrated for 4 hr with aqueous phases (750 ml). The aqueous phases were presaturated with the respective diluents and were buffered at *p*H 5 with acetic acid and sodium acetate; the ionic strength of the aqueous phases was maintained constant (0.1 *M*) with respect to chloride ion. After equilibration, the concentrations of the extracted ligand were determined spectrophotometrically[5]. K_{DR} values were then calculated.

Extraction procedure for equilibrium studies

The distribution of palladium(II)-LIX 63 complex between aqueous and organic phases was examined as a function of aqueous *p*H, chloride ion concentration, metal ion concentration and the reagent con-

centration in the bulk organic phase. LIX 63 was dissolved in seven different solvents to form the respective organic phases. A 10 ml portion of aqueous metal solution of known concentration was shaken for 2 hr with equal volume of ligand solution in the desired solvent. The metal concentration in the aqueous phase after the extraction was determined spectrophotometrically by potassium iodide[6] and extracted metal (as Pd-LIX 63 complex) concentration in the organic phase was also determined spectrophotometrically at the wavelength 330 nm against a blank solution, prepared similarly.

Procedure for determination of acid dissociation constant of the extractant

Acid dissociation constant of the extractant was determined by *p*H-metric titration of 0.01 *M* nitric acid in absence and in presence of 0.01 *M* LIX 63 at 30°C in ethanol-water medium (70% volume/volume) (having a constant ionic strength of 0.1 *M*) against 0.125 *M* sodium hydroxide solution. *p*H values were measured with reference to the 70% (v/v) ethanol-water standard state by applying appropriate correction factors[7]. the pK_a value, evaluated by the procedure of Irving and Rossotti[8], was found to be 10.73.

Results and Discussion

Distribution of LIX 63 between organic diluents and water

The distribution ratio D_R of LIX 63 was determined between various organic solvents and water at *p*H 5 and at temp. 25°C. A small variation in *p*H (around 5) had no significant effect on D_R.

Distribution ratio (D_R) of a weakly acidic reagent like LIX 63 between organic and aqueous media can be described in terms of its acid dissociation constant (K_a), its Nernst distribution constant (K_{DR}) and, when applicable, its organic phase polymerisation constant, (K_p).

As can be seen from Fig. 1, which summarises the results of the distribution experiments at *p*H 5, there is no concentration dependence on D_R of the extractant (LIX 63) for chloroform, toluene, dichloromethane and benzene; this signifies that polymer formation does not occur in the examined range of concentration (10^{-3} *M*-10^{-2} *M*) of LIX 63 in these solvents.

However, in carbon tetrachloride, *n*-hexane and *n*-heptane, the D_R values increased with an increase in the concentration of the extractant, probably owing to the self-association. The log K_{DR} values thus obtained in different diluents vary from 3.3 to 5.3 (Table 1, Fig. 1) depending upon the solvent in the following order: *n*-heptane < *n*-hexane < carbon tetrachloride < benzene < dichloromethane < toluene < chloroform.

Table 1—Extraction parameters of solvent extraction of palladium(II) with LIX 63 in seven organic diluents

Solvent	Dielectric constant	log K_{DR}	K_{ex}	log K_f K_{DC}
Chloroform	4.806	5.3	1.17	32.13
Toluene	2.438	4.9	0.94	31.23
Dichloromethane	9.08	4.6	0.95	30.64
Benzene	2.284	4.2	1.26	29.96
Carbon tetrachloride	2.238	4.1	1.62	29.87
n-Hexane	1.890	3.9	0.94	29.23
n-Heptane	—	3.3	0.91	27.96

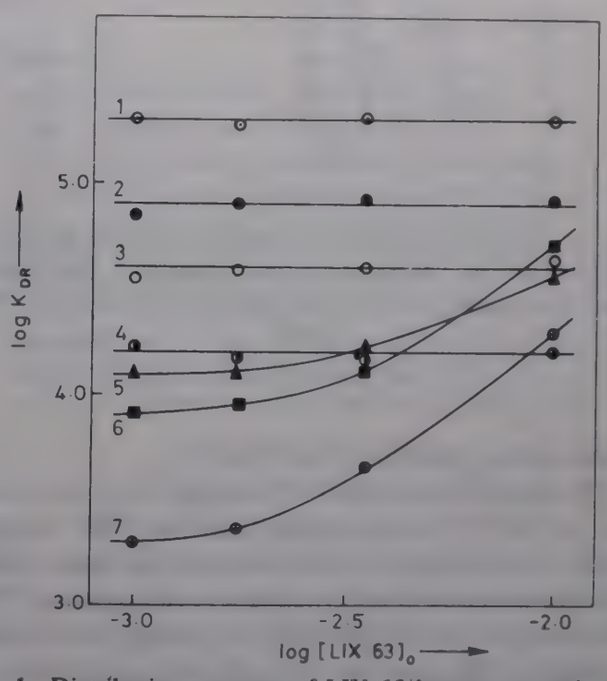

Fig. 1—Distribution constant of LIX 63 between organic solvents and the aqueous phase of *p*H 5 (I=0.1 *M* with NaCl) [1, Chloroform; 2, toluene; 3, dichloromethane; 4, benzene; 5, carbon tetrachloride; 6, *n*-hexane; 7, *n*-heptane].

It is thus observed from the distribution experiments that the possibility of self-association comes into play for the totally non-polar solvents. With increasing polarity of the solvents, this possibility diminishes, if not disappears completely.

Moreover, the log K_{DR} values of the extraction in different solvents showed an increasing trend with increasing dielectric constant, with a deviation in the case of dichloromethane. This might well be due to the fact that the contribution of the dispersion interaction (δ_d) to the solubility parameter (δ) for dichloromethane is significantly lower in comparison to that for other diluents used.

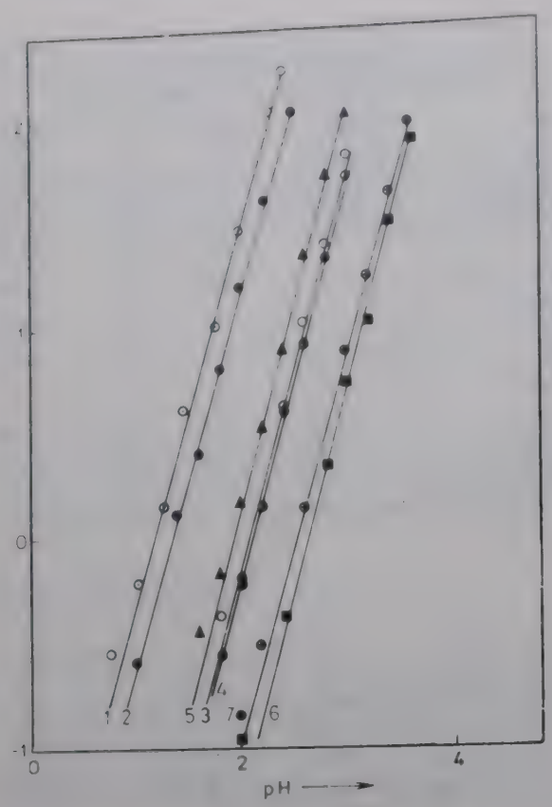

Fig. 2—Distribution ratio of palladium(II) as a function of *p*H at $[HL]_0 = 3.69 \times 10^{-2}$ *M* [1, chloroform; 2, toluene; 3, dichloromethane; 4, benzene; 5, carbon tetrachloride; 6, *n*-hexane; 7, benzene].

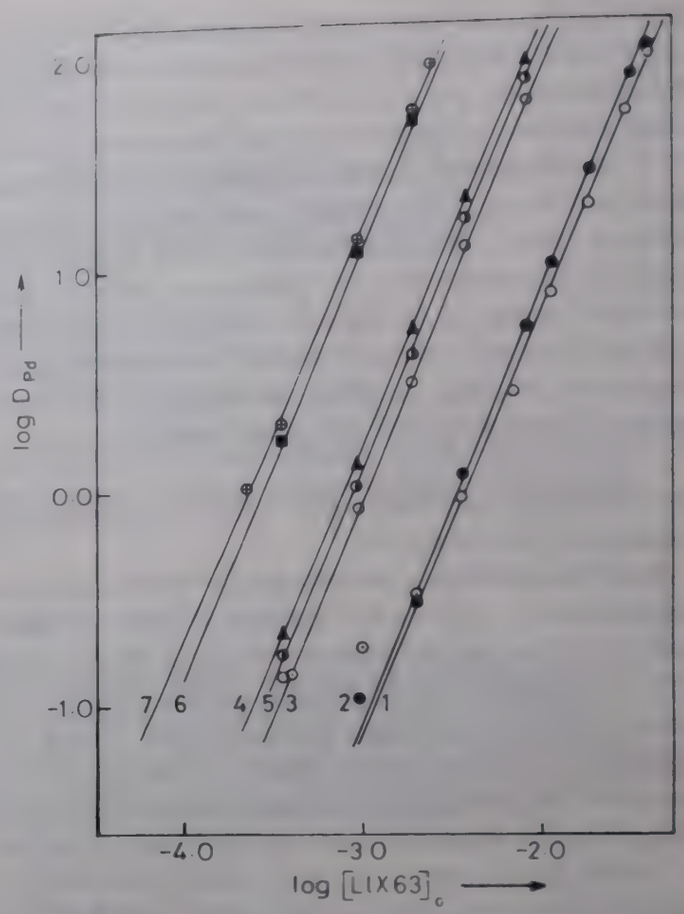

Fig. 3—Distribution ratio of palladium(II) as a function of LIX 63 concentration in the organic solvents [1, Chloroform *p*H 2.4; 2, toluene *p*H 2.5; 3, dichloromethane *p*H 3.0; 4, carbon tetrachloride *p*H 3.0; 5, benzene *p*H 3.0; 6, *n*-hexane *p*H 3.6; 7, *n*-heptane *p*H 3.6].

Extraction of palladium with LIX 63

The distribution ratio of the metal (D_{Pd}) as a function of LIX 63 concentration in the bulk organic phase and of aqueous metal ion concentration, chloride ion concentration and *p*H was determined. The distribution ratio of the metal was found to be independent of the aqueous chloride ion concentration in the $[Cl^-]$ range 0.005 *M* to 0.1 *M* and of the metal ion concentration as well, indicating that extraction of any polymeric species involving the metal is non-operative.

The log D_{Pd} vs *p*H plots at a constant extractant concentration and at a constant ionic strength (0.1 *M* with respect to chloride ion) of the aqueous phases yield a straight line (Fig. 2) with slopes nearly equal to two in each of the solvent systems. The analogous log D_{Pd} vs log $[LIX\ 63]_o$ plots at constant *p*H were also linear with slopes of around two in all of the diluents used (Fig. 3). These results indicate that a simple 1:2 (metal:ligand) chelate is extracted in the organic phase. The consistency of the K_{ex} values (~ 1) obtained from the corresponding log D_{Pd} vs log $[LIX63]_o$ plots for different solvents confirms that the overall extraction constant is independent of the nature of the solvents and a single metal species with identical stoichiometry is extracted in all the seven different organic diluents used. The linearity obtained in Figs 2 and 3 and the consistency of the slope values for the curves of different systems clearly indicate that self-association of the reagent (LIX 63) in carbon tetrachloride, *n*-hexane and *n*-heptane hardly has any significant effect on the overall metal-chelate-extraction systems.

Effect of solvent on extraction equilibria

Acid dissociation constant (K_a) of the reagent and the formation constant (K_f) of the complex are expected to be independent of the organic phase in extraction system, as they primarily are aqueous phase constants. On the other hand, the K_{DC} could be affected by the nature of the organic solvent. Solvent influence and hence the change in the distribution constants K_{DR} and K_{DC} is predictable from the extra-thermodynamic linear free energy relationship of Hansch and Leo[9]. When this approach is used, two hypotheses are to be applied. Firstly, if a simple chelate is extracted, the variation in the distribution constant of the metal chelate with solvent is related to the distribution constant of the ligand by the equation:

$$\log K_{DC} = n \log K_{DR} + C \qquad \ldots (1)$$

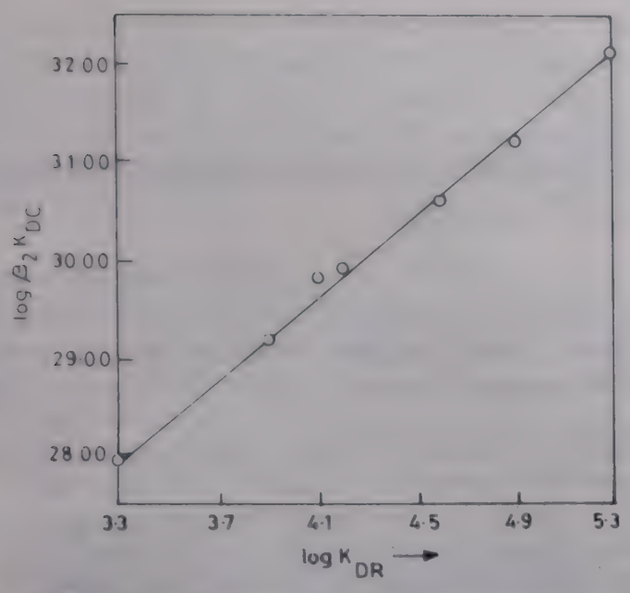

Fig. 4—Correlation between the distribution constant of LIX 63 and of its palladium-LIX 63 chelate.

where, C is a constant, accounting for other extraction parameters and 'n' is the number of ligand molecules bound to the central metal. Secondly, in systems where Eq. (1) holds good, the extraction constant will be essentially independent of the organic diluents. Hence, irregularities or deviations from the linearity in the curve, obtainable from Eq. (1), will suggest the possibility of stoichiometric differences in the extracted species in different solvents and/or existence of specific solvation effect. Fig. 4 illustrates the solvent effect where log $K_f K_{DC}$ are plotted against log K_{DR} values of the reagent (LIX 63) for respective organic diluents. Considering K_f as an organic phase-independent parameter, all variations in $K_f K_{DC}$ can be attributed to that in K_{DC} only. A reasonably good linear relationship between the two parameters (K_{DC} and K_{DR}) with a slope of two (Fig. 4) rules out any stoichiometric differences amongst the extracted species in different organic diluents, and the possibility of any specific solvent effect either. Any evidence of irregular trend had not been observed for the present Pd-LIX 63 complex as was reported in the extraction of copper with LIX 65 N[10].

References

1 Swanson R R, *U S Patent*, **3** (1965) 224, 853.
2 Feigl F, *Ber dt chem Ges*, 56 (1923) 2083.
3 Akiba K & Freiser H, *Sep Sci and Tech*, 17(5) (1982) 751.
4 Al-Bazi S J & Chow A, *Talanta*, 10A(31) (1984) 815.
5 Carter S P & Freiser H, *Anal Chem*, 52 (1980) 511.
6 Morrow J J & Markham J J, *Anal Chem*, 36(6) (1964) 1159.
7 Douheart G, *Bull Soc Chim Fr* (1968) 3222.
8 Irving H M & Rossotti H S, *J chem Soc* (1954) 2904.
9 Hansch C & Leo A J, *Substituent constant for correlation analysis in chemistry and biology* (Wiley, New York) 1979.
10 Akiba K & Freiser H, *Anal chem Acta*, 136 (1982) 329.

Indian Journal of Chemistry
Vol. 31A, February 1992, pp. 120-124

Study on the immobilization behaviour of barium, cadmium and antimony over Sn(IV) and Ce(IV) oxides

D K Bhattacharyya* & N C Dutta

Nuclear Chemistry Division, Saha Institute of Nuclear Physics, 1/AF, Bidhan Nagar, Calcutta 700 064

Received 24 July 1991; revised 10 October 1991; accepted 28 November 1991

Immobilization behaviour of barium, cadmium and antimony cations over Sn(IV) oxide and Ce(IV) oxide has been studied. High uptake for ^{125}Sb and an appreciable uptake for ^{140}Ba and ^{115}Cd is observed with both the oxides. Weighable quantities of Ba, Cd and Sb cations have been separately coprecipitated alongwith Sn(IV) and Ce(IV) hydroxides, the extent of adsorptions is found to be appreciable. After calcining the mixed mass at 1000°C for 20 hr soxhlet leach tests in deionised water at 97°C for 24 hr, repeated 7 times at an interval of one day, show low order of leachabilities for each of the cations. X-ray diffraction pattern of Sn(IV) oxide and Ce(IV) oxide contain the main reflections corresponding to the minerals cassiterite and cerianite respectively, which suffer some structural changes after adsorption of cations.

Radioactive wastes pose an alarming problem in relation to the spent nuclear fuels which are being produced from the nuclear power reactors and other sources all over the world. The process of immobilization of radioactive elements as nuclear wastes in solid forms and their subsequent disposal in the repository has attracted much attention in recent times. Various such wasteforms such as borosilicate glass[1], concrete[2], supercalcine[3,4], high alumina tailored ceramics[5], synroc[6] and silica matrix[1] have been reported. Also, immobilization of cations like Ba[7], Cs[8], Sr[9], transition elements[10] like Cu, Zn, Mn, Co, Ni, and some rare earth metal ions[11] over titania fibers in the form of mineral assemblage has been described.

Among these wasteforms described above, borosilicate glass, synroc and cement are the most thoroughly studied. Devitrification of borosilicate glass in severe hydrothermal conditions, complicated method of preparation of synroc and high leach rate of Cs and Sr in case of concretes, are some of the shortcomings because of which need is still being felt for an ideal immobilizer which might allow highest loading for a variety of cations of interest, with lowest leachability and which might withstand severe hydrothermal conditions.

Tin(IV) oxide a well known[12,13] inorganic ion exchanger, has been claimed[14] to be especially selective for bivalent transition elements and uranyl ion. The uptake characteristics of 22 cations at tracer concentrations have been also recently reported[15]. Also some fundamental properties of antimony-doped rutile related tin(IV) oxide have recently received much attention[16,17].

Tin(IV) oxide (cassiterite) has certain attractive properties[18] such as hardness 6 to 7 g/cm^3, m.p. 1127°C, insolubility (except strong alkali) in most solvents, great resistance to weathering, etc. Tetravalent Sn and Ti have many resemblances[19] such as similar values of ionic radii, octahedral covalent radii, isomorphism of SnO_2 (cassiterite) and TiO_2 (rutile), existence of distillable and readily hydrolysable tetrachlorides $SnCl_4$ and $TiCl_4$, etc. It was, therefore, expected that like titania[9,10], Sn(IV) oxide could act as a promising thermodynamically stable immobilizer for safe disposal of nuclear and industrial waste elements.

Since barium has high neutron fission yield, and its safe disposal has been always considered a problem, study on the extent of adsorption of Ba from an aqueous solution was taken up. Two other cations, viz, cadmium and antimony, though having low fission yields, have been also considered due to their well known toxic and hazardous behaviour as well as their association with industrial effluents.

A review of literatures[20] shows that while studies on ion exchange/adsorption behaviour of several quadrivalent metal oxides such as ZrO_2, TiO_2, SnO_2, SiO_2, MnO_2 and others have been reported to a considerable extent, such studies on Ce(IV) oxide are scanty, probably due to solubility limitations in mineral acids. Petro *et al.*[21] have recently reported the surface properties, structural behaviour, capacity, *pK* values etc. in respect of hydrous ceria as an ion exchanger. Ceria has a high melting point (2600°C), density (6.4 to 6.99 g/cm^3), it becomes very stable especially after strong ignition[22] and the aqueous chemistry of Ce(IV) is very much similar to

those of Zr, Hf, and tetravalent actinides. It was, therefore, decided to study it alongwith Sn(IV) oxide, as regards the extent of adsorption of Ba, Cd and Sb cations both at tracer and macro-concentrations, and the possibility of their immobilization over Ce(IV) oxide.

Materials and Methods

Stannic chloride, ceric sulphate, ammonia, sulphuric acid, hydrochloric acid and other reagents taken were of AR grade. The radioisotopes ^{140}Ba, ^{115}Cd and ^{125}Sb (in their chloride form) were supplied by BARC, Bombay, India.

Preparation of Tin(IV) oxide

Ammonia gas was bubbled through a solution of stannic chloride (100 ml, 2*M*) in HCl with vigorous stirring till precipitation was complete. Processing of the precipitate was carried out as already described[15], when a fine, granular white solid was obtained. It was stable in moderately dilute mineral acids and alkalis.

Preparation of Ce(IV) oxide

A solution of ceric sulphate in hot dil. sulphuric acid (1:6) was treated with gaseous ammonia till precipitation was complete. It was then washed with water till free from SO_4^{2-} ions, dried at ~70°C for 15 hr, ground and sieved through 120 mesh. The solid product was stable in water and moderately dilute acids.

Both Sn(IV) oxide and Ce(IV) oxide were studied by TGA and DTA techniques to ascertain the thermal stability, possible decompositions and purity (Fig. 1). A DT-40 Thermal Analyzer, Shimadzu (JAPAN) was used in the present studies.

The extent of uptake of ^{140}Ba, ^{115}Cd and ^{125}Sb over Sn(IV) oxide and Ce(IV) oxide was separately determined by equilibration for 24 hr of 0.5g of the oxide in 30 ml solution of each of the tracer cations at tracer level (~10,000 cpm) in closed L-shaped tubes at *p*H ~ 7 and room temperature. β-Activity in the solution part was measured with a Philips type G.M. liquid counter coupled with a scaler unit supplied by ECIL, Hyderabad, India. The extent of uptake and K_d values were determined in the usual way (Table 1).

The study on the uptake of these three cations was then extended to macro level concentration by separately taking Ba as $Ba(NO_3)_2$, Cd as $Cd(NO_3)_2.6H_2O$ and Sb as Sb_2O_3 in HCl and mixing with a known quantity of stannic chloride in HCl or ceric sulphate in H_2SO_4 solution, treating with ammonia till precipitation at *p*H 8-9 was complete, filtering, washing with demineralised water and making free from interfering ions. The amount of adsorbed cations was then determined knowing the amount of respective cations originally taken and that present in the filtrate, being determined spectrophotometrically. The extent of uptake limit for the cations was thus ascertained (Table 2). The mixed precipitate was then dried at ~70°C for 24 hr, powdered and pelletised (13mm × 0.5mm) by cold pressing under 50 MPa, subsequently calcined at 1000°C for 20 hr, thus converting to a compact and stable form.

Leach tests for the adsorbed Ba, Cd and Sb cations in the oxide matrices (0.5g) were then per-

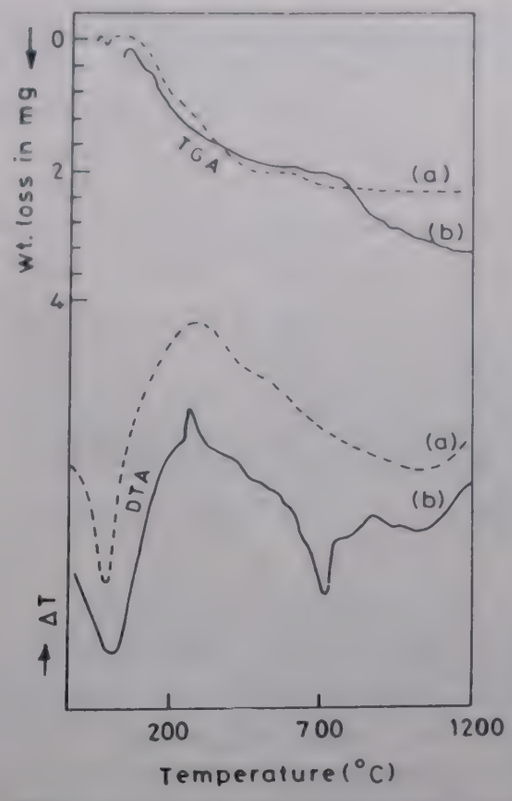

Fig. 1—TGA curves (ranges 20 mg):(a) Sn(IV) oxide and (b) Ce(IV) oxide. DTA curve (range 100mV): (a) Sn(IV) oxide and (b) Ce(IV) oxide. [Temperature increase rate = 20°C/min, upto 1200°C]

Table 1—Uptake of ^{140}Ba, ^{115}Cd and ^{125}Sb by Sn(IV) oxide and Ce(IV) oxide

Cations taken	Sn(IV) oxide		Ce(IV) oxide	
	Uptake(%)	K_d(ml/g)	Uptake(%)	K_d(ml/g)
*Ba^{2+} as ^{140}Ba (sp. activity, 4.02×10^{13} mci/g)	39.85	41.18	38.7	37.87
Cd^{2+} as ^{115}Cd (sp. activity, 5mci/g)	87.82	456.67	68.7	131.69
*Sb^{3+} as ^{125}Sb (sp. activity, 2.74×10^{11} mci/g)	99.79	23892.60	98.4	3690.00

*Supplied as carrier-free: sp. activity given as calculated.

Table 2—Wt% adsorption (maximum) of Ba, Cd and Sb cations on SnO_2 and CeO_2 adsorber

Adsorber	Adsorbed cations	Wt% adsorption
SnO_2	Ba	46.21
	Cd	54.71
	Sb	38.45
CeO_2	Ba	41.67
	Cd	62.42
	Sb	65.02

Table 3—Leachability of barium, cadmium and antimony over Sn(IV) oxide and Ce(IV) oxide immobilizers.

Adsorbed cations	Leachability ($g.cm^{-2}.d^{-1}$)						
	1	2	3	4	5	6	7
	*Immobilizer = Sn(IV) oxide**						
Ba	18.85	17.90	15.25	15.14	10.05	8.34	7.62
Cd	5.24	5.20	4.74	4.62	4.12	4.12	3.90
Sb	4.70	4.69	4.72	4.80	4.54	3.98	3.91
	*Immobilizer = Ce(IV) oxide***						
Ba	7.15	7.05	7.12	6.46	6.42	6.35	6.24
Cd	1.39	1.45	1.42	1.25	1.30	1.29	1.14
Sb	1.62	1.66	1.60	1.58	1.49	1.45	1.46

*Leachability is of the order of 10^{-7}, 10^{-12} and 10^{-6} for Ba, Cd and Sb respectively

**leachability is of the order of 10^{-7} for both Ba and Cd, and 10^{-10} for Sb.

formed in a Soxhlet apparatus by way of refluxing at 97°C for 24 hr with deionised water as leachant, repeating 7 times continuously with an interval of one day and the leached out solution was analysed by a UV spectrophotometer (Table 3).

Leachability (L_i) of the 'i'th element was determined from the following equation.

$$L_i = M_i/(C_i.S.T) \qquad (g.cm^{-2},d^{-1})$$

where,

M_i = content of the leached element 'i' (g)
C_i = content of the element 'i' (g) in the immobilizer
S = specific surface area of the immobilizer (cm^2g^{-1})
T = immersion time, days (d).

The specific surface area of the oxide sample was determined in a Surface Area Analyser (Fabricated by BARC, Bombay, India) by the single point BET method based on the physical adsorption, and using a flowing mixture of nitrogen and hydrogen. The changes in the nitrogen concentration of the flowing gas stream, were monitored by a thermal conductivity detector. The desorption signal was electronically integrated and therefrom the surface area of the sample was computed using the BET equation.

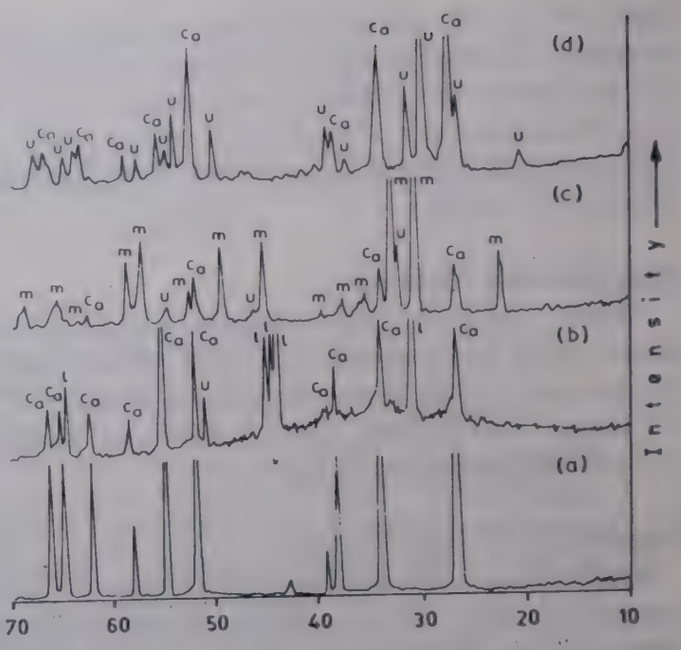

Fig. 2—X-ray diffraction patterns of (a) Sn(IV) oxide, and Sn(IV) oxide adsorbed with (b) Ba, (c) Cd and (d) Sb; symbols C_a, l, m and u identify peaks for cassiterite (SnO_2), $BaSnO_3$, $CdSnO_3$ and unknown phases respectively.

The calcined oxide samples, after adsorption of Ba/Cd/Sb cations, were analysed through X-ray powder diffraction operated in a PW 1830 Phillips Automated Diffractogram with N_2 filtered Cu-K_α radiation ($\lambda = 1.5406$ Å). The results are shown in Figs 2 and 3.

Results and Discussion

Fig. 1 shows the DTA and TGA curves of Sn(IV) oxide and Ce(IV) oxide. From the weight loss curves the formulae were ascertained to be $SnO_2.1.7H_2O$ and $CeO_2.2.2H_2O$. DTA curves indicated endothermic peaks at 80°C for both Sn(IV) and Ce(IV) oxides, which may be assigned to loss of moisture adhering to the samples. The second endotherm in case of Sn(IV) oxide corresponds to the beginning of melting whereas the endotherm in the case of Ce(IV) oxide at 720°C might be due to rapid loss of water. The exothermic peaks at 350°C for Sn(IV) oxide and at 260°C and 900°C for Ce(IV) oxides are probably due to transformation and modifications into some intermediate phases, which, however, require further investigations.

A preliminary study of heterophase distributions of tracer cations (^{140}Ba, ^{115}Cd and ^{125}Sb) in preformed hydrous oxides by batch technique at $pH \sim 7$ showed appreciable uptake indicating that these oxides were affected mainly by adsorption. It appears that a process of primary adsorption of cations takes place at the solid surface; the secondary adsorption due to tracer concentration of

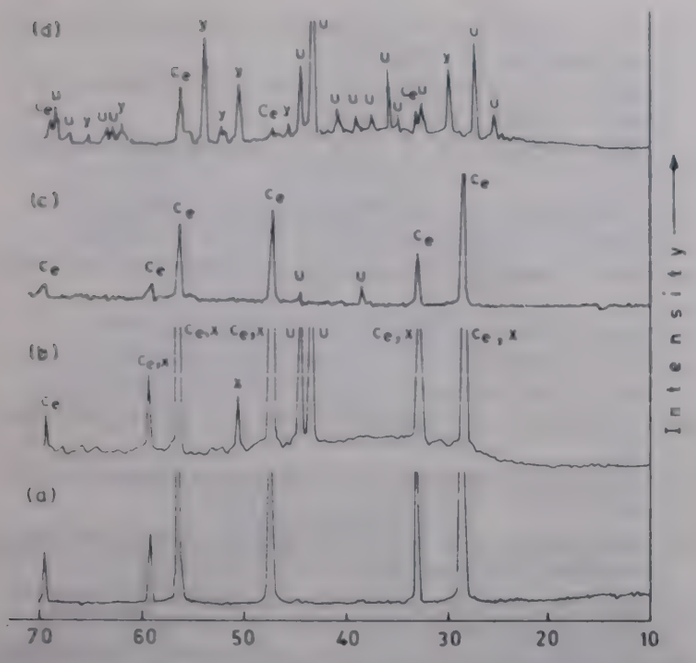

Fig. 3—X-ray diffraction patterns of (a) Ce(IV) oxide, and Ce(IV) oxide adsorbed with (b) Ba, (c) Cd and (d) Sb; symbols C_e, x, y and u identify peaks for cerianite (CeO_2), $BaCeO_3$, Ce_2O_2Sb and unknown phases respectively.

cations is negligible. The comparatively low uptake (%) and K_d values of Ba^{2+} at tracer concentration, seems to be due to its comparatively large ionic radius, low ionic charge (compared to Sb^{3+} ion) and hence low polarizability (α) which do not allow it to occupy suitable positions in the outerpart of the double layer because of weak electrostatic and dipole interactions with the potential forming ions. Also, the ionic radius of $Cd^{2+} > Sb^{3+}$, and charge of $Cd^{2+} < Sb^{3+}$. Consequently, the polarizability of $Cd^{2+} < Sb^{3+}$ which favours the uptake order: Ba < Cd < Sb (Table 1).

The interactions of cations at macro scale were studied by precipitating hydroxides of the Sn(IV) and Ce(IV) (fixed quantity) in presence of varying proportions Ba, Cd and Sb cations separately at *p*H 8-9. The wt% adsorptions (Table 2) were apparently much more than the tracer scale activity adsorption percentage. In fact, at the macro scale, metal hydroxides were the adsorbents, which adsorbed the cations more easily than that expected from hydrous oxides on the basis of the mechanism stated above and the secondary adsorption, which is more feasible in the concentrated solution. Moreover, on aging the precipitate, the cations may go into the bulk of the solid forming ionic cage by way of coulombic interactions and thus get trapped. It was observed that the tracer scale adsorption order Ba < Cd was maintained also in macro scale. But the adsorption of Sb^{3+} was found to be lesser than that of Ba^{2+} or Cd^{2+} ion in the Sn(IV)-Sb(III) system, probably due to the possibility of colloid formation, partial hydrolysis in the solution due to the amphoteric character of the cations concerned during the process of co precipitation at alkaline *p*H.

However, this effect was not observed in the adsorption order for Ba < Cd < Sb in the Ce(IV) hydroxide system, which may be attributed to the difference of properties of Sn^{4+} and Ce^{4+} ions in solution.

The leachability data showed that cations were released in the order Cd < Ba < Sb from Sn(IV) oxide, and in the order Sb < Cd < Ba from Ce(IV) oxide host. However, the range lies within 10^{-1} - 10^{-6} $g.cm^{-2}.d^{-1}$ for all the cases, which shows high leach-resistant property of both host matrices after incorporation of Ba, Cd and Sb cations.

It was observed that amorphous mixed precipitates turned into rigid, stable crystalline phases in the calcination process, on which immobilization of cations occurred. Each of the mixed calcined samples of Sn(IV) and Ce(IV) oxides were characterised by X-ray powder diffraction analysis. It was found that the original oxide matrices, which manifested main reflection of cassiterite and cerianite minerals respectively, suffered some structural changes after incorporation of guest cations (Figs 2, 3). Ba^{2+} ions were immobilized into the mineral assemblages of $BaSnO_3$ (cubic), with a little of unknown phase besides cassiterite (Fig. 2a). Similarly, Cd^{2+} ions were immobilized in the mineral assemblages of $CdSnO_3$ (cubic), with a little of unknown phase besides cassiterite (Fig. 2a). Similarly, Cd^{2+} ions were immobilized in the mineral assemblages of $CdSnO_3$ (rhombohedral) with a little of unknown phase alongwith cassiterite (Fig. 2b). Sb^{3+} ions also were found to be fixed in the cassiterite crystal lattice with some unidentified new phases (Fig. 2c). In all cases cassiterite is present as a matrix mineral. On the other hand, in Ce(IV) oxide systems, Ba^{2+} and Sb^{3+} ions were found to be accommodated in the cerianite crystal forming new mineral phases of $BaCeO_3$ (orthorhombic), and Ce_2O_2Sb (tetragonal) respectively (Figs 3a, b), accompanied by a little of unidentified phase. But in case of Cd-CeO_2 system only a small change in the composition of cerianite was observed, wit a little contributions of unknown phase (Fig. 3c), although peak height and corresponding intensities of cerianite were found to be reduced. This, however, requires a detailed crystallographic study.

These observations indicated that the wt% loading of all the three cations was appreciable in the hydrothermally stable hosts. Formation of new mineral phases in each case, although there is no major structural change of host material in Cd-CeO_2 sys-

tem, has been noted, which confirms immobilization of all the cations, as also manifested in their leach-resistant properties. From physical properties and other characteristics Sn(IV) oxide seems to be a better immobilizer.

Acknowledgement

The authors are thankful to Head, Analytical Chemistry Division, BARC, Bombay, India for providing surface area measurement facilities and to Mr. S.N. Dutta for L.T.P. Division, SINP, and Department of Mineralogy, G.S.I, Calcutta for X-ray Diffractograms.

References

1 Bernadzikowski T B, Allender J S, Stone J A, Gordon D E, Gould (Jr). T H & Westberry C F, III, *Am Ceram Soc Bull*, 62 (1983) 1364, 1390.

2 Dole L R, Moore J G, Rogers G C, West G A, Devaney H E, Morgan M T, McDaniel E W & Kessler J H, "Cementitious radioactive waste hosts formed under elevated temperatures and pressures Fuetap Concretes", in *Scientific basis for nuclear waste management*, edited by S V Topp (North-Holland, New York) 1982, 585.

3 McCarthy G J & Davidson M T, *Am Ceram Soc Bull*, 54 (1975) 782.

4 McCarthy G J & Davidson M T, *Am Ceram Soc Bull*, 55 (1976) 190.

5 Jentzen C M, Clarke D R, Morgan P E D & Harker A B, *J Am ceram Soc*, 65 (1982) 292.

6 Ringwood A E, Kesson A E, Ware N G, Hibberson W & Major A, *Nature*, 278 (1979) 219.

7 Fujiki Y, Komatsu Yu & Sasaki T, *Yogyo-Kyokai-Shi*, (1986) 94.

8 Fujiki Y, Komatsu Y & Ohta N, *Chem Lett*, (1980) 1023.

9 Sasaki T, Komatsu Yu & Fujiki Y, *Chem Lett* (1981) 957.

10 Fujiki Y, Sasaki T & Komatsu Yu, *Yogyo-Kyokai-Shi*, (1985) 93.

11 Sasaki T, Komatsu Yu & Fujiki Y, *Chem Lett*, (1987) 95.

12 Kraus K A, Philips H O, Carlson T A & Johnson J S, *Proc 2nd Int Conf Peaceful Uses Atomic Energy*, 28 (1958) 3.

13 Donaldson J D & Fuller M J, *J inorg nucl Chem*, 30 (1968) 1083.

14 Donaldson J D & Fuller M J, *J inorg nucl Chem*, 32 (1970) 1703.

15 Bhattacharyya D K, Dutta N C & De A, *J radioanal & nucl Chem Art*, 140 (1990) 121.

16 Berry F K, Holbourne P E & Woodhams F W D, *J chem Soc, Dalton Trans*, (1980) 2241.

17 Pyke R, Reid R & Tilley R J D, *J chem Soc, Faraday Trans* 1, (1980) 1174.

18 Hodgman C D, Weast R C & Selby S M, *Handbook of chemistry and physics* (The Chemical Rubber Co., Cleveland, Ohio) 1960.

19 Cotton F A & Wilkinson G, *Advanced inorganic chemistry* (John Wiley & Sons) 1988, 652.

20 Vesely V & Pekarek V, *Talanta*, 19 (1972) 219.

21 Petro N S, El-Naggar I M, Shabana E I & Misk N Z, *Colloids and Surfaces*, 49 (1990) 211.

22 Hopkins B, *Chemistry of less familiar elements, Vol* 1 (Stipes Publ. Co, Champaign, Illinois), 1939.

Indian Journal of Chemistry
Vol. 31A, February 1992, pp. 125-127

Notes

Kinetics of oxidation of bis(2,2′,6′,2″-terpyridine)iron(II) by cerium(IV)

T Satyanarayana & N R Anipindi*
School of Chemistry, Andhra University, Visakhapatnam 530 003

and

V Subbiah & M W Pandit
Centre for Cellular and Molecular Biology, Hyderabad 500 007

Received 31 July 1991; revised and accepted 7 October 1991

The oxidation of bis(2,2′,6′,2″-terpyridine)iron(II), $Fe(tpy)_2^{2+}$ by cerium(IV) has been studied in sulphuric acid using stopped-flow spectrophotometry. The reaction is overall second order, first order in each reactant. The rate of the reaction increases with increase in $[H_2SO_4]$. Three cerium(IV) species viz., $CeSO_4^{2+}$, $Ce(SO_4)_2$ and $Ce(SO_4)_3^{2-}$ are considered to be the reactive oxidising species.

There are a few reports available on the oxidation of iron(II) and its complexes by cerium(IV) in literature[1-4]. Dulz and Sutin[5] studied the oxidation of iron(II), ferroin and substituted ferroins and Miller and Prince[6] studied the oxidation of 3-, 5-sulphonic substituted ferroins. Both these groups discussed their kinetic data in terms of Marcus theory of electron-transfer reactions and they made no attempt to explain the effect of acid on the reaction. Bis(terpyridine)iron(II), $Fe(tpy)_2^{2+}$, has a stability constant (log $B_x = 21.16$) which is equal to that of ferroin (log $B_x = 21.30$) and its dissociation constant (1.0×10^{-6} s^{-1}) is also less than that of ferroin (7.5×10^{-5} s^{-1}). Its oxidised product is also more stable than ferroin and other iron(III)-polypyridyl complexes. Inspite of this, the kinetic and mechanistic aspects of the oxidation of $Fe(tpy)_2^{2+}$ have not received much attention. In view of this, the title investigation has been carried out.

Experimental

All the chemicals used were of analytical reagent grade. Doubly distilled water, passed through a millipore column was used for the preparation of the solutions. Iron(II) solution was prepared by dissolving requisite quantity of iron wire (E. Merck) in warm dilute sulphuric acid. Ceric sulphate (G.F.S. Chemical Co.) and 2,2′,6′,2″-terpyridine (G.F.S. Chemical Co.) were used. Bis(terpyridine)iron(II) was prepared by mixing stoichiometric amounts (1:2) of iron(II) and terpyridine.

Table 1 — Effect of $[H_2SO_4]$ on rate {$[Fe(tpy)_2^{2+}] = 1.0 \times 10^{-5}$ mol dm^{-3}; $[Ce(IV)] = 1.0 \times 10^{-4}$ mol dm^{-3}; $[HSO_4^-] = 1.0$ mol dm^{-3}}

$[H_2SO_4]$, mol dm^{-3}	k_{obs}, s^{-1}		
	25°C	30°C	35°C
0.05	2.03 ± 0.09	2.45 ± 0.15	2.90 ± 0.10
0.10	2.22 ± 0.05	2.70 ± 0.26	3.22 ± 0.08
0.20	2.76 ± 0.03	3.25 ± 0.18	4.01 ± 0.21
0.30	3.47 ± 0.22	4.27 ± 0.24	4.97 ± 0.15
0.40	4.37 ± 0.15	5.51 ± 0.27	6.62 ± 0.30
0.50	5.64 ± 0.11	7.07 ± 0.11	8.63 ± 0.25

The absorption spectra of the reactants and products were recorded using Shimadzu UV-260 recording spectrophotometer. A Hi-Tech stopped-flow spectrophotometer (with support unit SF-3L and control unit SF-40C) equipped with APPLE II data acquisition and storage system was used for fast reaction kinetics.

Kinetic runs were carried out under pseudo-first order conditions ([oxidant] > > [substrate]). The reaction was monitored at 552 nm where $Fe(tpy)_2^{2+}$ has the absorption maximum. Requisite volumes of the reactants were taken in two syringes, syringe A containing $Fe(tpy)_2^{2+}$ and syringe B containing Ce(IV), H_2SO_4 and $NaHSO_4$ solutions such that their concentrations in the reaction mixture were exactly half (1:1 mixing). All kinetic runs were performed with a sweep-time equal to 10 half-lives of the corresponding reaction. The data acquisition system acquired the absorbance/voltage versus time data and computed the rate constants from log $(A_t - A_\alpha)$ versus time plots (with a standard least squares programme) where A_t and A_α correspond to absorbance/voltage at time t and infinite time (after completion of the reaction) respectively. Each kinetic run was performed six times and the average k_{obs} values evaluated.

Product analysis

The oxidation product of $Fe(tpy)_2^{2+}$ was $Fe(tpy)_2^{3+}$ and it was identified by its visible absorption spectrum which has maximum absorbance at 702 nm (ref. 7). Results of thin layer chromatographic analysis showed that the products contain no free terpyridine.

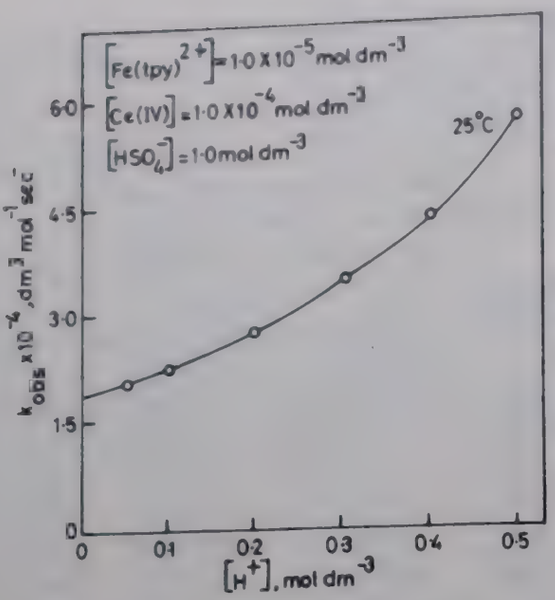

Fig. 1—Effect of [hydrogen ion] on rate

Results and discussion

The reaction is first order eachin [substrate] and [oxidant]. The rate of reaction increases with an increase in $[H_2SO_4]$ (Table 1) and decreases with increase in $[HSO_4^-]$.

Under the present experimental conditions cerium(IV) exists mainly as $CeSO_4^{2+}$, $Ce(SO_4)_2$ and $Ce(SO_4)_3^{2-}$ and all the three species are considered to react with the substrate in rate-limiting steps to give the products. The mechanism is given in Scheme 1.

$$CeSO_4^{2+} + HSO_4^- \overset{K_1}{\rightleftharpoons} Ce(SO_4)_2 + H^+ \quad \ldots(1)$$

$$Ce(SO_4)_2 + HSO_4^- \overset{K_2}{\rightleftharpoons} Ce(SO_4)_3^{2-} + H^+ \quad \ldots(2)$$

$$CeSO_4^{2+} + Fe(tpy)_2^{2+} \xrightarrow{k_3} Ce(III) + Fe(tpy)_2^{3+} \quad \ldots(3)$$

$$Ce(SO_4)_2 + Fe(tpy)_2^{2+} \xrightarrow{k_4} Ce(III) + Fe(tpy)_2^{3+} \quad \ldots(4)$$

$$Ce(SO_4)_3^{2-} + Fe(tpy)_2^{2+} \xrightarrow{k_5} Ce(III) + Fe(tpy)_2^{3+} \quad \ldots(5)$$

Scheme 1

$$\begin{aligned} \text{Rate} &= k_3[CeSO_4^{2+}]_e[Fe(tpy)_2^{2+}] \\ &\quad + k_4[Ce(SO_4)_2]_e[Fe(tpy)_2^{2+}] \\ &\quad + k_5[Ce(SO_4)_3^{2-}]_e[Fe(tpy)_2^{2+}] \quad \ldots(6) \\ &= [Fe(tpy)_2^{2+}]\{k_3[CeSO_4^{2+}]_e + k_4[Ce(SO_4)_2]_e \\ &\quad + k_5[Ce(SO_4)_3^{2-}]_e\} \quad \ldots(7) \end{aligned}$$

$$k_{obs} = k_3[CeSO_4^{2+}]_e + k_4[Ce(SO_4)_2]_e + k_5[Ce(SO_4)_3^{2-}]_e \quad \ldots(8)$$

$$[Ce(IV)]_t = [CeSO_4^{2+}]_e + [Ce(SO_4)_2]_e + [Ce(SO_4)_3^{2-}]_e \quad \ldots(9)$$

By calculating $[CeSO_4^{2+}]_e$, $[Ce(SO_4)_2]_e$ and $[Ce(SO_4)_3^{2-}]$ from Eqs (1) and (2) and substituting in Eq. (9), we get

$$[CeSO_4^{2+}]_e = \frac{[Ce(IV)]_t[H^+]^2}{\{[H^+]^2 + K_1[H^+][HSO_4^-] + K_1K_2[HSO_4^-]^2\}} \quad \ldots(10)$$

$$[Ce(SO_4)_2]_e = \frac{K_1[Ce(IV)]_t[H^+][HSO_4^-]}{\{[H^+]^2 + K_1[H^+][HSO_4^-] + K_1K_2[HSO_4^-]^2\}} \quad \ldots(11)$$

$$[Ce(SO_4)_3^{2-}]_e = \frac{K_1K_2[Ce(IV)]_t[HSO_4^-]^2}{\{[H^+]^2 + K_1[H^+][HSO_4^-] + K_1K_2[HSO_4^-]^2\}} \quad \ldots(12)$$

Substituting the values of $[CeSO_4^{2+}]_e$, $[Ce(SO_4)_2]_e$ and $[Ce(SO_4)_3^{2-}]_e$ in Eq. (8), we get

$$k_{obs} = [Ce(IV)]_t \left\{ \frac{k_3[H^+]^2 + k_4K_1[H^+][HSO_4^-] + k_5K_1K_2[HSO_4^-]^2}{[H^+]^2 + K_1[H^+][HSO_4^-] + K_1K_2[HSO_4^-]^2} \right\} \quad \ldots(13)$$

Table 2—Comparison of observed and calculated rate constants in [oxidant] variation

{$[Fe(tpy)_2^{2+}] = 5.0 \times 10^{-6}$ mol dm^{-3}; $[H_2SO_4] = 2.5 \times 10^{-1}$ mol dm^{-3}; $[HSO_4^-] = 2.5 \times 10^{-1}$ mol dm^{-3}; temp. = 25°C}

$10^4[Ce(IV)]_t$, mol dm^{-3}	k	
	obs.	cal.
0.5	8.37	8.34
1.0	17.10	16.67
1.5	25.89	25.02
2.0	35.63	33.36
2.5	41.66	41.69

Table 3—Comparison of observed and calculated rate constants in [bisulphate ion] variation

{$[Fe(tpy)_2^{2+}] = 1.0 \times 10^{-5}$ mol dm^{-3}; $[Ce(IV)] = 1.0 \times 10^{-4}$ mol dm^{-3}; $[H_2SO_4] = 1.0 \times 10^{-1}$ mol dm^{-3}; temp. = 25°C}

$[HSO_4^-]$, mol dm^{-3}	k	
	obs.	cal.
0.1	15.76	16.67
0.2	6.10	5.96
0.4	2.95	3.09
0.6	2.55	2.51
0.8	2.40	2.29
1.0	2.25	2.18

This reaction has been carried out at an ionic strength of 1.0 (using $NaHSO_4$) and hence the K_1 and K_2 values of 120 and 5 respectively reported in literature[8] at $\mu = 1.0$ are used in arriving at the mechanism of this reaction. Hence, $K_1K_2[HSO_4^-]^2 > \{[H^+]^2 + K_1[H^+][HSO_4^-]\}$. Then Eq. (13) transforms to

$$k_{obs} = [Ce(IV)]_t \left\{ \frac{k_3[H^+]^2 + k_4K_1[H^+][HSO_4^-] + k_5K_1K_2[HSO_4^-]^2}{K_1K_2[HSO_4^-]^2} \right\} \quad \ldots(14)$$

$$k'_{obs} = \frac{k_3[H^+]^2}{K_1K_2[HSO_4^-]^2} + \frac{k_4[H^+]}{K_2[HSO_4^-]} + k_5 \quad \ldots(15)$$

where $k'_{obs} = k_{obs}/[Ce(IV)]_t$.

A plot of k'_{obs} versus $[H^+]$ gave a curve concave to the rate axis making an intercept on it (Fig. 1). Adopting the approach of Liebhafsky[9] and Peard and Wells[10] envisaged in the $H_2O_2 - IO_3^-$ reaction, this curve is extrapolated to zero $[H^+]$. The intercept on the rate axis gives the k_5 value. Equation (15) can be rearranged as

$$\frac{(k'_{obs} - k_5)}{[H^+]} = \frac{k_4}{K_2[HSO_4^-]} + \frac{k_3[H^+]}{K_1K_2[HSO_4^-]^2} \quad \ldots(16)$$

Using the k_5 value obtained, $(k'_{obs} - k_5)/[H^+]$ against $[H^+]$ was plotted. From the slope and intercept of this plot the values of k_3 and k_4 have been evaluated. The values of k_3, k_4 and k_5 at 25°C are 8.0×10^7, 7.3×10^4 and 1.9×10^4 dm^3 mol^{-1} s^{-1} respectively. This shows that $CeSO_4^{2+}$ is highly reactive when compared to $Ce(SO_4)_2$ and $Ce(SO_4)_3^{2-}$. This is due to the fact that the potentials for the cerium(IV)-cerium(III) couple decreases with increase in the number of sulphate groups coordinated to the cerium(IV) centre.

Substituting the values of k_3, k_4 and k_5 in rate equation, the rate constants are calculated for the oxidant and the bisulphate ion variations at 25°C. These values are presented in Tables 2 and 3.

It can be seen from the Tables 2 and 3 that the observed and calculated rate constants agree well giving support to the mechanism. The overall activation energy, E_a for this reaction is 28 ± 9 kJ mol^{-1}.

Acknowledgement

Prof. M.N. Sastri is thanked for useful discussions.

References

1 Chum H L & Krumholz P, *Inorg Chem*, 13 (1974) 519.
2 Chum H L & Helene M E M, *Inorg Chem*, 19 (1980) 876.
3 Soria D, De Castro M L & Chum H L, *Inorg Chim Acta*, 42 (1980) 121.
4 Adamson M G, Dainton P S & Glentworth P, *Trans Faraday Soc*, 61 (1965) 689.
5 Dulz G & Sutin N, *Inorg Chem*, 2 (1963) 917.
6 Miller J D & Prince R H, *J chem Soc (A)*, (1966) 1370.
7 Ford-Smith M H & Sutin N, *J Am chem Soc*, 83 (1961) 1830.
8 Hanna S B & Sarac A S, *J org Chem*, 42 (1977) 2063.
9 Liebhafsky H A, *J Am chem Soc*, 53 (1931) 896.
10 Peard M G & Wells C F, *Trans Faraday Soc*, 47 (1951) 616.

Indian Journal of Chemistry
Vol. 31A, February 1992, pp. 128-130

Reactivity of bismuth(III) dichlorodithiocarbamate: Synthesis and spectroscopic characterisation of mixed bismuth-molybdenum and bismuth-tungsten complexes

Subrata Mandal, G C Mandal, R Shukla & P K Bharadwaj*

Department of Chemistry, Indian Institute of Technology, Kanpur 208 016, India

Received 21 June 1991; revised and accepted 4 November 1991

Sulphur bridged dinuclear bismuth-molybdenum and bismuth-tungsten complexes are isolated when a DMSO solution of the bismuth complex (dtc)$BiCl_2$ (dtc = diethyldithiocarbamate) is allowed to react with $(NH_4)_2MS_4$ (M = Mo, W). The two chloride ions are replaced by the tetrathiometallato group which coordinates the bismuth moiety in a bidentate fashion forming two neutral complexes, (dtc)$Bi(MS_4)$ (M = Mo, W) in high yields (65-75%). The bidentate coordination of tetrathiometallates has been concluded on the basis of conductivity, infrared, elemental analysis and electronic and NMR spectral data.

Oxo-bridged bismuth-molybdate or bismuth-tungstate compounds are important heterogeneous catalysts. They are used commercially in the well-known SOHIO process[1-3] for the selective oxidation and amoxidation of propylene to form acrolein and acrylonitrile respectively. Mechanism of any of these catalytic reactions is not known at the molecular level due to the lack of knowledge on structure and bonding of these systems. Naturally, studies of bismuth-transition metal complexes are of considerable current interest. However, most of the studies have been carried out with transition metal carbonyls where bismuth is directly bonded to transition metal ion(s)[4-9].

Our efforts[10] in this area have been aimed at isolation of sulphur/oxygen bridged bismuth-transition metal complexes to obtain systems that might prove to be catalysts or catalyst precursors. In order to synthesize mixed dinuclear/polynuclear complexes of bismuth with transition metal ions it is necessary first to synthesize stable Bi(III) complexes and then use them as ligands to bind various molybdenum and tungsten species. Coordination chemistry of Bi(III) is a relatively unexplored area and only a few complexes have been characterized. This is partly due to the ready conversion of Bi(III) into BiO^+ in presence of traces of moisture even at low *p*H values[11]. Therefore, it is essential to have ligands that can form stable Bi(III) complexes even in presence of moisture.

An aqueous solution of dialkyldithiocarbamate reacts readily with $BiCl_3$ in alcohol to form a tris-complex in high yields[12]. Even when BiOCl is allowed to react with an excess of dithiocarboxylate, the tris-complex can be isolated[13]. The facile formation of these complexes reflects the affinity of Bi(III) towards sulphur. If mixed halo-dithiocarbamato complexes of Bi(III) could be isolated, then the halides could possibly be replaced by suitable metal oxo-/thio-species giving rise to the desired sulphur/oxygen bridged complexes. In order to explore this possibility, we synthesized Bi(dtc)Cl_2 in high yields[14] and allowed it to react with thiometallates. Thiomolybdates and thiotungstates occupy a special position in coordination chemistry as they are unique ligands which are purely inorganic in nature and give rise to sulphur bridged multimetallic complexes[15,16]. In the present note, we describe the facile synthesis of neutral Bi−S−Mo and Bi−S−W species by reacting Bi(dtc)Cl_2 with the tetrathiometallates. This work provides a convenient route to isolation of sulphur bridged bismuth-transition metal complexes.

Experimental

Bismuth trichloride, carbon disulphide and diethyl amine were of reagent grade and used as received. All the solvents were purified prior to use following standard methods of purification[17]. $(NH_4)_2MS_4$ (M = Mo, W) complexes were obtained as crystalline solids following published procedures[15].

Infrared spectra were recorded on a Perkin-Elmer model 580 spectrophotometer. Electronic spectral data were collected on a Perkin-Elmer Lambda 2 spectrophotometer in freshly distilled dimethylformamide (DMF). The conductivity data of the compounds were collected in DMF solutions using an Elico model CM-82T conductivity bridge. The proton NMR data were collected on a Bruker 80W NMR instrument. The elemental analyses (C, H, N & S) were performed at the Microanalytical Laboratories of IIT, Kanpur and CDRI, Lucknow, India.

Synthesis of Bi(dtc)Cl_2 **1**

$BiCl_3$ (630 mg; ~ 2 mmol) was dissolved in 25 ml

Table 1—Selected IR and UV-Vis spectral data of the complexes

Compound	IR data (cm^{-1})	Assignment	UV-Vis data (nm) (ε in $M^{-1}\,cm^{-1}$)	Ref.
$(NH_4)_2MoS_4$	480	ν_{as} (MoS)	467 (11850)	19
			316 (16750)	
			241 (24700)	
$(NH_4)_2WS_4$	460	ν_{as} (WS)	393 (15710)	19
			277 (24500)	
$(Ph_4P)_2[Zn(WS_4)_2]$	489	$\nu(WS_{term})$	460	15
	446	$\nu(WS_{br})$	395	
$Bu_4N[Bi(MoS_4)_2]$	505 (sb)	$\nu(MoS_{term})$	445 (6100)	10
	465 (mb)	$\nu(MoS_{br})$	285 (16000)	
$Bu_4N[Bi(WS_4)_2]$	495 (sb)	$\nu(WS_{term})$	375 (8100)	10
	440 (mb)	$\nu(WS_{br})$	280 (20600)	
(dtc)Bi(MoS_4)	505 (sb)	$\nu(MoS_{term})$	445 (2540)	This work
	450 (mb)	$\nu(MoS_{br})$	370 (3950)	
(dtc)Bi(WS_4)	485 (sb)	$\nu(WS_{term})$	395 (4100)	This work
	440	$\nu(WS_{br})$	360 (5625)	

dry CH_3CN. A freshly prepared solution of $Bi(dtc)_3$ (650 mg; ~ 1 mmol) in 10 ml dry $CHCl_3$ was added to the above solution dropwise with stirring under an atmosphere of N_2 to get a yellow solution. After the addition was complete, the solution was filtered and kept in the freeze at 5°C. After about 12 h, yellow crystals of the product were collected and air dried (yield 60%). The compound was found to be stable in air. Infrared spectrum of the compound showed a strong band at 380 cm^{-1} which is not present in $Bi(dtc)_3$ and is attributed to Bi−Cl stretching vibration[14]. ^{1}H-NMR spectral data of the compound in d_6-DMSO showed the presence of dtc group.

Analytical data: Found % (calc. for $C_5H_{10}Cl_2NS_2Bi$): C, 13.97 (14.03); H, 2.21 (2.35); N, 3.30 (3.27); S, 14.86 (14.98).

Synthesis of (dtc)Bi(MoS_4) **2**

(dtc)$BiCl_2$ (428 mg; ~ 1 mmol) was dissolved in 5 ml dry DMSO and heated to about 60°C for 5 min under N_2. The yellow solution was allowed to cool to RT and added dropwise with constant stirring under nitrogen to an ice-cold solution of freshly prepared $(NH_4)_2MoS_4$ (260 mg; ~ 1 mmol) dissolved in 10 ml of degassed water. A brown microcrystalline solid separated immediately which was collected by filtration using a Schlenk apparatus and dried in a stream of dry N_2 gas (yield 60%). The complex was found to be moderately soluble in DMF and DMSO. ^{1}H-NMR data showed the presence of the dtc group and qualitative test for chloride was negative.

Analytical data: Found % (calc. for $C_5H_{10}NS_2Bi.MoS_4$): C, 10.19 (10.33); H, 1.79 (1.72); N, 2.44 (2.41); S, 32.62 (33.05).

Synthesis of (dtc)Bi(WS_4) **3**

This complex was synthesized by reacting a freshly prepared aqueous solution of $(NH_4)_2WS_4$ with a DMSO solution of (dtc)$BiCl_2$ as described in the preparation of **2** (yield 75%). Presence of the dtc group could be ascertained from the ^{1}H-NMR data of the compound and absence of chloride was confirmed by qualitative silver nitrate test.

Analytical data: Found % (calc. for $C_5H_{10}NS_2Bi.WS_4$): C, 8.83 (8.97); H, 1.51 (1.49); N, 2.21 (2.09); S, 28.14 (28.71).

Results and discussion

The facile formation of $Bi(dtc)_3$ in aqueous alcoholic medium and the affinity of Bi(III) for soft S-donors suggest that new complexes could be isolated by reacting (dtc)$BiCl_2$ with tetrathiometallates. In the present case, use of two-fold excess of MS_4^{2-} in the reactions affords only the 1 : 1 complexes indicating the stability of neutral (dtc)Bi(MS_4) species giving Bi(III) a tetracoordination. However, without crystal structural data no comment could be made whether or not Bi(III) is coordinated to sulphur

from neighbouring molecules at least in the solid state. All our attempts to grow single crystals of the complexes have been unsuccessful so far although efforts are still on.

The compounds behave as nonelectrolytes in DMF solutions as inferred from their conductivity data. This means that the compounds are neutral as indicated and the integrity of the complexes remains intact in the DMF solution further signifying the stability of the bonds formed between the tetrathiometallates and $(dtc)Bi^{2+}$ ions.

Selective infrared spectral data for the complexes are given in Table 1. Infrared spectral band positions for the thiometallato complexes are diagnostic. In the free $(MS_4)^{2-}$ ion which has T_d symmetry, the IR-active triply degenerate Mo − S stretching vibration occurs at 480 cm^{-1} while for WS_4^{2-} it occurs at 460 cm^{-1} (refs 18, 19). When a binuclear complex is formed, the MS_4^{2-} anion binds in a bidentate fashion leaving a pair of terminal M − S bonds. As a result, the local symmetry of the tetrathiometallate group reduces from T_d to C_{2v} and four bands are expected to appear in the IR spectrum of which two bands corresponding to $\nu(M-S_{term})$ are expected at higher frequencies while the other two due to $\nu M-S_{br}$ are expected at lower frequencies. Usually, however, only two broad bands appear, one for each type[15]. For complex **2**, broad peaks appearing at 505 and 450 cm^{-1} are attributed to νMo − S (terminal) and ν Mo − S (bridging) vibrations respectively. The corresponding bands for the bismuth-tungstate complex appear at 485 and 440 cm^{-1} respectively. The 1450-1550 cm^{-1} region is primarily associated with the C − N stretching vibrations. Both the complexes in the present study show two peaks in this region, which falls between the C − N single bond (1250-1350 cm^{-1}) and C = N double bond (1640-1690 cm^{-1}) regions[20] signifying partial double bond character. The 950-1050 cm^{-1} region is associated primarily with ν(CSS) vibrations. Both the complexes **2** and **3** show that the peak around 1000 cm^{-1} is split although the extent of splitting is small which may be due to asymmetric binding of the dithio-group to Bi(III) ion. The far-IR region was not studied to locate Bi − S stretching vibrations as the complexes could be unequivocally characterised without it.

The electronic spectra of the complexes showed internal transitions of the ligand, corresponding to the thiometallate ion as well as the dithiocarbamate ion. The LMCT or MLCT transitions involving Bi(III) were not seen. Bi(III) has a stereochemically active lone pair. Although crystal structures of the two complexes **2** and **3** are not known, coordination geometry around Bi(III) is expected to be distorted in each case.

Acknowledgement

We thank the CSIR, New Delhi and IIT, Kanpur for financial support.

References

1 Grasselli R K & Burrington J D, *Adv Catal*, 30 (1981) 133.
2 Grasselli R K, *J chem Educ*, 63 (1986) 216.
3 Dadyburjor D B, Jewur S S & Ruckenstein E, *Catal Rev*, 19 (1979) 293; Bielanski A & Haber J, *Catal Rev*, 19 (1979) 1; Gates B C, Katzer J R & Schuit G C A, *Chemistry of catalytic processes*, (McGraw-Hill, New York), 1979, 325-389; Anderson A B, Ewing D W, Kim Y, Grasselli R K, Burrington J D & Brazdil J F, *J Catal*, 96 (1985) 222.
4 Etzrodt G, Boese R & Schmid G, *Chem Ber*, 112 (1979) 2574.
5 Wallis J M, Muller G & Schmidbaur H, *Inorg Chem*, 26 (1987) 458.
6 Whitmire K H, Shieh M & Cassidy J, *Inorg Chem*, 28 (1989) 3164.
7 Cullen W R, Patmore D J, Sams J R, Newlands M J & Thompson L K, *J chem Soc Chem Commun*, (1971) 952; Cullen W R, Patmore D J & Sams J R, *Inorg Chem*, 12 (1973) 867; Kaul H A, Greissinger D, Luksza M & Malisch W, *J organomet Chem*, 228 (1982) C29.
8 Seyerl J von & Huttner G, *J organomet Chem*, 195 (1980) 207.
9 Clegg W, Compton N A, Errington R J, Norman N C, Tucker A J & Winter M J, *J chem Soc Dalton Trans*, (1988) 2941.
10 Srinivasan B R & Bharadwaj P K, *Inorg chim Acta*, 178 (1991) 165.
11 Baes C F & Mesmer R E, *The hydrolysis of cations* (John Wiley & Sons, New York), 1976, 377.
12 Coucouvanis D, *Progr inorg Chem*, 26 (1979) 301.
13 Bharadwaj P K & Musker W K, *Inorg Chem*, 26 (1987) 1453.
14 To be published.
15 Diemann E & Muller A, *Coord Chem Rev*, 10 (1973) 79; Muller A, Diemann E, Jostes R & Bogge H, *Angew Chem Int Ed Engl*, 20 (1981) 934.
16 Srinivasan B R, *Ligational behaviour of thiomolybdates and thiotungstates towards Mn(II), Fe(II), Co(II) and Ni(II) in the presence of aromatic diimines*, Ph.D. Thesis, IIT, Kanpur, 1987.
17 Perrin D D, Armargo W L F & Perrin D R, *Purification of laboratory chemicals*, (Pergamon, Oxford), 1980.
18 Cormier A, Nakamoto K, Ahlborn E & Muller A, *J molec Struct*, 25 (1975) 43.
19 McDonald J W, Friesen G D, Rosenhein L D & Newton W E, *Inorg chim Acta*, 72 (1983) 205.
20 Nakamoto K, *Infrared and Raman spectra of inorganic and coordination compounds*, 4th Edn, (John Wiley & Sons, NY), 1986, 346 and references cited therein.

Indian Journal of Chemistry
Vol. 31A, February 1992, pp. 131-133

Trimethylplatinum(IV) complex with diphenylthiophosphinic acid

S Chaudhury

Fuel Chemistry Division, Bhabha Atomic Research Centre, Trombay, Bombay 400 085

and

V K Jain*

Chemistry Division, Bhabha Atomic Research Centre, Trombay, Bombay 400 085

Received 27 June 1991; revised and accepted 18 November 1991

A dinuclear trimethylplatinum(IV) complex $[PtMe_3(SOPPh_2)]_2$ incorporating a diphenylthiophosphinate ligand has been prepared. The complex has an octahedral environment around platinum with diphenylthiophosphinate acting as a tridentate ligand. Bridge cleavage reactions of this complex with neutral bidentate nitrogen donor ligands give mononuclear complexes in which thio ligand behaves in a monodentate fashion coordinating through sulphur.

As a part of our continuing research programme on organoplatinum(IV) complexes[1-4], we have synthesised a series of trimethylplatinum (IV) complexes containing diphenylthiophosphinate moiety.

Experimental

Trimethylplatinum iodide[5], diphenylthiophosphinic acid[6] and neutral nitrogen donor ligands[7] were prepared according to literature methods. The ^1H NMR spectra were recorded on a Bruker AM-200 or Varian FT-80A NMR spectrometer in $CDCl_3$. Chemical shifts are reported in δ, ppm with reference to internal chloroform peak (δ 7.26 ppm). Variable temperature ^1H NMR spectra of $[PtMe_3(SOPPh_2)]_2$ were recorded on a Bruker-500 MHz NMR spectrometer. The ^{31}P NMR spectra were recorded on a Varian FT-80A spectrometer operating at 32.203 MHz and chemical shifts are reported with reference to external 85% H_3PO_4. Microanalyses were performed at the Analytical Chemistry Division of this research centre.

Preparation of $[PtMe_3(SOPPh_2)]_2$

To a benzene solution of trimethylplatinum iodide (99 mg, 0.067 mmol), a solution of diphenylthiophosphinic acid (63 mg, 0.27 mmol) in benzene (5 ml) containing 0.2 ml triethylamine was added dropwise with vigorous stirring at room temperature. Reactants were stirred for 2 hr. The solvent was stripped off *in vacuo*. To the residue, dichloromethane (20 ml) and water (20 ml) were added and contents were shaken for 2 min. Dichloromethane layer was separated and dried *in vacuo* to obtain a white solid. This was recrystallized twice from dichloromethane/hexane mixture to obtain a white crystalline solid (97 mg; 76%).

Preparation of $[PtMe_3(SOPPh_2)(bipy)]$

To a benzene solution (10 ml) of $[PtMe_3(SOPPh_2)]_2$ (49 mg, 0.052 mmol) a solution of 2,2′-bipyridine (16 mg, 0.103 mmol) was added and the contents were stirred at room temperature for 2 hr. The solvent was evaporated *in vacuo* to obtain a white crystalline solid. It was recrystallized from dichloromethane/hexane (1:5, v/v) at 0°C as colourless crystalline solid (46 mg, 71%). Similarly, other compounds with neutral nitrogen donor ligands were prepared. The analytical data are summarized in Table 1.

Results and discussion

Reaction of trimethylplatinum iodide with $[Et_3NH][SOPPh_2]$ in benzene gave a dinuclear platinum complex, $[PtMe_3(SOPPh_2)]_2$. The latter

Table 1—Analytical data for trimethylplatinum diphenylthio phosphinate complexes

Compound*	m.p. (yield, %)	Found (Calc.), %		
		C	H	N
$[PtMe_3(SOPPh_2)]_2$	150 (76)	37.0 (38.0)	4.4 (4.0)	—
$[PtMe_3(SOPPh_2)(bipy)]$	193 (71)	47.4 (47.7)	4.3 (4.3)	4.4 (4.4)
$[PtMe_3(SOPPh_2)(Me_2bipy)]$	212 (82)	48.6 (49.3)	4.8 (4.7)	4.2 (4.3)
$[PtMe_3(SOPPh_2)(phen)]$	112 (61)	48.7 (49.6)	4.2 (4.2)	4.3 (4.3)
$[PtMe_3(SOPPh_2)(pypz)]$	185 (85)	44.3 (44.7)	4.2 (4.2)	6.7 (6.8)
$[PtMe_3(SOPPh_2)(pyMe_2pz)]$	195 (57)	46.1 (46.4)	4.7 (4.7)	6.5 (6.5)
$[PtMe_3(SOPPh_2)(pz_2CH_2)]$	85 (82)	40.7 (42.5)	4.3 (4.4)	8.5 (9.0)

*All the compounds were recrystallized from dichloromethane/hexane.

complex on treatment with neutral bidentate nitrogen donor ligand afforded mononuclear complexes (Eq. 1).

$$[PtMe_3I]_4 + 4[Et_3NH][SOPPh_2] \rightarrow 2[PtMe_3(SOPPh_2)]_2 + 4Et_3NHI$$
$$\downarrow 4\widehat{NN}$$
$$4[PtMe_3(SOPPh_2)(\widehat{NN})] \quad \ldots (1)$$

[where $\widehat{NN}$ = 2,2′bipyridine(bipy); 4,4′-dimethyl-2,2′-bipyridine (Me_2bipy); 1,10-phenanthroline (phen); 1-(2-pyridyl)pyrazole (pypz); 1-(2-pyridyl)--3,5-dimethylpyrazole ($pyMe_2pz$) and bis(1-pyrazolyl)methane (pz_2CH_2)].

The ^{31}P NMR spectra (Table 2) of these complexes exhibit a single resonance flanked by platinum satellites. Shielding of the ^{31}P NMR signal in these complexes with respect to the free ligand has been observed. Shielding is maximum in mononuclear complexes. The $^2J(^{195}Pt-^{31}P)$ lies in the range 32-54 Hz. For similar complexes of dithio acid ligands[3,4] the $^2J(^{195}Pt-^{31}P)$ varies in the range 54-95 Hz.

The ^1H NMR spectrum of $[PtMe_3(SOPPh_2)]_2$, recorded on 80 and 500 MHz at room temperature, showed two broad signals attributable to Pt-Me protons with platinum satellites. On cooling the $CDCl_3$ solution of this complex down to 0°C both the resonances sharpened and the spectrum remained unaffected on further lowering the temperature down to −50°C. This suggests that either the complex is fluxional even at −50°C or the four-membered Pt_2S_2 ring is symmetrical. Recent X-ray structural studies of $[PtMe_3(SSAsMe_2)]_2$[8] and $[PtMe_3(SSPh_2)]_2$[4] have revealed that the four-membered Pt_2S_2 ring in these compounds is asymmetrical. In both the cases, three platinum methyl signals, for the former at room temperature (rigid structure) and for the latter at lower temperatures (non-rigid structure), have been observed. The signal at δ 0.24 ppm with integration corresponding to six protons has been assigned to the methyl groups *trans* to the bridging sulphur atoms. The signal at δ 1.17 ppm has been attributed to the methyl group *trans* to the oxygen. A structure with an oxygen and a sulphur or both oxygen bridges can be ruled out on the basis of NMR data. For the former species three Pt-Me signals are expected while for the latter the integration for downfield signal should correspond to two methyl groups.

The mononuclear compounds exhibit two resonances for Pt-Me protons for the complexes containing symmetrical $\widehat{NN}$ ligands, while three

Table 2—^{31}P and ^1H NMR data for trimethylplatinum (IV) complexes with diphenylthiophosphinic acid in $CDCl_3$

Compound	^{31}P NMR data		^1H NMR data	
	δ in ppm	^2J(Pt−P) in Hz	Pt-Me protons	Ligand protons
$Ph_2P(S)OH$	76.3[a]	—	—	7.90-7.78 (m, 2 & 6 Ph, 4H), 7.47-7.35 (m, 3-5-Ph, 6H), 5.42 (br, acidic proton)
$[PtMe_3(SOPPh_2)]_2$	54.3	32	1.17 (1 Me, 86 Hz) *trans* to O, 0.24 (2 Me, 72.7 Hz *trans* S)	7.87-7.96 (m) 7.26-7.42 (m)
$[PtMe_3(SOPPh_2)(bipy)]$	44.3	48	1.10 (2 Me, 69 Hz) 0.10 (1 Me, 69 Hz)	6.80-8.55 (m)
$[PtMe_3(SOPPh_2)(Me_2bipy)]$	43.8	48	1.20 (2 Me, 69 Hz) 0.23 (1 Me, 68.7 Hz)	2.50 (s, Me) 7.13-8.51 (m)
$[PtMe_3(SOPPh_2)(phen)]$	43.1	47	1.42 (2Me, 69.7 Hz) 0.24 (1 Me, 69.0 Hz)	9.15 (q), 8.34 (d) 7.80, 7.25 (d,d) 6.86-7.03 (m)
$[PtMe_3(SOPPh_2)(pypz)]$	44.5	46	1.31 (1 Me, 72 Hz) 1.19 (1 Me, 71.9 Hz) 0.36 (1 Me, 69.0 Hz)	6.50 (br, s) 7.19-8.35 (m)
$[PtMe_3(SOPPh_2)(pyMe_2pz)]$	43.4	47	1.37 (1 Me, 72.7) 1.26 (1 Me, 71.5) 0.34 (1 Me, 68.7)	2.61 (s, Me), 2.35 (s, Me) 6.05 (pz, 3-H), 7.2-8.6 (m)
$[PtMe_3(SOPPh_2)(pz_2CH_2)]$	45.0	54	0.77 (2 Me, 71.6 Hz) 0.36 (1 Me, 69 Hz)	5.15 (s, CH_2), 6.16 (t) 7.09-7.98 (m)

(a) Reported 74.0 ppm (ref. 12)

signals are observed in the case of the complexes containing unsymmetrical NN′ ligands. In both the cases neutral nitrogen donor ligand acts in a bidentate mode and the $Ph_2P(O)S^-$ binds through sulphur in a monodentate fashion. The assignment of NMR data of these complexes are based on the data reported for other trimethylplatinum(IV) complexes[2-4,8-11]. The resonance at the highest field is attributed to the methyl group *trans* to sulphur, while the lower field signals are assigned to the methyl groups *trans* to N. The observed values of $^2J(^{195}Pt-^1H)$ and chemical shifts are comparable to those of the complexes having monodentate anionic dithio ligand[3,4], indicating a sulphur bonded complex rather than the oxygen bonded. In the latter case the magnitude of $^2J(Pt-H)$ is expected to be ≈ 75 Hz with chemical shift signal appearing at lower fields[10,11].

References

1 Jain V K, Rao S & Jain L, *Adv organometal Chem*, 27 (1987) 113.

2 Jain V K, *Indian J Chem*, 26A (1987) 1019.

3 Visalakshi R & Jain V K, *Trans Met Chem*, 15 (1990) 278.

4 Chaudhury S, Jain V K, Jakkal V S & Venkatasubramanian K, *J organometal Chem*, (in press).

5 Baldwin J C & Kaska W C, *Inorg Chem*, 14 (1975) 2020.

6 Hopkins T R & Vogel P W, *J Am chem Soc*, 78 (1956) 4447; Pitts J J, Robinson M A & Trotz S I, *J inorg nucl Chem*, 30 (1968) 1299.

7 Visalakshi R, Jain V K, Kulshreshtha S K & Rao S, *Inorg chim Acta*, 118 (1986) 119.

8 Abel E W, Beckett M A, Bates P A & Hursthouse M B, *Polyhedron*, 7 (1988) 1855.

9 Clark H C, Ferguson , Jain V K & Parvez M, *J organometal Chem*, 270 (1984) 365.

10 Hall J R & Swile A, *Aust J Chem*, 28 (1975) 1507.

11 Romano V, Badalamenti R, Pizzino T & Maggio F, *J organometal Chem*, 42 (1972) 199.

12 Kumara Swamy K C, Schmid C , Day R O & Holmes R R, *J Am chem Soc*, 110 (1988) 7067.

Indian Journal of Chemistry
Vol. 31A, February 1992, pp. 134-135

Determination of microquantities of fluoride by ion-exchange spectrophotometry

Anjali Nayar & Surekha Devi*

Department of Chemistry, M S University, Baroda 390 002, India

Received 26 September 1991; revised and accepted 20 November 1991

Amberlite IRA 400 in the thiocyanate form is used for the estimation of fluoride by ion exchange spectrophotometry. Various reaction conditions have been optimised and interferences due to other anions have been removed. The method is used for the estimation of fluoride in drinking water.

Numerous methods have been proposed for the determination of fluoride because of its ecological importance in natural and waste waters. They are mainly spectrochemical and electrochemical in nature. Most of the existing spectrophotometric methods are based on the bleaching action of fluoride either on aqueous metal complexes[1,2] or on complexes in micellar medium[3]. Some other direct spectrophotometric methods[4,5] are based on the formation of ternary metal complexes of fluoride. Atomic absorption, molecular absorption and emission methods are also used in the determination of microquantities of fluoride. However, all these methods are either complex or require specialised instruments. In the present note we are reporting a very simple and economical method for the estimation of fluoride. The method is reproducible, sensitive and allows fluoride estimation in the presence of halides, sulphide and sulphate.

Experimental

AR grade chemicals and doubly deionised water were used throughout the course of the work. Absorbance was measured on a Spectronic 20, Baush and Lomb photometer.

In a glass column of 18 cm in length and 1.2 cm int. dia slurry of the Amberlite-IRA 400 resin in the thiocyanate form was poured to achieve a uniform packing. Excess water was drained and air gaps were avoided to overcome the eddy diffusion. The length of the resin bed was maintained at 10 cm. A resin pre-column of 5 cm length was prepared as described earlier using Dowex 50W-XB (mesh 20-50) cation exchange resin in silver ion form.

Stock solutions (10^{-2} *M*) of the anions required for the study were prepared by dissolving appropriate amounts of AR grade sodium salts in deionised water.

Determination of fluoride

Sodium fluoride solution (10 ml, 10^{-3} *M*) was passed through the SCN^- form column at the flow rate of 1 ml min^{-1}. The column was washed with 10 ml of deionised water. The column effluents were collected alongwith the washings and diluted to 25 ml with deionised water. The iron-thiocynate complex was developed at *p*H 1.5-1.8 by using appropriate quantity of 10^{-2} *M* ferric solution and the column effluent. The absorbance was measured at 480 nm against reagent blank. Operational conditions were optimised by varying column length, ferric ion concentration and flow rate. A calibration curve was plotted by using 10^{-4}-10^{-5} *M* fluoride solution.

Results and discussion

The method is based on the displacement of equimolar quantity of SCN^- by fluoride. The displaced thiocynate when treated with ferric ion at *p*H 1.5-1.8 forms ion-thiocynate complex which absorbs at 480 nm. Fluoride was estimated at preoptimised conditions using calibration plot constructed for complexes formed from 10^{-4}-10^{-3} *M* KCNS solutions and 10^{-2} *M* iron(III) solution. A linear plot with the correlation coefficient 0.9998 and least square equation, $A = 1031\ [SCN^-\ M] - 0.013$, was obtained. In the study of effect of resin bed length (2-10 cm) on fluoride estimation it was observed that resin bed of 2 cm length was sufficient for the quantitative displacement of thiocynate by fluoride. It was also observed that flow rate of column effluents from 1 ml to 8 ml min^{-1} does not influence the displacement of thiocynate from the column by fluoride. It was observed that a linear plot (correlation coefficient = 0.9998) was obtained from the 10^{-3} to 10^{-5} *M* sodium fluoride concentration and displaced thiocynate in terms of iron-thiocynate complex. Fluoride concentration as low as 10^{-6} *M* also displaced SCN^- from the column, but the absorbance developed was not accurately measurable. By developing a flow manifold with a microcolumn of resin (4×0.2 cm), determination of fluoride upto 10^{-7} *M* was possible. The least square equation obtained for these results was, $A = 958\ [M$ conc. of $F^-] - 0.013$. In the study of interference due to displacement by other anions it was observed that equimolar solutions of the ions thiosulphate, chloride,

Table 1—Analysis of drinking water

Water source at Tavadia	*p*H	Fluoride (μg ml^{-1}) (mean of 5 determinations)	
		proposed method	SPADNS method
Water works (bore well)	7.45	3.85	3.7
Municipal (tube well)	7.4	5.05	4.9
Water works (tube well)	8.1	4.0	4.0
Private (tube well)	7.9	4.35	4.30

bromide, iodide, nitrate, sulphate, hydrogen phosphate and sulphide do not displace thiocynate to the same extent. The displacement of SCN^- by equimolar solutions depends upon the charge present on the anion indicating the relationship between the absorbance and the concentration of anions in terms of normality. The interference due to chloride, bromide, iodide and sulphide was eliminated by introducing a precolumn in Ag^+ form. For the removal of sulphate along with earlier mentioned interferring ions a precolumn made up of Ag^+ and Ba^{2+} form resin was efficient and effective.

In the estimation of fluoride in the presence of chloride, bromide, iodide, sulphide and sulphate, thiocynate column coupled with precolumn in the form of Ag^+ and Ba^{2+} was used. It was observed that all these interferring ions are quantitatively masked by the precolumn and displacement of SCN^- is only due to fluoride in the solution. Proportionate increase in the displacement of thiocynate was observed when only thiocynate column was used. It was further confirmed by passing the fluoride, chloride, iodide, bromide, sulphide and sulphate solutions separately through combined column. It was observed that displacement of SCN^- by fluoride remains unchanged whereas for all other anions combined column suppresses the displacement of thiocynate from the column quantitatively.

Analysis of drinking water

In Gujarat (India) fluoride content in drinking water is in the range of 3.8 to 4.2 μg ml^{-1} particularly in Mehsana district. This value is much higher than the US public health drinking water standards (1.5 μg ml^{-1}). It is even higher than the permissible values given by Indian Standards Institution[6] (3.0 μg ml^{-1}). The analysis of samples collected from various sources used for drinking water at Tavadia is given in Table 1. From the results in Table 1, it is observed that the results obtained by the proposed method are in good agreement with those obtained by SPADNS method.

References

1 Einaga H & Iwasaki I, *Talanta*, 18 (1981) 889.
2 Naidu A & Devarajulin K V R, *Indian J Chem*, 19A (1980) 177.
3 Long D & Huang Q, *Yejun Fenxi*, 7 (1987) 21.
4 Dean S F & Leonard M A, *Analyst*, 102 (1977) 340.
5 Mori I, Fujita Y, Fujita K, Nakahasi Y & Kishida Y, *Anal Lett*, 21 (1988) 563.
6 De A K, *Environmental chemistry* (Wiley Eastern, New Delhi) 1987, 157.

Indian Journal of Chemistry
Vol. 31A, February 1992, pp. 136-138

The efficacy of antimony(III) molybdotungstate as an exchanger for the separation of lead

C Janardanan & S M K Nair*

Department of Chemistry, University of Calicut, Calicut 673 635, India

Received 27 May 1991; revised and accepted 31 October 1991

A new thermally stable heteropolyacid inorganic ion exchanger, antimony(III) molybdotungstate, has been synthesised and characterised. The chemical composition (Sb:Mo:W::1:2.5:1.5), chemical stability, distribution coefficients for eight metal ions, change in capacity with ionic radii, effect of temperature on ion exchange capacity and effect of electrolyte concentrations on distribution coefficients for certain metal ions have been studied. Its properties have been compared with those of antimony(III) molybdate and antimony(III) tungstate. It has been used as an elegant exchanger for the separation of lead from other metals such as mercury, copper, zinc and magnesium.

Ion exchangers based on heteropolyacids with polyvalent metals are important as they show selective ion exchange behaviour. Qureshi *et al.* have studied tungstoarsenate[1,2], vanadophosphate[3], molybdoarsenate[4], vanadotungstate[5], molybdosilicate[6] and tungstophosphate[7] of tin(IV). However, heteropolyacid exchangers based on antimony(III) have not been studied in detail so far. The known antimony(III) based ion exchangers are antimony(III) arsenate, antimony(III) molybdate[8], antimony(III) selenite and antimony(III) tungstate[9]. But a heteropolyacid ion exchanger based on antimony(III) has not yet been reported. This note describes the synthesis, ion exchange properties and comparison of exchange properties of antimony(III) molybdotungstate with those of antimony(III) molybdate and antimony(III) tungstate and its efficacy in the separation of lead from other metal ions.

Experimental

Antimony(III) chloride, sodium tungstate (BDH) and sodium molybdate (V O Sojuz Chimexport) were used as such. All the other reagents used were of AR grade.

Synthesis

Antimony(III) molybdotungstate was prepared by adding a mixture containing 250 ml of 0.05 *M* sodium molybdate and 250 ml of 0.05 *M* sodium tungstate to 500 ml of 0.05 *M* acidic solution of antimony(III) chloride with constant stirring. The *p*H of the mixture was adjusted to 1 using dil. HCl and NaOH. On allowing to stand for 24 h, the precipitate settled. It was filtered, washed first with dil. HCl at the same *p*H as that at which the precipitation was made and then with demineralised water and dried at room temperature. The material was then converted into H^+ form by treatment with 1.0 *M* HNO_3 for 24 h with occasional shaking and intermittent changing of the acid when dark green antimony(III) molybdotungstate was obtained.

Determination of ion exchange capacity

The ion exchange capacity of the sample was determined by column operation. The exchanger in the H^+ form was placed in the column with a glass wool support. 1.0 *M* sodium chloride was used as the eluant and 200 ml of eluate was collected in each case. The hydrogen ions eluted from the column were determined titrimetrically with standard NaOH. One gram of the exchanger was used in each case to determine the capacity. The exchanger could be regenerated five times without any appreciable loss of exchange capacity.

For chemical analysis, 100 mg of the well-powdered material was dissolved in conc. H_2SO_4 and heated. Antimony was determined as antimony pyrogallate[10a], molybdenum as oxinate[10b] and tungsten as barium tungstate[10c].

Distribution coefficients

The distribution studies were carried out for eight metal ions by a batch process in the usual manner[11] by equilibrating the metal ion solution with the exchanger beads for 6 h at room temperature (30 ± 1°C). The K_d values were calculated using the expression,

$$K_d = \frac{I - F}{F} \times \frac{20}{0.1}$$

where I is the volume of EDTA consumed by the original solution and F is the volume of EDTA consumed at equilibrium. The total volume of the solution was 20 ml and the amount of exchanger used was 0.1 g. The concentrations of the metal ions were found out by EDTA titration[10d].

The effect of heating on ion exchange capacity was studied by heating 1 g of the exchanger in H^+ form in a thermostatically controlled oven at various

temperature for 6 h. After cooling the samples, their ion exchange capacities were determined.

The effect of electrolyte concentrations on the K_d values of certain metal ion solutions

Certain metal ion solutions in 1.0, 0.1, 0.01 and 0.001 *M* HNO_3 and NH_4NO_3 respectively were equilibrated with the exchanger and their coefficients were determined as described above. A comparison of properties such as exchange capacity, distribution coefficients, separation factors, efficiency in binary separation, etc., of antimony(III) molybdotungstate with those of antimony(III) molybdate and antimony(III) tungstate is given in Table 1. The importance of antimony(III) molybdotungstate as an efficient exchanger is evident from the data listed in Table 1.

Separation of metal ion solutions

For binary separation studies, 5.0 g of the exchanger in the H^+ form was taken in a glass column (30 cm × 1.1 cm dia). The rate of flow of all the separations was 0.5 ml/min. The separation of metal ions was tried in cases where the separation factor was greater than 5. In all separations the metal ion concentration was maintained at 0.005 *M* and 5 ml of each metal ion solution was taken. The details are given in Table 2.

Table 1—Properties of antimony(III) molybdate, antimony(III) tungstate and antimony(III) molybdotungstate.

Properties		Antimony(III) molybdate	Antimony(III) tungstate	Antimony(III) molybdotungstate
Ion exchange capacity	Li(I)	0.56	0.25	0.33
	Na(I)	1.02	0.60	0.80
	K(I)	1.20	0.73	0.97
	Mg(II)	0.96	0.58	0.63
	Ca(II)	1.40	0.81	0.65
	Ba(II)	1.60	0.83	0.76
Effect of temp. on i.e.c.	50	0.98	0.58	0.73
	150	0.86	0.32	0.61
	200	0.52	0.21	0.31
	300	0.15	0.08	0.07
K_d values (ml/g) of metal ions on	Zn(II)	115.38	21.50	26.74
	Mg(II)	76.19	19.80	20.24
	Pb(II)	800.00	145.40	427.78
	Co(II)	120.32	27.70	34.67
	Ca(II)	139.50	25.30	53.70
	Ni(II)	106.15	24.40	22.35
	Cu(II)	212.50	45.00	61.76
	Hg(II)	150.00	104.00	17.65
Separation factors for	Pb-Hg	6	1.5	23
	Pb-Zn	6.8	6.7	10.6
	Pb-Mg	10.5	7	20.14
	Pb-Cu	3.8	3.2	6.9
% Efficiency in binary separations	Hg-Pb	90.95	90.91	99-100
	Zn-Pb	90-92	94-95	96-100
	Mg-Pb	95-96	95-96	98-100
	Cu-Pb	90-92	94-95	95-100

Results and discussion

Antimony(III) molybdotungstate was obtained as a dark green hardmass, amorphous in nature. It is stable in 2 *M* HNO_3, 2 *M* H_2SO_4, 1 *M* HCl and salt solutions but dissolves in sodium hydroxide. The maximum ion exchange capacity was found to be 0.80 for Na^+ ion. The proportion of Sb:Mo:W was found to be 1:2.5:1.5 with a variation of ±0.01% for successive determinations.

The effect of size and charge of the ingoing ion on the capacity of the exchanger was studied. For all the alkali and alkaline earth metal ions the sequence shown by antimony(III) molybdotungstate is as follows:

$$Li^+(0.33) < Na^+(0.80) < K^+(0.97)$$

$$Ba^{2+}(0.76) > Sr^{2+}(0.68) > Ca^{2+}(0.65) > Mg^{2+}(0.63)$$

The exchange capacities are given in parentheses. The ion exchange capacity increases with decrease in hydrated ionic radii. This trend in the exchange capacities confirms that the ion exchange takes place in the hydrated form.

The study of the effect of temperature on the ion exchange capacities revealed that the ion exchange capacity decreased with increase in temperature and the sample retained the ion exchange capacity even on heating to 300°C.

Studies on the effect of electrolyte concentration (HNO_3, NH_4NO_3) on the distribution coefficients of metal ion such as zinc, copper and lead revealed that

Table 2—Separation of binary mixtures

Mixtures with eluants	Loaded (mg)	Recovered (mg)
Hg(II) 0.1 *M* HNO_3 + 0.1 *M* NH_4NO_3	4.91	4.90
Pb(II) 0.5 *M* HNO_3 + 0.5 *M* NH_4NO_3	6.50	6.50
Zn(II) 0.2 *M* HNO_3 + 0.2 *M* NH_4NO_3	1.91	1.91
Pb(II) 0.5 *M* HNO_3 + 0.5 *M* NH_4NO_3	6.50	6.49
Mg(II) 0.2 *M* HNO_3 + 0.2 *M* NH_4NO_3	0.62	0.60
Pb(II) 0.5 *M* HNO_3 + 0.5 *M* NH_4NO_3	6.50	6.50
Cu(II) 0.2 *M* HNO_3 + 0.2 *M* NH_4NO_3	1.30	1.28
Pb(II) 0.5 *M* HNO_3 + 0.5 *M* NH_4NO_3	6.50	6.49

the uptake of ions decreased with increase in electrolyte concentration. This may be due to the competitions of ions.

The distribution studies of eight metal ions have shown that antimony(III) molybdotungstate has affinites as follows: Zn(II) (26.74), Mg(II) (20.24), Pb(II) (427.78), Co(II) (34.67), Ca(II) (53.70), Ni(II) (22.35) Cu(II) (61.76) and Hg(II) (17.65). Antimony(III) molybdate and antimony(III) tungstate have high affinity for lead. Similarly, antimony(III) molybdotungstate also shows high affinity but the separation factors for the metal ions were found to be two to four times greater than those of the other simple ion exchangers. This fact is more pronounced when the binary separations are carried out. Also, separations were found to be more elegant and distinct on the molybdotungstate columns. A 100% efficiency of separation in the case of lead was achieved.

References

1 Qureshi M, Kumar R, Sharma V & Khan T, *J Chromatogr*, 118 (1976) 125.

2 Qureshi M, Sharma V, Kaushik R L & Khan T, *J Chromatogr*, 128 (1976) 149.

3 Qureshi M & Kaushik R C, *Anal Chem*, 49 (177) 165.

4 Qureshi M, Kumar R & Kaushik R C, *Sep Sci Technol*, 13 (1978) 185.

5 Qureshi M & Kaushik R C, *Sep Sci Technol*, 17 (1982) 739.

6 Qureshi M, Gupta A P, Rizvi S M A & Shakeel N A, *Reactive Polym*, 3 (1984) 23.

7 Qureshi M, Gupta A P, Sharma V, Kaushik R C & Gupta H O, *J Indian chem Soc*, 63 (1986) 206.

8 Janardanan C & Madhavankutty Nair S, *Analyst* 115 (1990) 85.

9 Janardanan C & Madhavankutty Nair S, *Proceedings of Kerala Science Congress*, (1991) 285.

10 Vogel A I, *A text book of quantitative inorganic analysis*, 4th Edn. (Longmans, London) 1978; a, 366; b, 472; c, IIIrd edn, p, 567; d, 324.

11 Qureshi M, Varshney K G & Israili A H, *J Chromatogr*, 50 (1972) 141.

Indian Journal of Chemistry
Vol. 31A, February 1992, pp. 139

Book Review

The structure, dynamics and equilibrium properties of colloidal system, edited by D M Bloor & E Wyn-Jones (Kluwer, The Netherlands), 1990, pp. XI + 888, Price US $ 220.

Over the last two decades, there has been prolific research endeavour on colloidal systems including micelles and microemulsions, specially with a view to understanding the structure and function of biological maeromolecular systems (biopolymers and biological amphiphiles are colloidal in nature). Numerous applications of amphiphilic and colloidal systems in pharmacy, enhanced-oil-recovery, cleaning, detergency, lubrication, water-conservation, sewage treatment, etc., have added new dimensions to the study of colloidal systems. The excellent promise of microemulsions and reverse micelles in the fields of biophysical and photophysical chemistry has ushered in new impetus in this branch of science all over the world.

The present book is, therefore, a useful document. It will positively serve the purpose of enlightening researchers and scientists (engaged in the field of colloid and surface science as well as in the borderline areas) and make them up-to-date about the state-of-the-art. The articles, authored by distinguished scientists, are versatile in nature. The structure, dynamics and equilibrium studies of collidal systems encompass the basic understanding of reverse micelles and collidal phenomena and the modern trend in the field baed on sophisticated techniques and fundamental-logical concepts of analysis blended with accurate experimental results. There are 57 articles in this 885-page volume. Studies on both conventional and non-conventional systems have been presented.

The editing job of the book has been done with great care; there are negligible printing errors in the volume of considerable bulk. The balance of the articles is, however, weighted towards the micelle and microemulsion side; articles on hydrocolloids, gels, vesicles, foams and liquid crystals are relatively less in number. There is only one article on colloidal semiconductors and one on wetting phenomenon. The applicability of colloidal system is the main potential of the field, and as expected several articles on this aspect and also on biological assemblies and biocolloids have been included. Comprehensive presentations point to the versatility of the topic. The subject matter of some of the articles by way of their presentation will fresh the reader's mind about the basic premises and the fundamental principles of the colloidal systems. On the whole, the endeavour has been fruitful. It is expected that such efforts would continue in future to enrich this important branch of physical science.

S P Moulik
Department of Chemistry
Jadavpur University
Calcutta 700 032

Indian Journal of Chemistry
Vol. 31A, February 1992, p. 140

ANNOUNCEMENT

National Symposium on Recent Advances in Chiral Synthesis

A National Symposium on Recent Advances in Chiral Synthesis will be held during 2-3 April 1992 at the Indian Institute of Chemical Technology (IICT), Hyderabad. Organised as a part of the CSIR Golden Jubilee celebrations, the symposium plans to bring together people engaged in various aspects of synthesis of chiral compounds. The programme will consist of invited talks and presentation of papers in the following areas:

(i) New strategies in the synthesis of chiral compounds
(ii) Modern techniques for the analysis of optically active compounds

Further information regarding the symposium may be obtained from Dr U T Bhalerao, Convenor, National Symposium on Recent Advances in Chiral Synthesis, Indian Institute of Chemical Technology, Hyderabad 500 007.

Errata

Paper entitled, "Standard potentials of Ag-AgX (X = Br and I) electrodes at different temperatures and the related transfer energetics of HX in quasi-isodielectric aqueous ethylene carbonate solvents" by Subrata Sinha and Kiron K Kundu, *Indian J Chem*, 30A (1991) 920-928.

(i) Structure D on p. 926 has been printed wrongly. The correct structure is shown below:

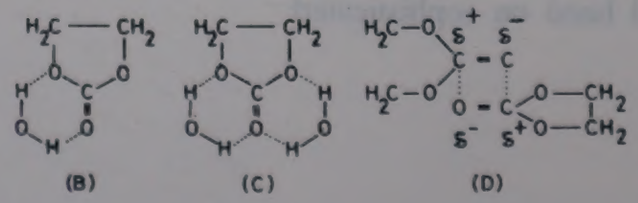

(B) (C) (D)

(ii) In the title of Table 1 on pages 921 and 922, KBr and AgBr/Ag should read as KX and AgX/Ag. X = Br before 10 wt% ethylene carbonate at the top of the page 921 and X = I before 10wt% ethylene carbonate near the bottom of the page 921.

Paper entitled "Organometallic derivatives of diphosphazanes: Part 3—The reaction of $PhN\{P(OPh)_2\}_2$ with $[Fe(\eta^5-C_5H_5)(CO)_2]_2$, unusual cleavage of a P–N bond to yield a complex containing $P(OPh)_2$ and $PhNP(OPh)_2$ units" by M S Balakrishna and S S Krishnamurthy, *Indian J Chem.*, 30A (1991) 536-537.

The 11th line from top right hand column of page 537 should read as: "groups whereas for **2** ν(CO) appears at 1960 cm^{-1}.

CSIR GOLDEN JUBILEE SERIES

BODY'S BATTLES

BAL PHONDKE

WAR makes rattling good history", said Oscar Wilde referring to the struggles of nations to capture new and to retain old territories. But other battles not visible to the naked eye are equally fascinating. An account of the miniscule wars fround witnin the confines of the human body is breathtaking if only for the fact that these are being fought every single living moment. The human body is continually besieged and attacked by a multitude of microbial enemies of great cunning and guile. However, nature has endowed the human body with an unique built-in defence organization that can be envy of the most modern technologically advanced nation.

This attractive and lavishly illustrated book, written especially for the non-specialist, unfolds the dramatic story of this inner defence organization, the diversity and specificity of its armament, and the methodical way in which it maintains a round the clock vigil to meet squarely every imaginable threat to the human body and also how it wins the body's battles most of the time.

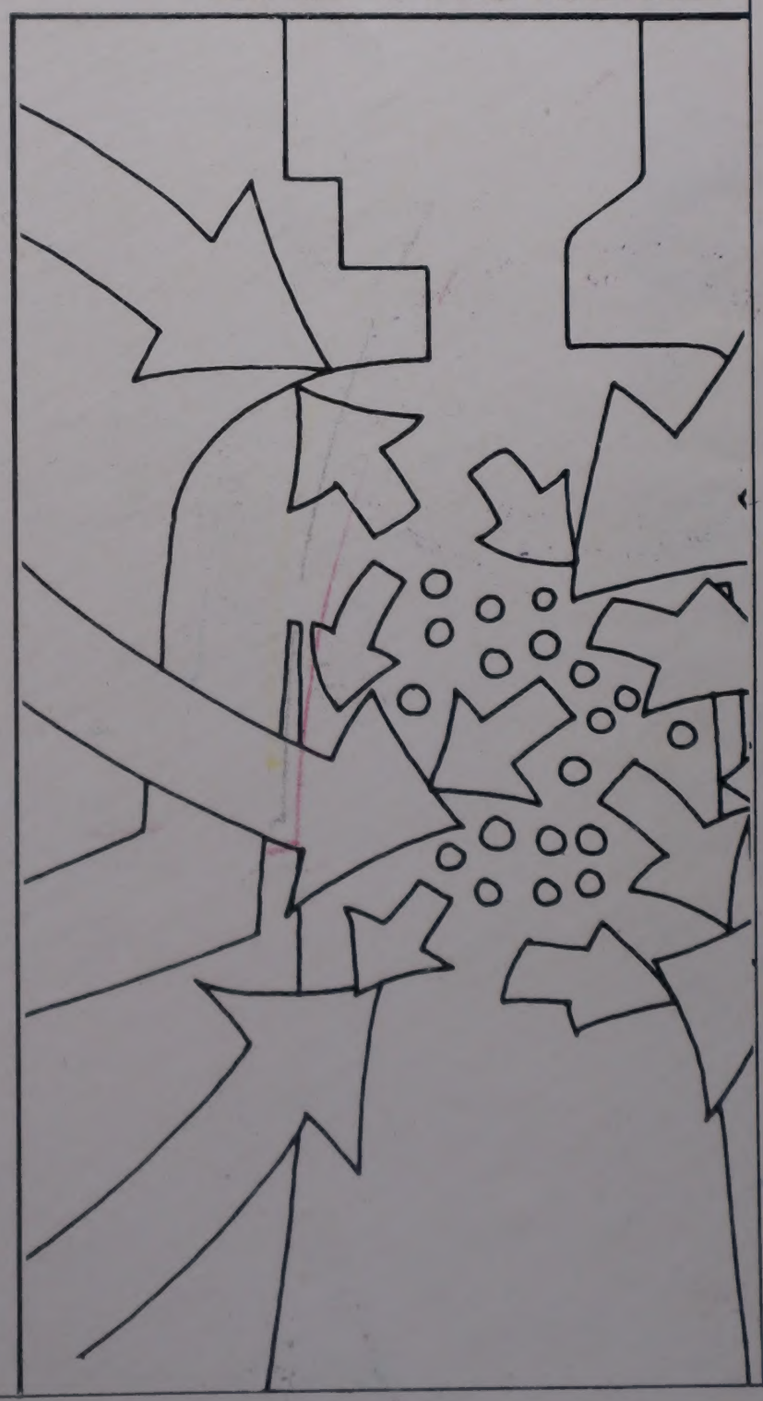

Price : Rs.9/- Paper back
:Rs.18/- Hard Bound

Orders should be accompanied by money order or Demand Draft made payable to PUBLICATIONS & INFORMATION DIRECTORATE, NEW DELHI and sent to:

The Senior Sales & Distributions Officer,
Publications & Information Directorate, CSIR
Dr K.S. Krishnan Marg,
New Delhi - 110 012

Printed & Published by Dr G.P. Phondke, Publications & Information Directorate (PID)
Dr K.S. Krishnan Marg, New Delhi 110 012, at PID Printing Unit

Unnecessary roughness.

action® For a different kind of Playing

D(W) 103
RN 7090/63